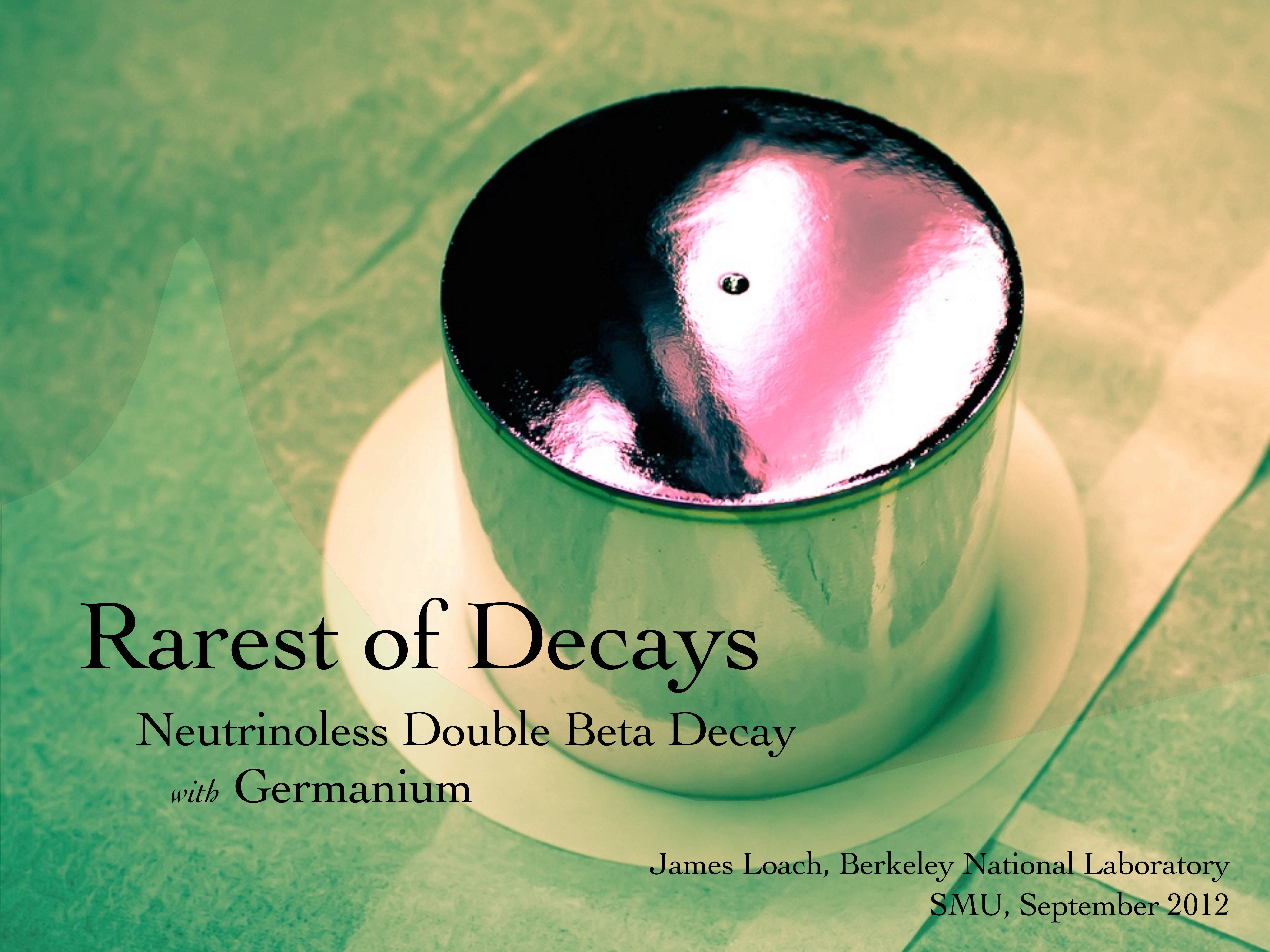

Rarest of Decays

Neutrinoless Double Beta Decay *with* Germanium

James Loach, Berkeley National Laboratory
SMU, September 2012

Double beta decay

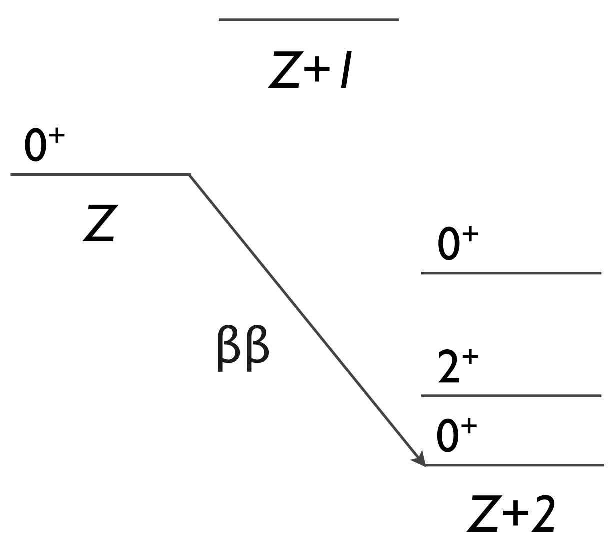

Can be observed when pairing forces forbid normal beta decay

$\beta^+\beta^+$, β^+EC & ECEC are phase space surpassed

Two neutrino

$$ {}^{A}_{Z}\mathrm{N} \rightarrow {}^{A}_{Z+2}\mathrm{N}' + e^- + e^- + \nu_e + \nu_e $$

$T_{1/2} \sim 10^{20}$ y

Rarest nuclear process observed

Neutrinoless

$$ {}^{A}_{Z}\mathrm{N} \rightarrow {}^{A}_{Z+2}\mathrm{N}' + e^- + e^- $$

$T_{1/2} > 10^{25}$ y

As yet unobserved

Two neutrino

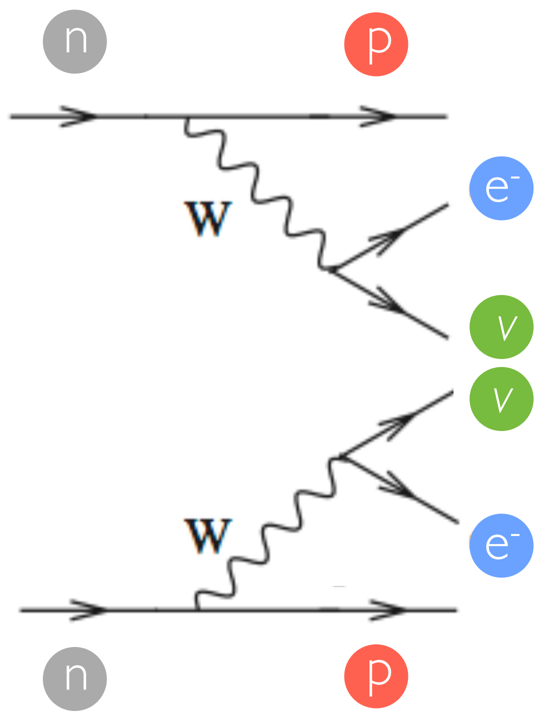

Phase space factor

$$(T^{2\nu}_{1/2})^{-1} = G_{2\nu}(Q_{\beta\beta}, Z)|M_{2\nu}|^2$$

Matrix element

$T_{1/2}$ (2ν) (y)

^{48}Ca	$(4.4 \pm 0.6) \cdot 10^{19}$
^{76}Ge	$(1.5 \pm 0.1) \cdot 10^{21}$
^{82}Se	$(0.92 \pm 0.07) \cdot 10^{20}$
^{96}Zr	$(2.3 \pm 0.2) \cdot 10^{19}$
^{100}Mo	$(7.1 \pm 0.4) \cdot 10^{18}$
^{116}Cd	$(2.8 \pm 0.2) \cdot 10^{19}$
^{128}Te	$(1.9 \pm 0.4) \cdot 10^{24}$
^{130}Te	$(1.5 \pm 0.1) \cdot 10^{20}$
^{150}Nd	$(8.2 \pm 0.9) \cdot 10^{18}$
^{238}U	$(2.0 \pm 0.6) \cdot 10^{21}$
^{136}Xe	$(2.1 \pm 0.2) \cdot 10^{22}$

A.S. Barabash, Phys. Rev. C **81**, 035501 (2010).
(With errors symmetrized)
+ arXiv:1108.4193v2

1935 Prediction of 0νββ

M. Goeppert-Mayer, Phys. Rev. **48**, 512 (1935).

1957 Geochemical observation (Te)

M.G. Inghram and J.H. Reynold, Phys. Rev. **78**, 822 (1950).

1987 Laboratory observation (Se)

S.R. Elliott et al., Phys. Rev. Lett. **59**, 2020 (1987).

Neutrinoless

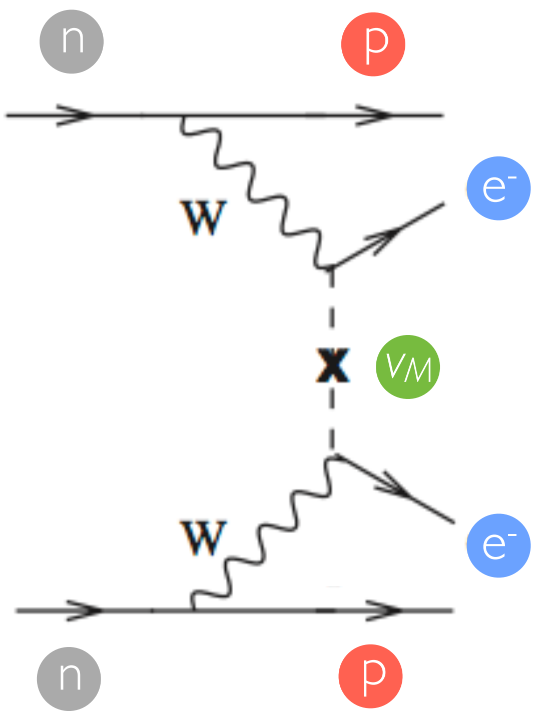

Phase space factor — Matrix element

$$(T^{0\nu}_{1/2})^{-1} = G_{0\nu}(Q_{\beta\beta}, Z)|M_{0\nu}|^2\langle m_{\beta\beta}\rangle^2$$

$$\langle m_{\beta\beta}\rangle \equiv \left|\sum_k m_k U^2_{ek}\right|$$

Effective Majorana neutrino mass

$T_{1/2}$ (0ν) (y)

^{76}Ge	> 1.9 · 10^{25}
	> 1.6 · 10^{25}
^{130}Te	> 2.8 · 10^{24}
^{100}Mo	> 1.1 · 10^{24}
^{136}Xe	> 1.6 · 10^{25}
^{82}Se	> 3.6 · 10^{23}
^{116}Cd	> 1.7 · 10^{23}

A.S. Barabash, Phys. Rev. C **81**, 035501 (2010).
(Limits at 90% c.l.)
+ arXiv:1205.5608v2

1937 Majorana neutrino

E. Majorana, Nuovo Cimento **14**, 171 (1937).

1937 Suggestion of 0νββ

G. Racah, Nuovo Cimento **14**, 322 (1937).

2002 Claimed observation (Ge)

H.V. Klapdor-Kleingrothaus et al.,
Phys. Lett. B **586**, 198 (2004).
Mod. Phys. Lett. A **21**, 1547 (2006).

Neutrinoless

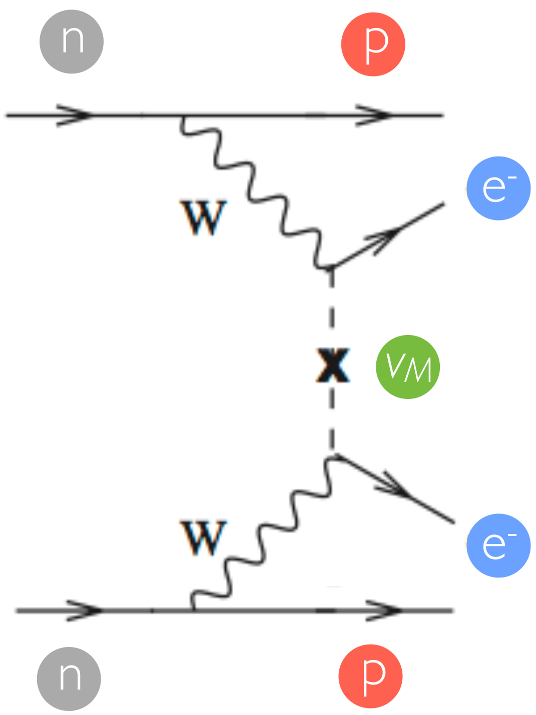

Phase space factor

Matrix element

$$(T^{0\nu}_{1/2})^{-1} = G_{0\nu}(Q_{\beta\beta}, Z)|M_{0\nu}|^2\langle m_{\beta\beta}\rangle^2$$

S.R. Elliott and P. Vogel, Annu. Rev. Nucl. Part. Sci. **52**, 115 (2002).

$$\langle m_{\beta\beta}\rangle \equiv \left|\sum_k m_k U_{ek}^2\right|$$

Effective Majorana neutrino mass

1937 Majorana neutrino

E. Majorana, Nuovo Cimento **14**, 171 (1937).

1937 Suggestion of 0νββ

G. Racah, Nuovo Cimento **14**, 322 (1937).

2002 Claimed observation (Ge)

H.V. Klapdor-Kleingrothaus et al.,
Phys. Lett. B **586**, 198 (2004).
Mod. Phys. Lett. A **21**, 1547 (2006).

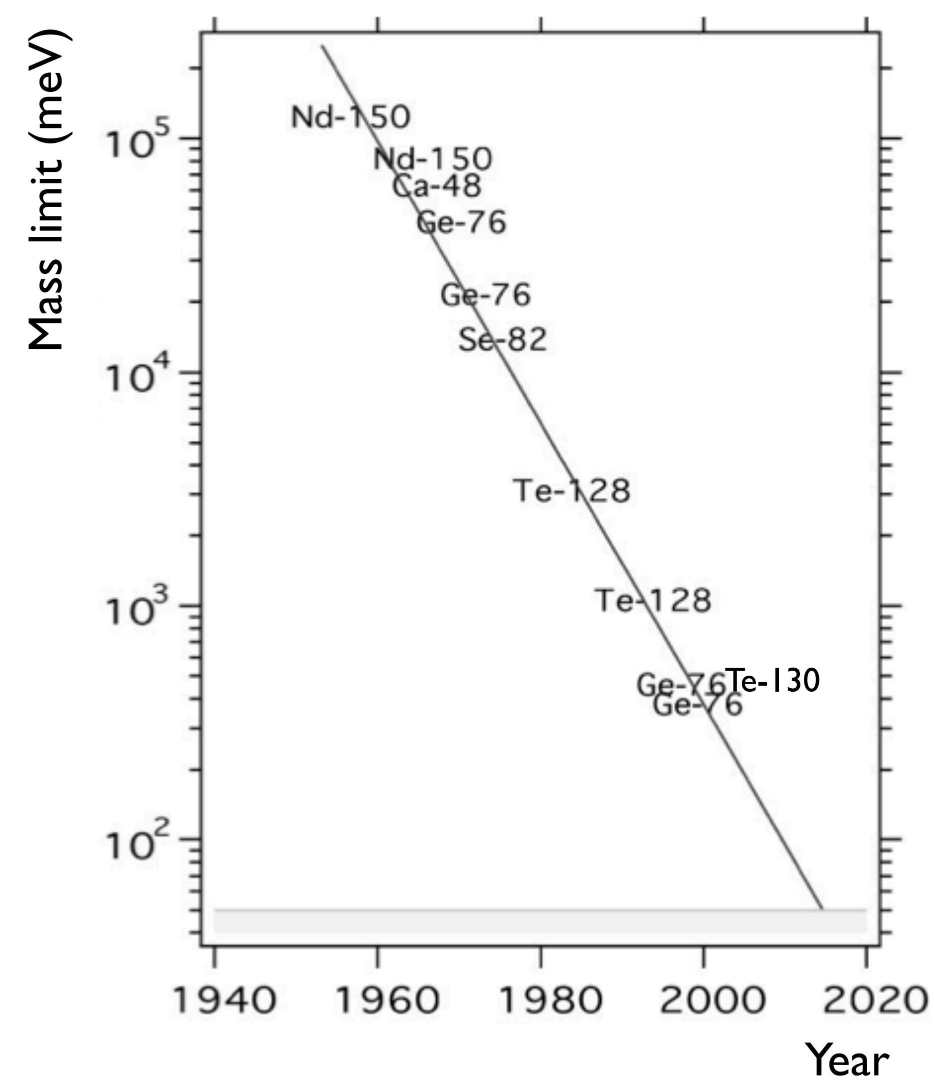

What we would learn

The neutrino is a Majorana particle

though other mechanisms may contribute to the 0νββ decay rate

Schechter, J., and J. W. F. Valle, Phys. Rev. D **25**, 2951 (1982).

$$\nu^D = \begin{pmatrix} \nu_L \\ \bar{\nu}_L \\ \nu_R \\ \bar{\nu}_R \end{pmatrix}$$

Dirac neutrino

Conventional
Redundant information

$$\nu^M = \begin{pmatrix} \nu_L \\ \nu_R \end{pmatrix}$$

Majorana neutrino

Efficient
New

What we would learn

The neutrino is a Majorana particle

though other mechanisms may contribute to the $0\nu\beta\beta$ decay rate

Schechter, J., and J. W. F. Valle, Phys. Rev. D **25**, 2951 (1982).

Its mass can be explained naturally via the seesaw mechanism

- natural explanation for the mass scale
- important for leptogenesis

Lepton number is violated

- a prerequisite for leptogenesis

A.D. Sakharov, JETP Lett. **91B** (1967).

The neutrino mass

Measure the effective Majorana neutrino mass

$$\langle m_{\beta\beta} \rangle \equiv \sum_k m_k U_{ek}^2$$

Neutrino mixing (MNSP) matrix

$$\begin{pmatrix} \nu_e \\ \nu_\mu \\ \nu_\tau \end{pmatrix} = \begin{pmatrix} U_{e1} & U_{e2} & U_{e3} \\ U_{\mu 1} & U_{\mu 2} & U_{\mu 3} \\ U_{\tau 1} & U_{\tau 2} & U_{\tau 3} \end{pmatrix} \begin{pmatrix} \nu_1 \\ \nu_2 \\ \nu_3 \end{pmatrix}$$

$c = \cos \quad s = \sin$

$$U = \begin{pmatrix} 1 & 0 & 0 \\ 0 & c_{23} & s_{23} \\ 0 & -s_{23} & c_{23} \end{pmatrix} \begin{pmatrix} c_{13} & 0 & s_{13}e^{-i\delta} \\ 0 & 1 & 0 \\ -s_{13}e^{-i\delta} & 0 & c_{13} \end{pmatrix} \begin{pmatrix} c_{12} & s_{12} & 0 \\ -s_{12} & c_{12} & 0 \\ 0 & 0 & 1 \end{pmatrix}$$

Atmospheric   Theta-13 & phase   Solar

The neutrino mass

Measure the effective Majorana neutrino mass

$$\langle m_{\beta\beta} \rangle \equiv \sum_k m_k U_{ek}^2$$

Neutrino mixing (MNSP) matrix

$$\begin{pmatrix} \nu_e \\ \nu_\mu \\ \nu_\tau \end{pmatrix} = \begin{pmatrix} U_{e1} & U_{e2} & U_{e3} \\ U_{\mu 1} & U_{\mu 2} & U_{\mu 3} \\ U_{\tau 1} & U_{\tau 2} & U_{\tau 3} \end{pmatrix} \begin{pmatrix} \nu_1 \\ \nu_2 \\ \nu_3 \end{pmatrix}$$

$c = \cos \quad s = \sin$

$$U = \begin{pmatrix} 1 & 0 & 0 \\ 0 & c_{23} & s_{23} \\ 0 & -s_{23} & c_{23} \end{pmatrix} \begin{pmatrix} c_{13} & 0 & s_{13}e^{-i\delta} \\ 0 & 1 & 0 \\ -s_{13}e^{-i\delta} & 0 & c_{13} \end{pmatrix} \begin{pmatrix} c_{12} & s_{12} & 0 \\ -s_{12} & c_{12} & 0 \\ 0 & 0 & 1 \end{pmatrix} \begin{pmatrix} e^{i\alpha_1/2} & 0 & 0 \\ 0 & e^{i\alpha_2/2} & 0 \\ 0 & 0 & 1 \end{pmatrix}$$

Atmospheric — Theta-13 & phase — Solar — Majorana phase

The neutrino mass

Cosmology

$$m_{sum} = \sum_k m_k = m_1 + m_2 + m_3$$

$m_{sum} < \sim 0.7$ eV

Beta decay

$$m_\beta = \sqrt{\sum_k m_k^2 |U_{ek}|^2}$$

$m_\beta < \sim 2$ eV

Oscillation

$$\Delta m_{ij}^2 = m_j^2 - m_i^2$$

U_{ik}, Δm_{12}, Δm_{23}

Neutrinoless double beta decay

$$\begin{aligned}\langle m_{\beta\beta} \rangle \equiv \sum_k m_k U_{ek}^2 \\ = \cos^2\theta_{12}\cos^2\theta_{13} e^{i\alpha} m_1 \\ + \sin^2\theta_{12}\cos^2\theta_{13} e^{i\beta} m_2 \\ + \sin^2\theta_{13} e^{-2i\delta} m_3\end{aligned}$$

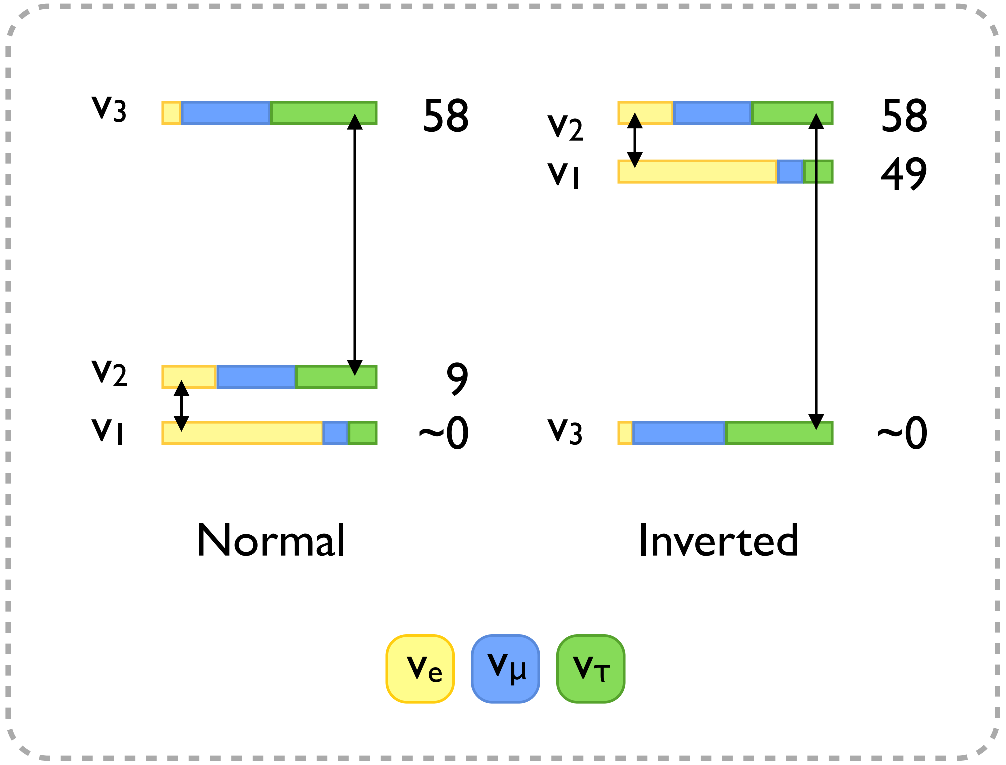

The neutrino mass

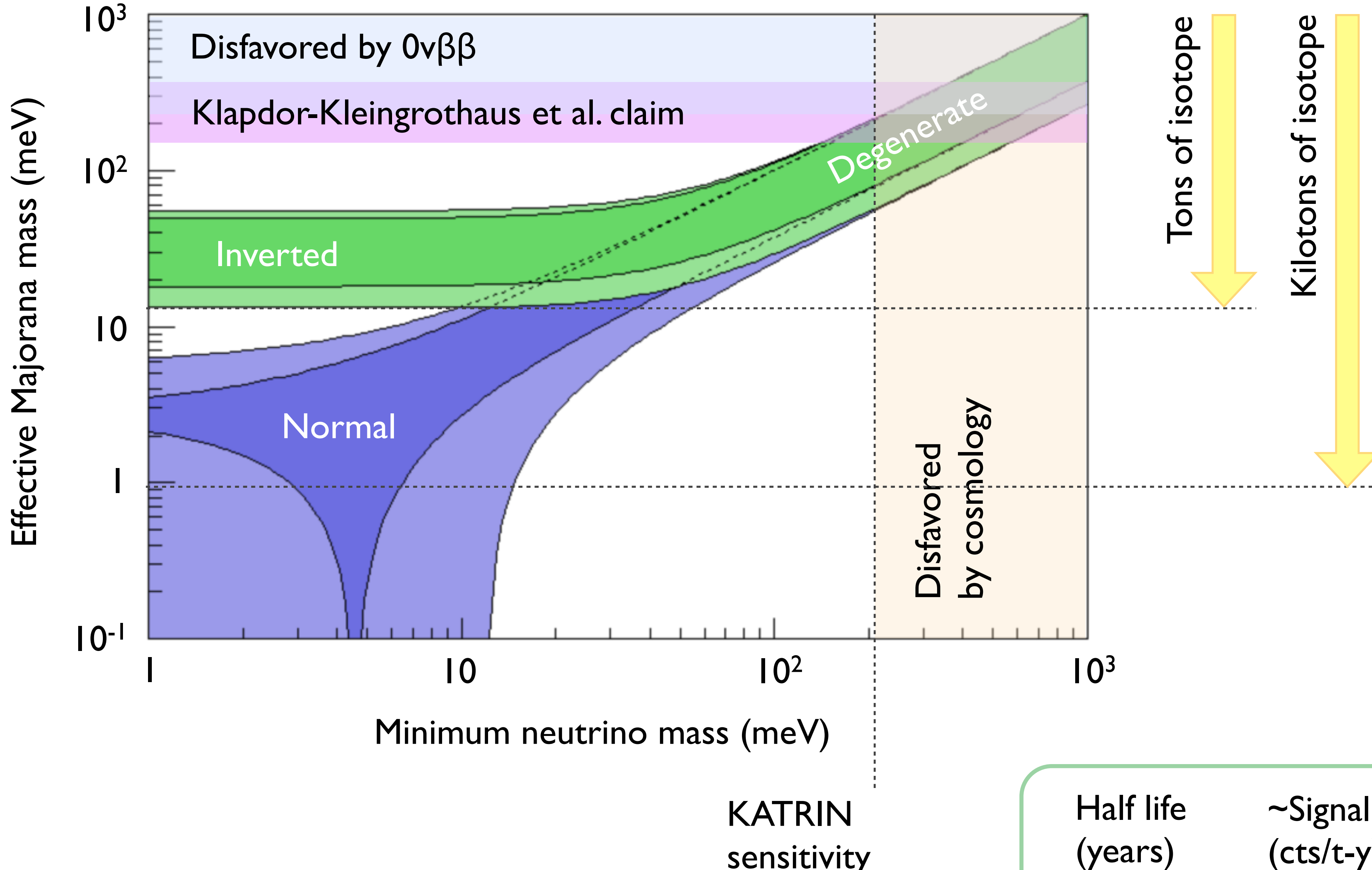

Half life (years)	~Signal (cts/t-y)	~Neutrino mass scale (meV)	
10^{25}	530	400	Degenerate
5×10^{26}	10	100	
5×10^{27}	1	40	Atmospheric
$>10^{29}$	<0.05	<10	Solar

The next generation of experiments will reach the inverted hierarchy

Experimental signatures

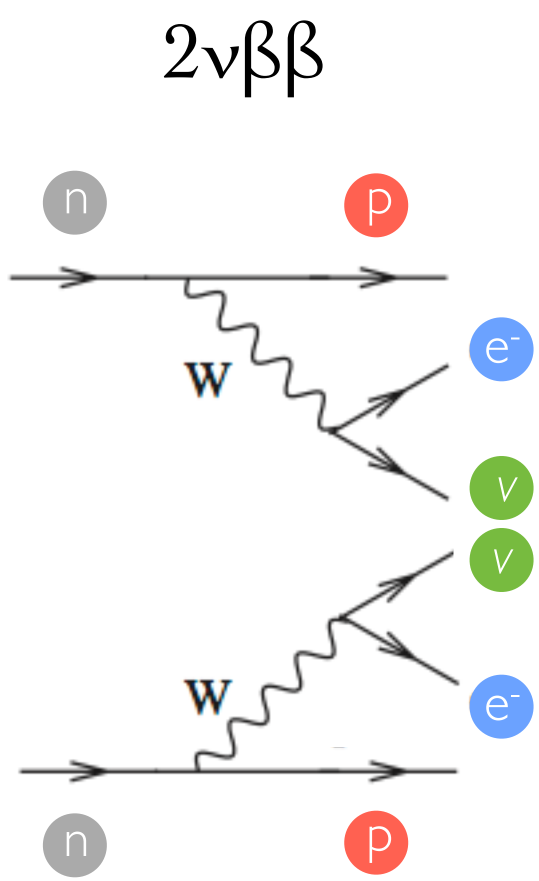

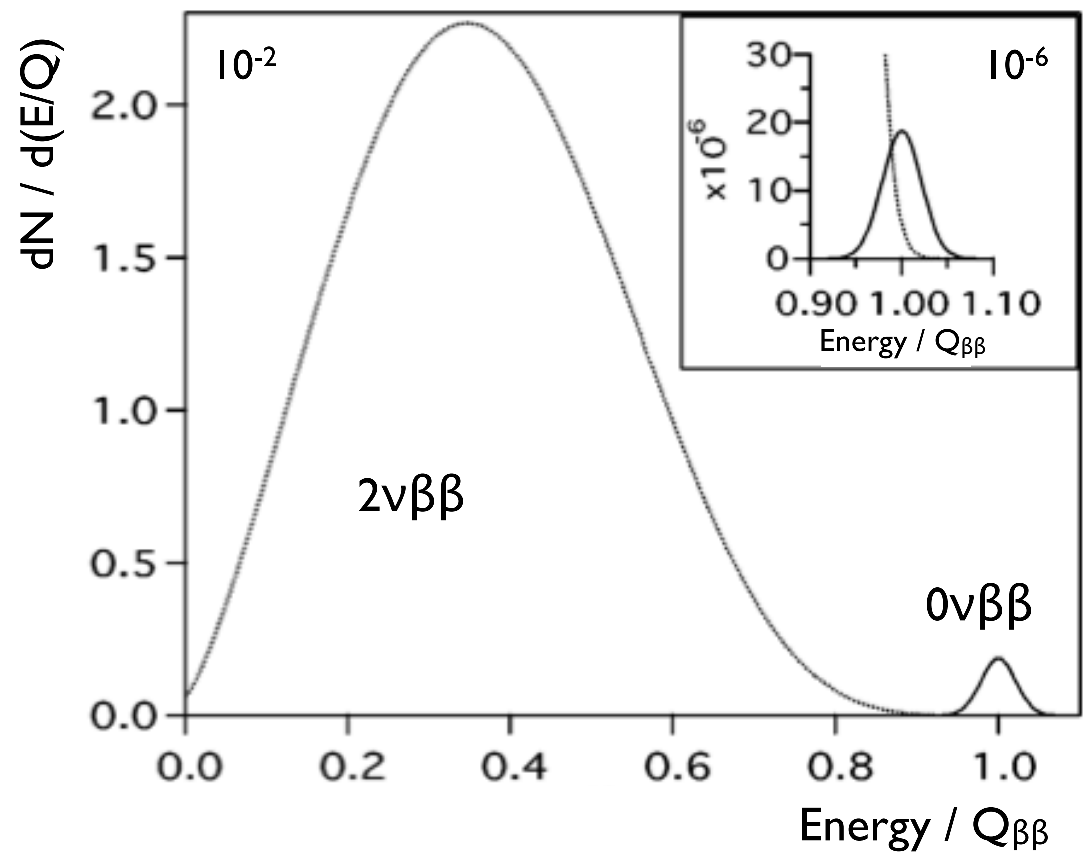

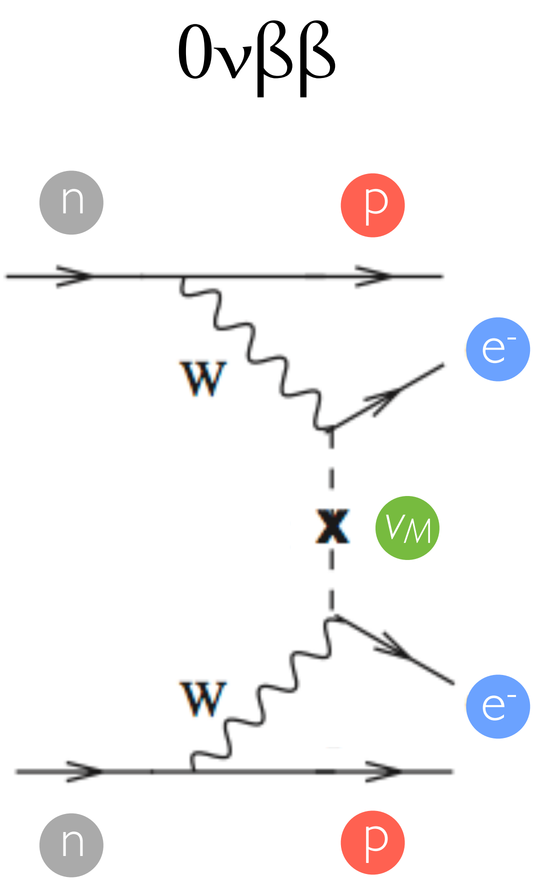

Elliott, S. R., and Vogel, P., Annu. Rev. Nucl. Part. Sci. **52**, 115 (2002).
(5% energy resolution; relative normalization 10^{-2}, 10^{-6} in insert)

0νββ characterized by a sharp peak in deposited energy

Rate heavily suppressed relative to 2νββ

Making a discovery

Evidence

- Peak at the correct energy
- Single-site deposition
- Correct event distributions

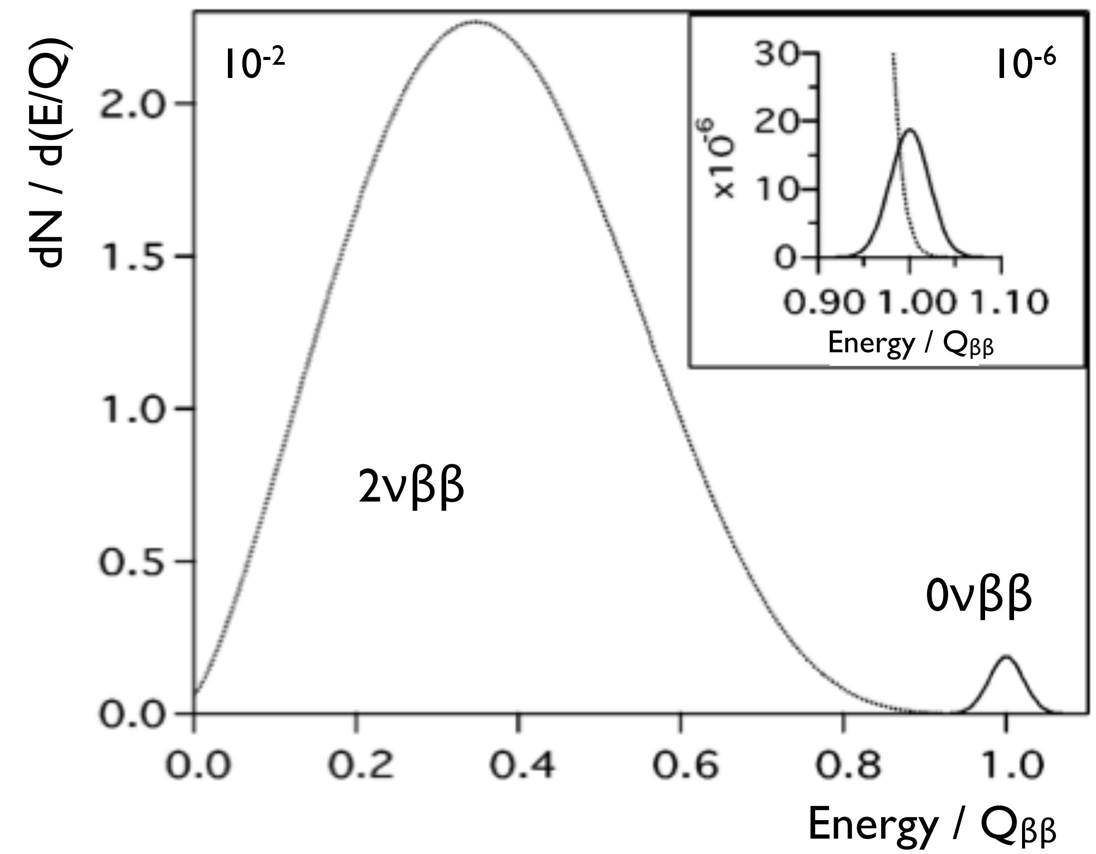

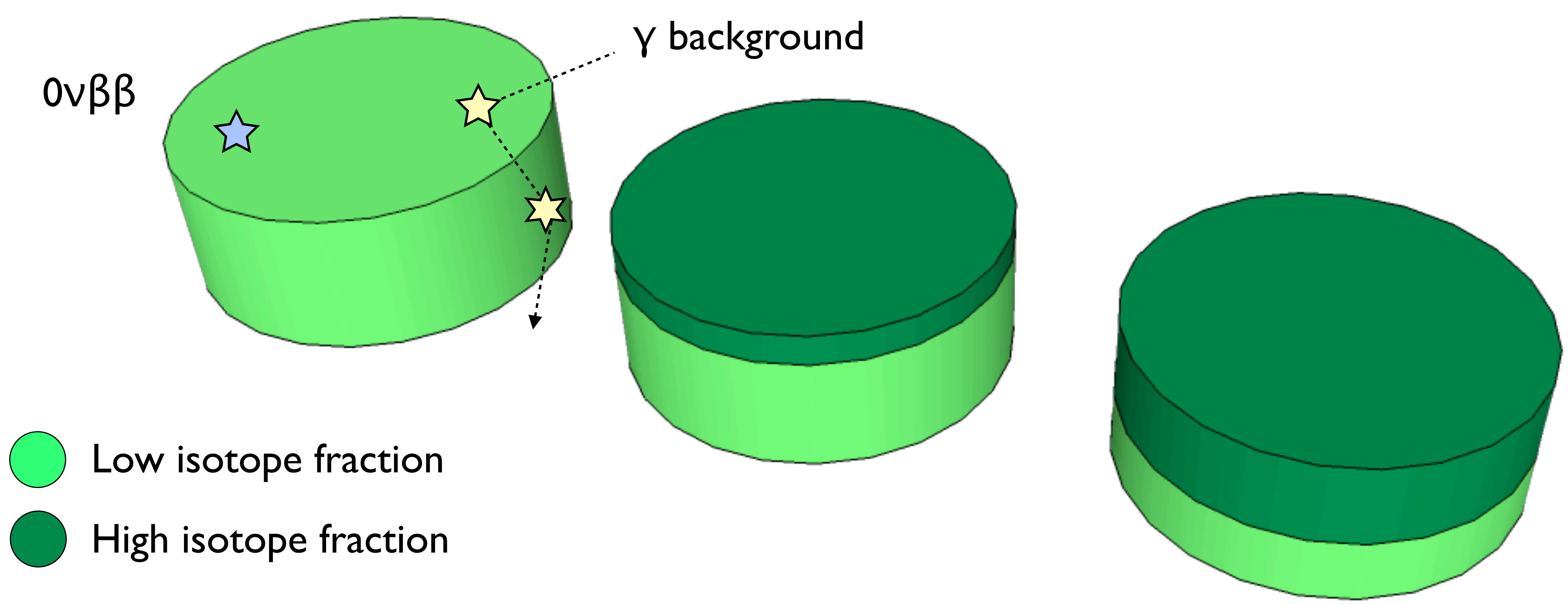

Making a discovery

Evidence

- Peak at the correct energy
- Single-site deposition
- Correct event distributions

Convincing evidence

- Observe the 2-electron nature
- Correct kinematic distributions
- Observe t-correlated daughter
- Observe excited-state decay

Compelling evidence

- Consistent results using different isotopes

A broad experimental program is required

Sensitivity

$$\langle m_{\beta\beta} \rangle^2 = \frac{1}{T^{0\nu}_{1/2} \cdot G_{0\nu}(Q_{\beta\beta}, Z)|M_{0\nu}|^2}$$

Zero background

$$m_{\beta\beta} \sim \sqrt{1/\varepsilon} \cdot \frac{1}{\sqrt{Mt}}$$

Background-limited

$$m_{\beta\beta} \sim \sqrt{1/\varepsilon} \cdot \left(\frac{b\Delta E}{Mt} \right)^{1/4}$$

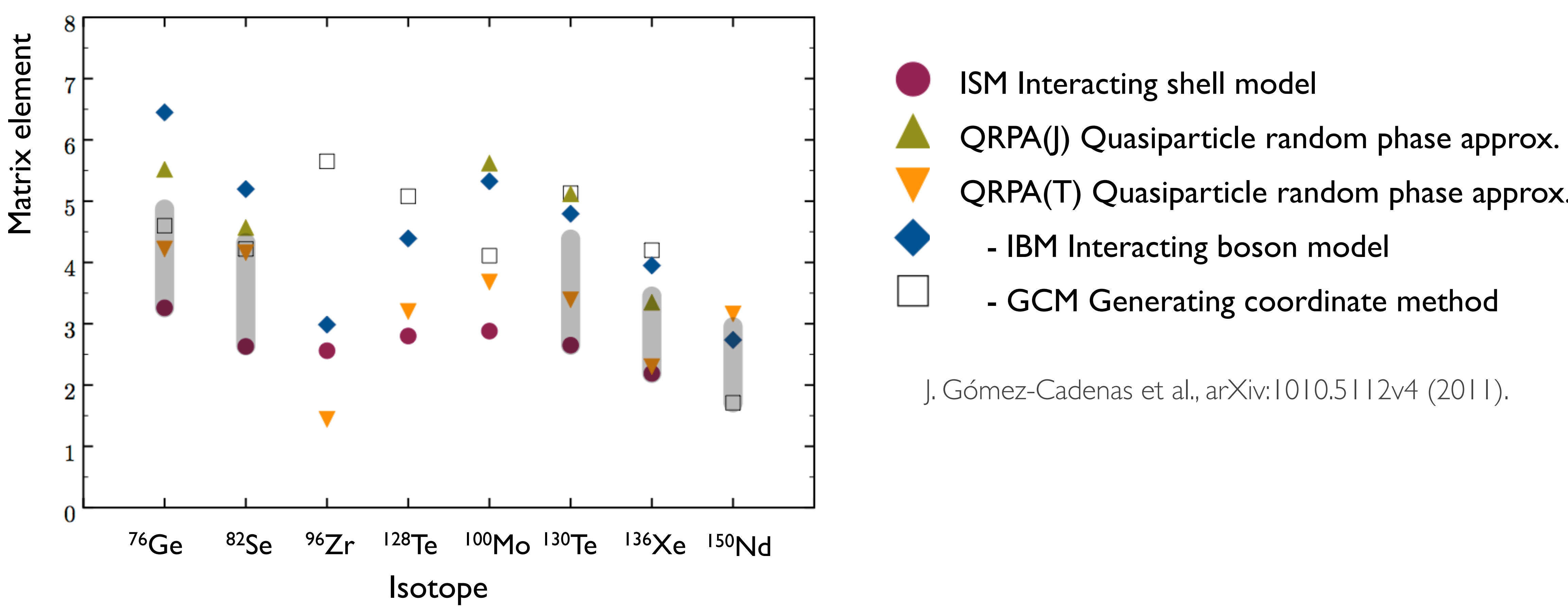

J. Gómez-Cadenas et al., arXiv:1010.5112v4 (2011).

Isotope

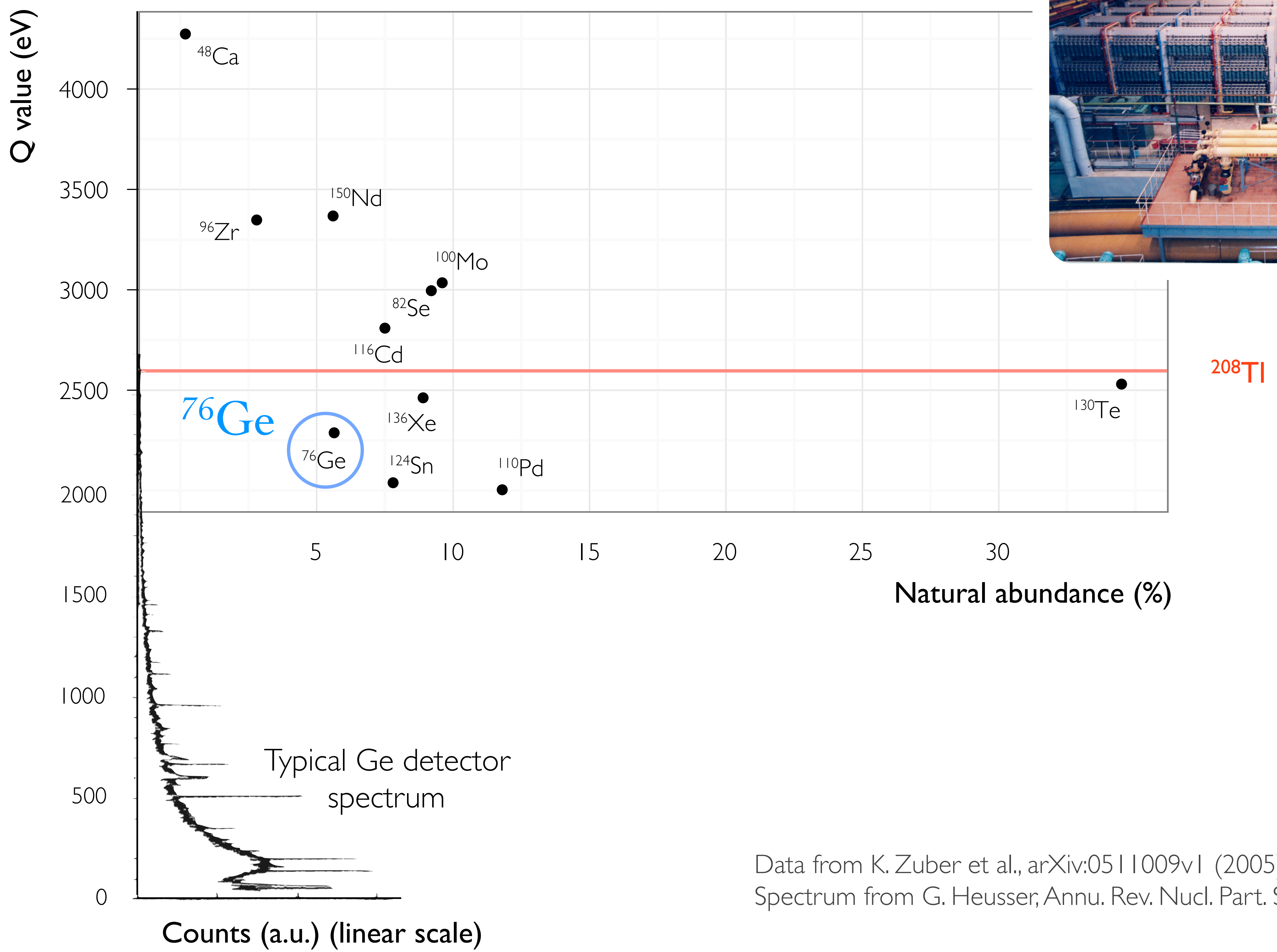

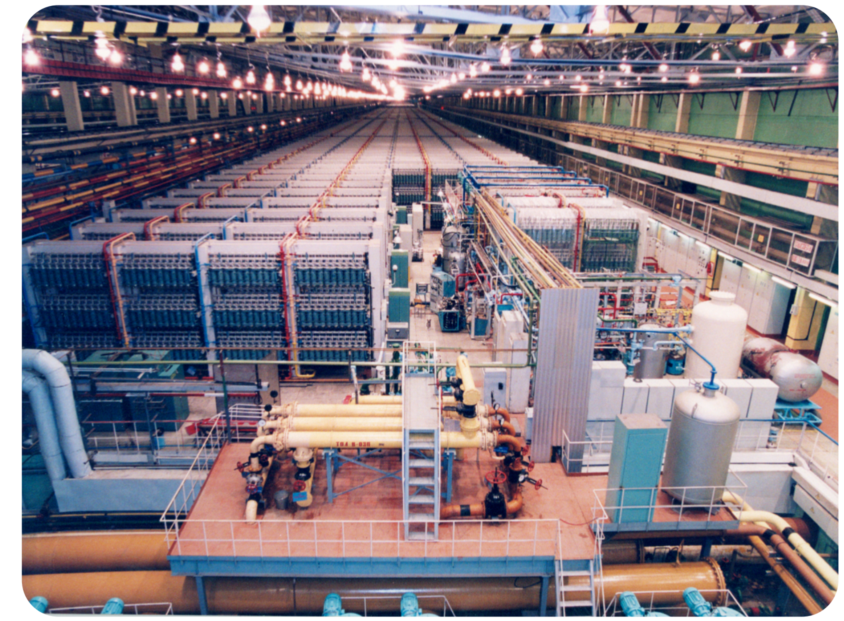

Data from K. Zuber et al., arXiv:0511009v1 (2005).
Spectrum from G. Heusser, Annu. Rev. Nucl. Part. Sci. **45** (1995).

Current experimental efforts

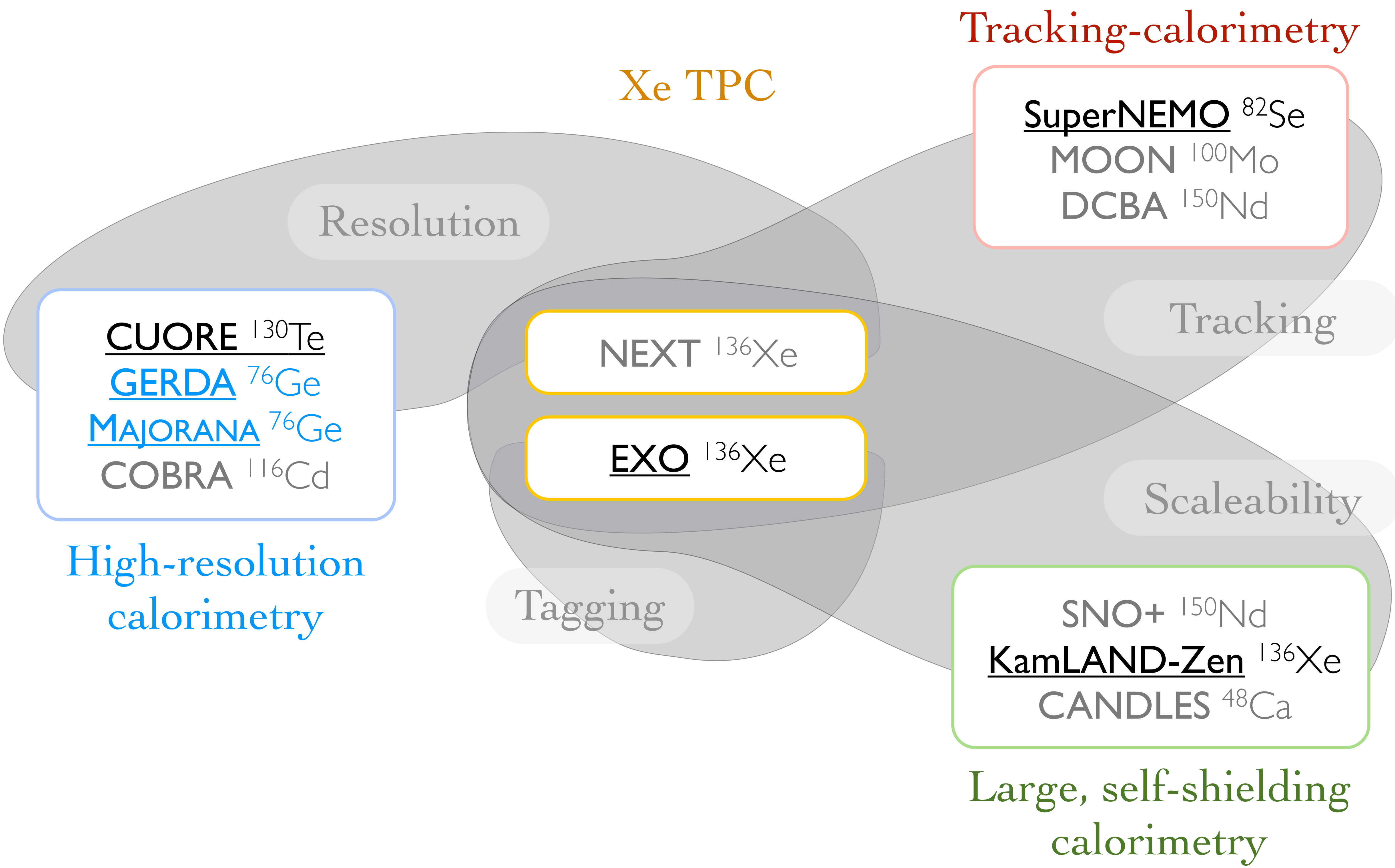

KamLAND-Zen

Xenon-loaded liquid scintillator

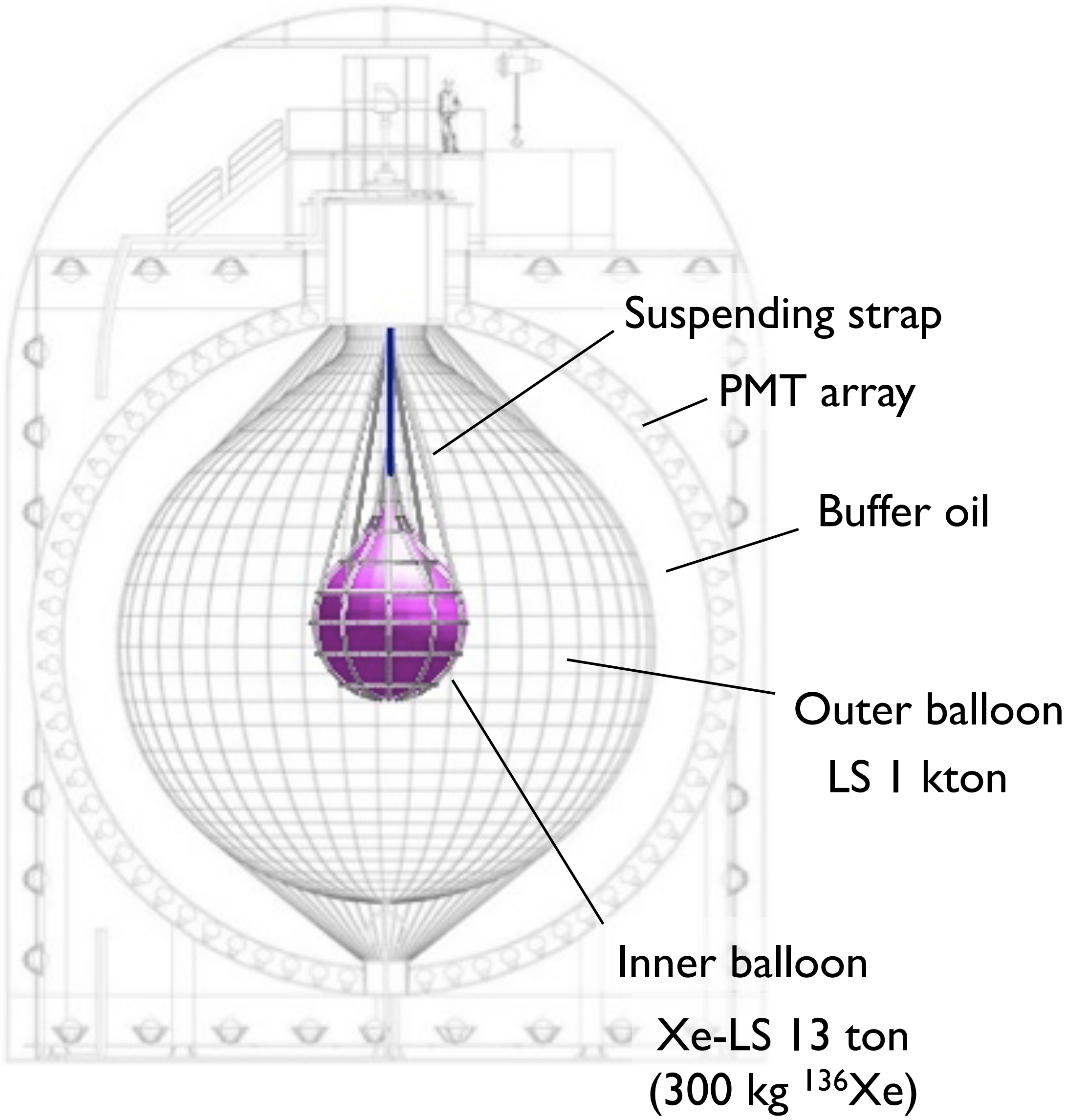

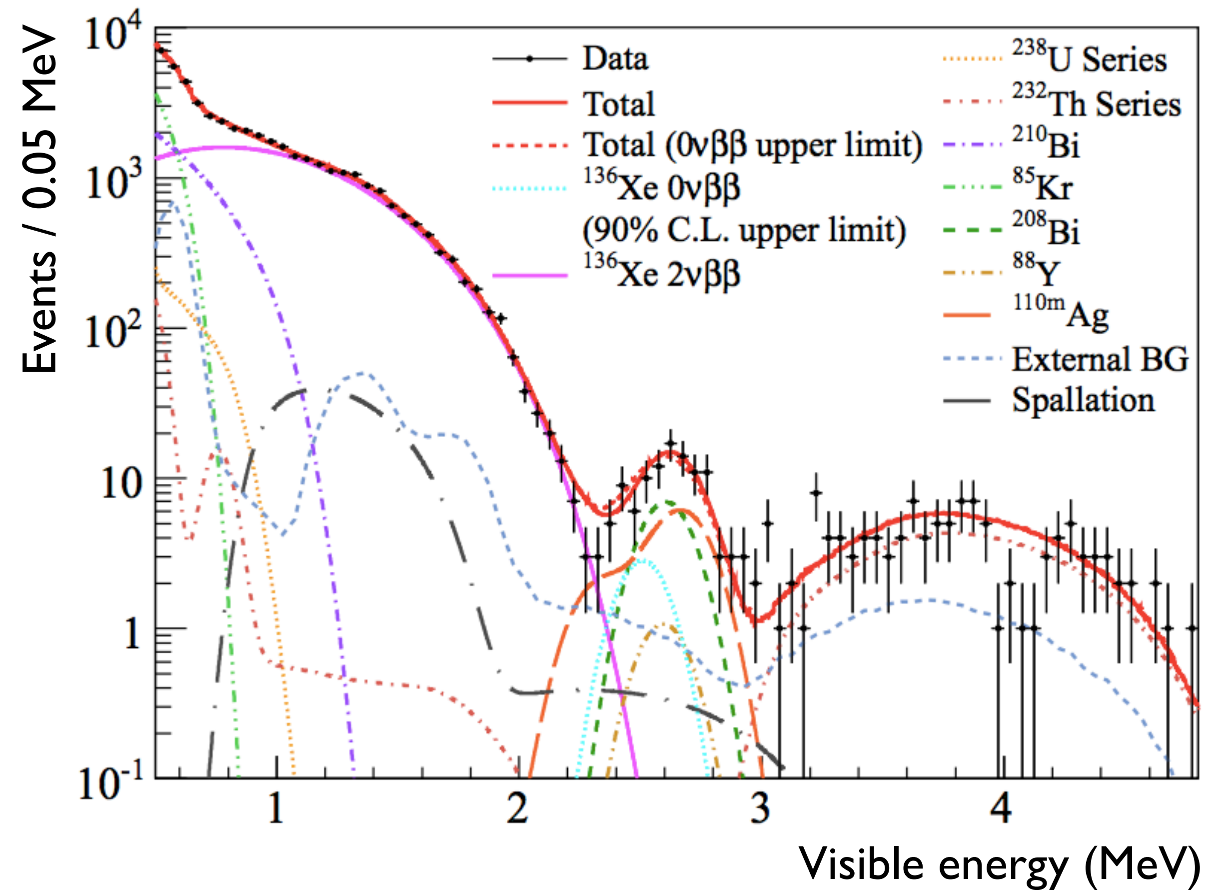

$$T_{1/2}^{0\nu} > 5.7 \times 10^{24}\,\mathrm{y}\ (90\%\ \mathrm{c.l.})$$

$$T_{1/2}^{2\nu} = 2.38 \pm 0.02\,(\mathrm{stat}) \pm 0.14\,(\mathrm{sys}) \times 10^{21}\,\mathrm{y}$$

A. Gando et al. (KamLAND-Zen Collaboration) (2012).

EXO-200

Xenon time projection chamber

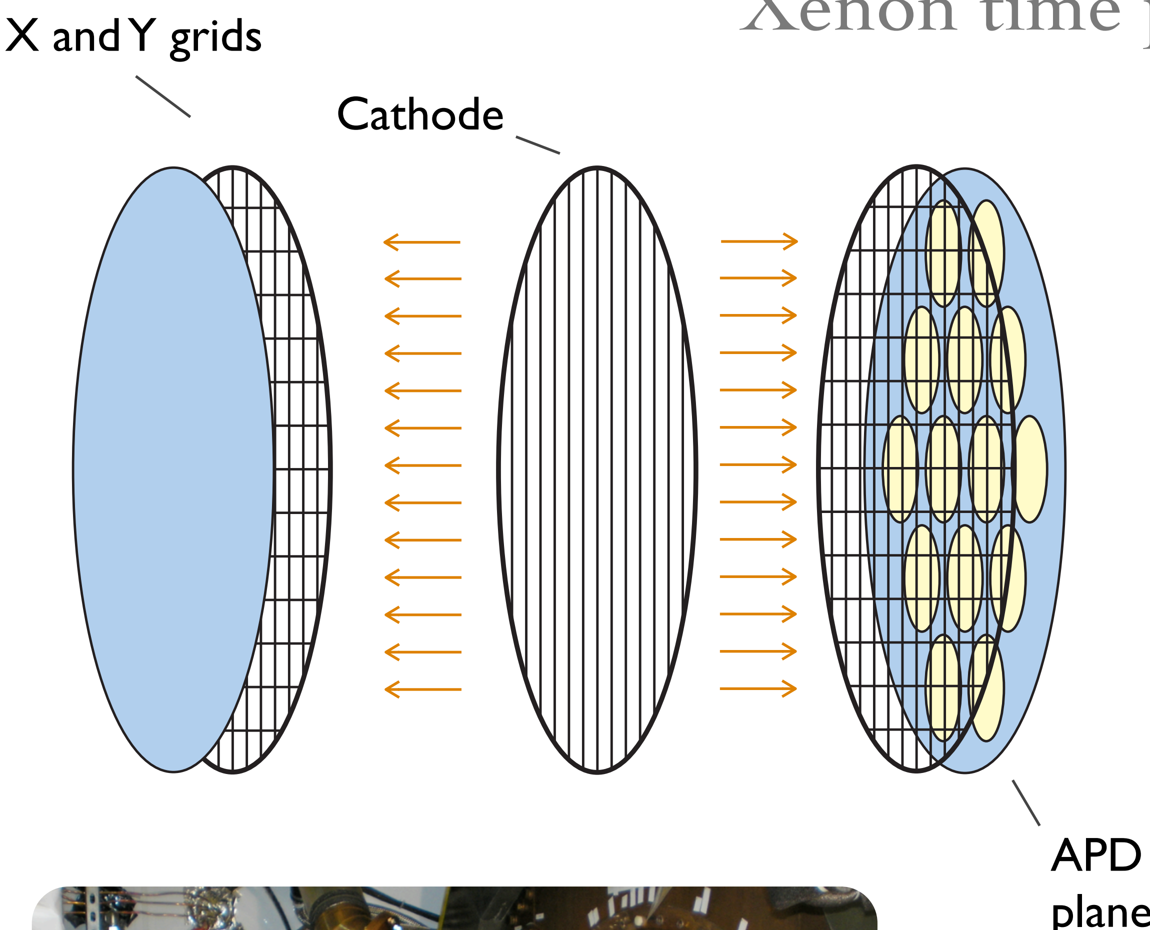

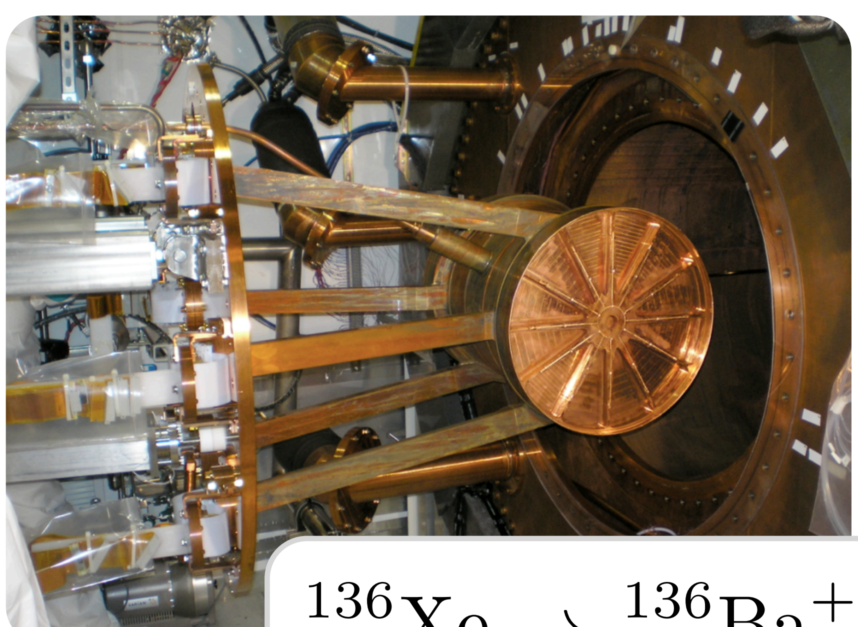

$$^{136}\mathrm{Xe} \to {}^{136}\mathrm{Ba}^{++} + 2\,\mathrm{e}^-$$

$$T^{2\nu}_{1/2} = 2.11 \pm 0.04\,(\mathrm{stat}) \pm 0.21\,(\mathrm{sys}) \times 10^{21}\,\mathrm{y}$$

$$T^{0\nu}_{1/2} > 1.6 \times 10^{25}\,\mathrm{y}\;(90\%\ \mathrm{c.l.})$$

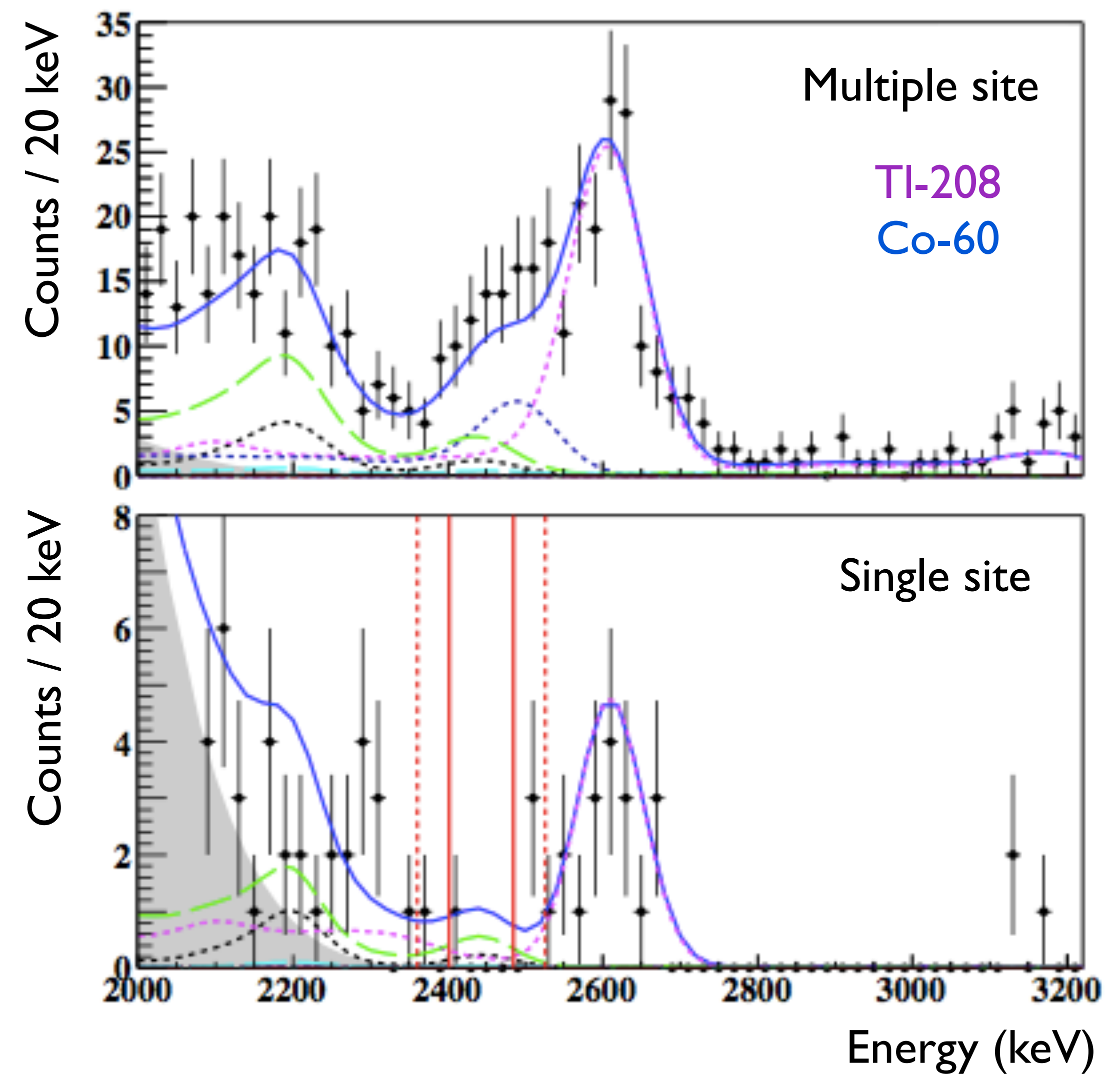

N. Ackerman et al. (EXO Collaboration), Phys. Rev. Lett. 107, 212501 (2011).

supernemo collaboration

NEMO & SuperNEMO

Foils, tracking and calorimetry

Beautiful measurements of two-neutrino angular distributions and half-lives

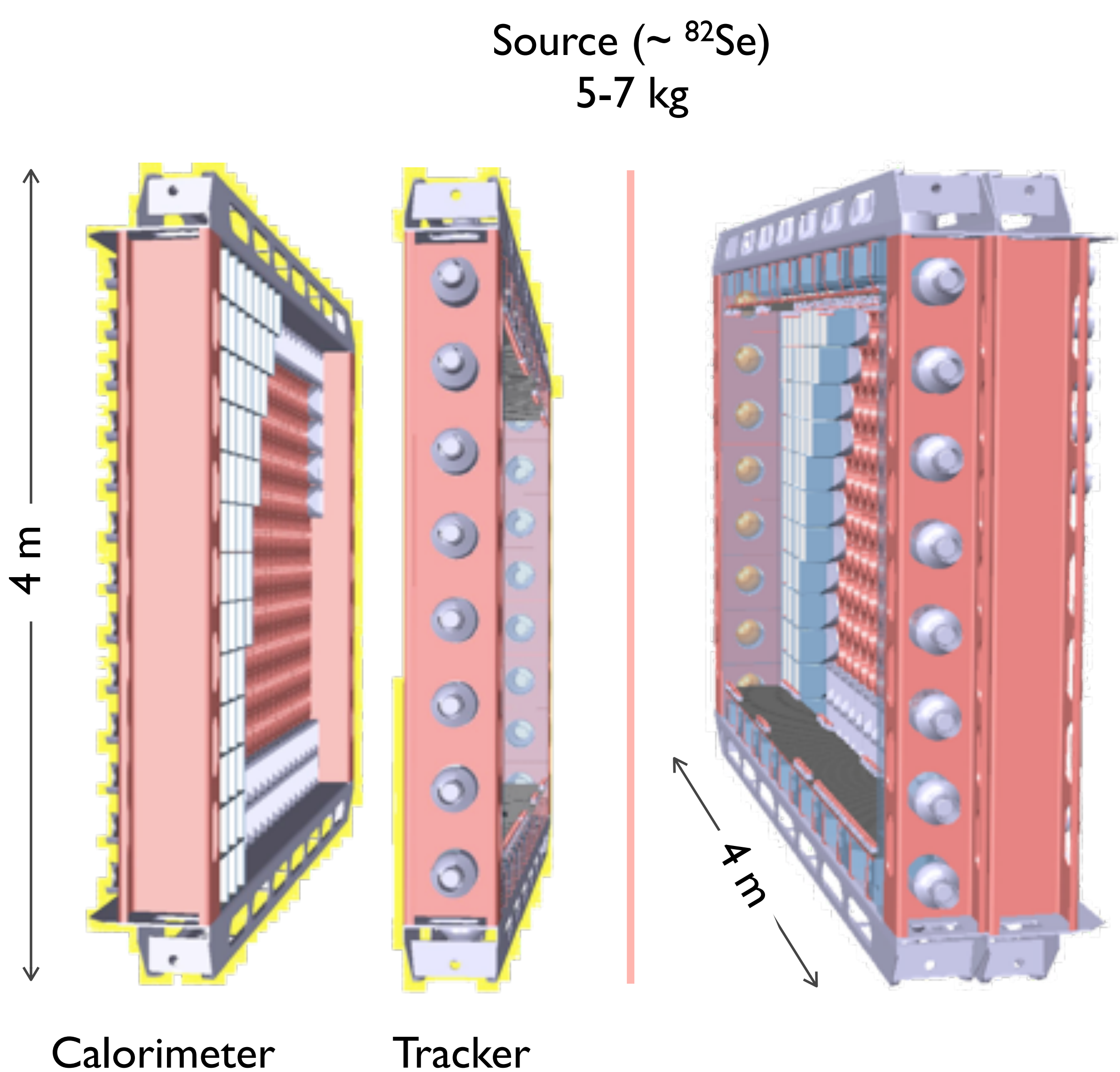

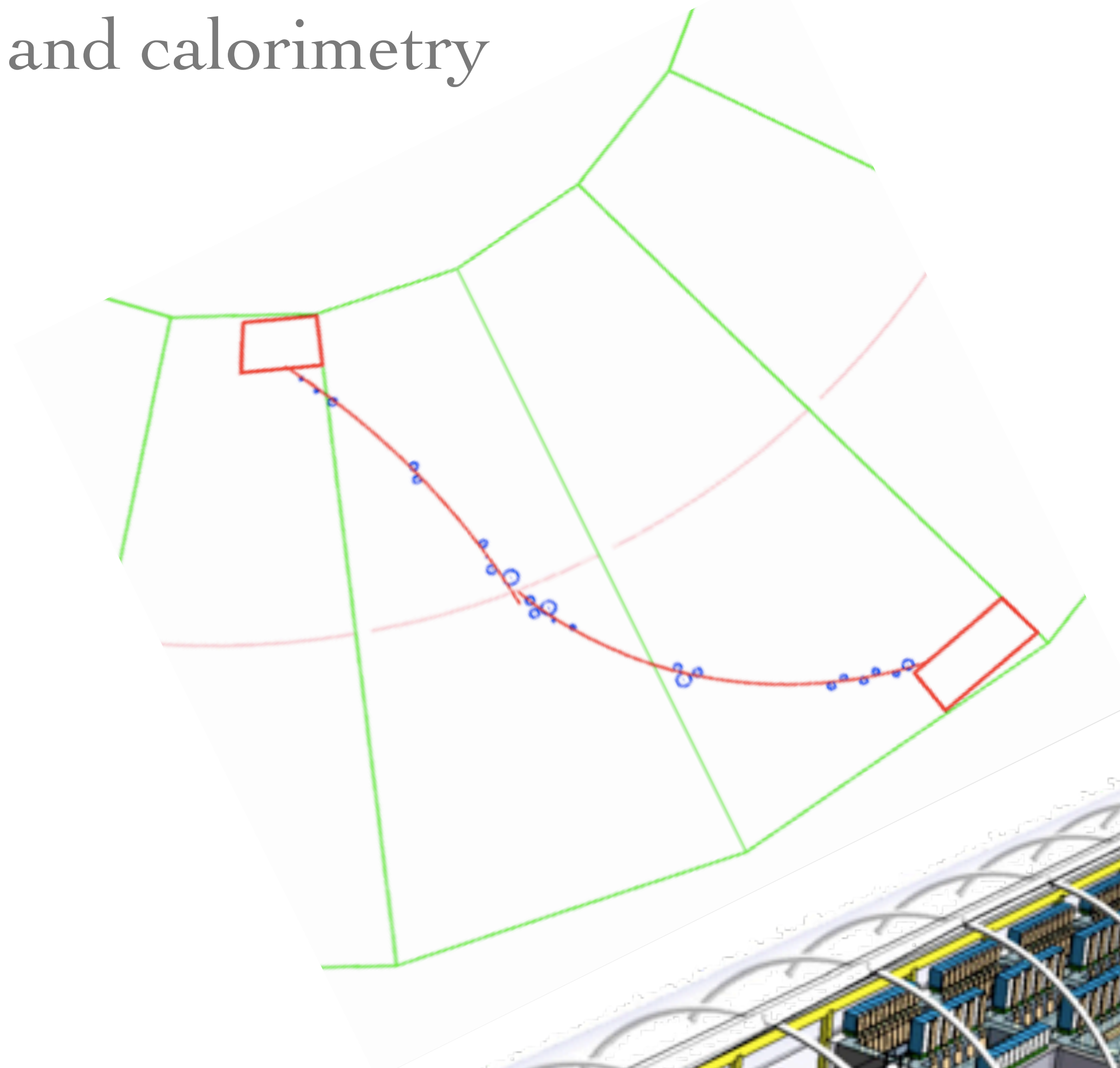

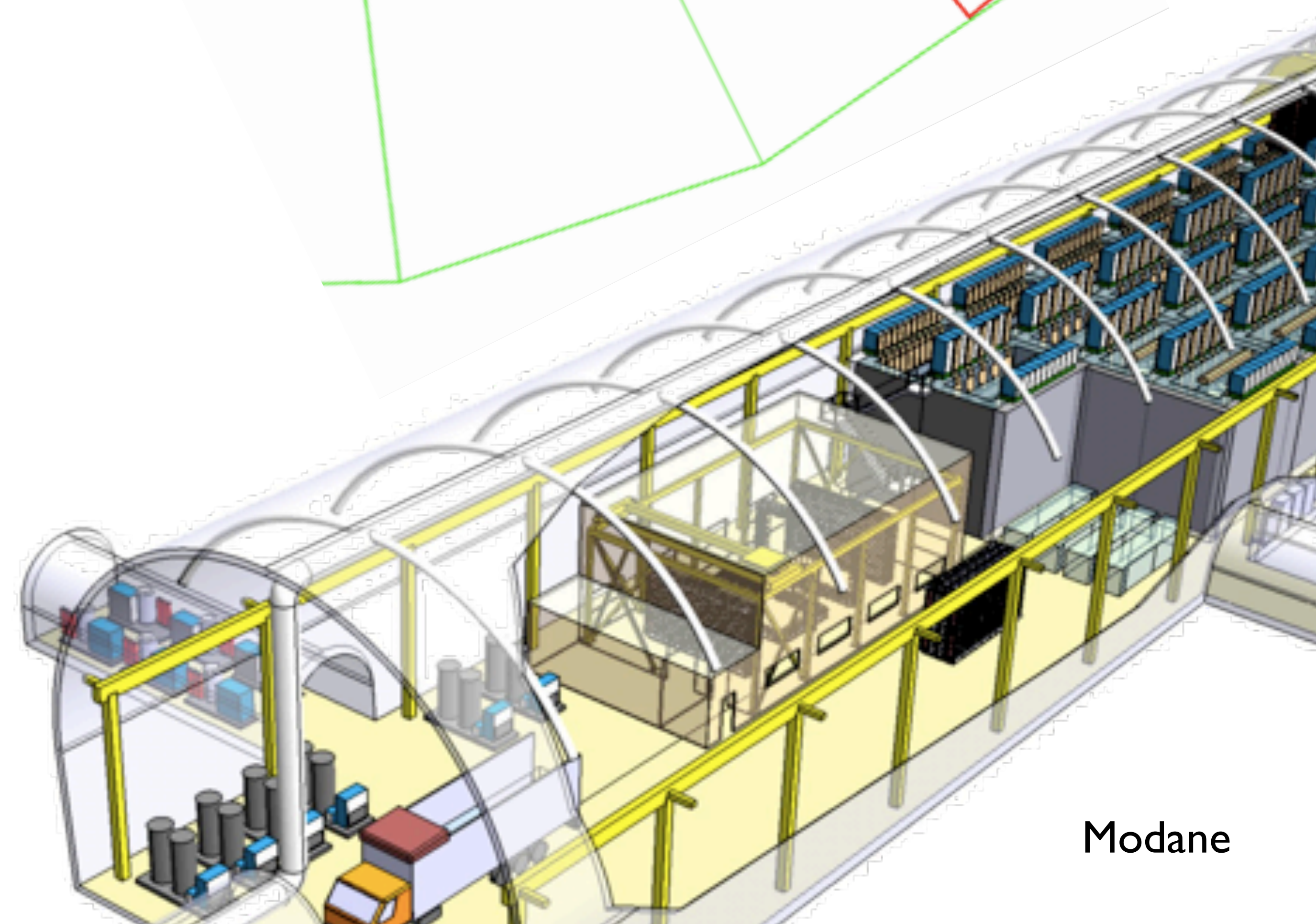

CUORE

Tellurium oxide bolometers

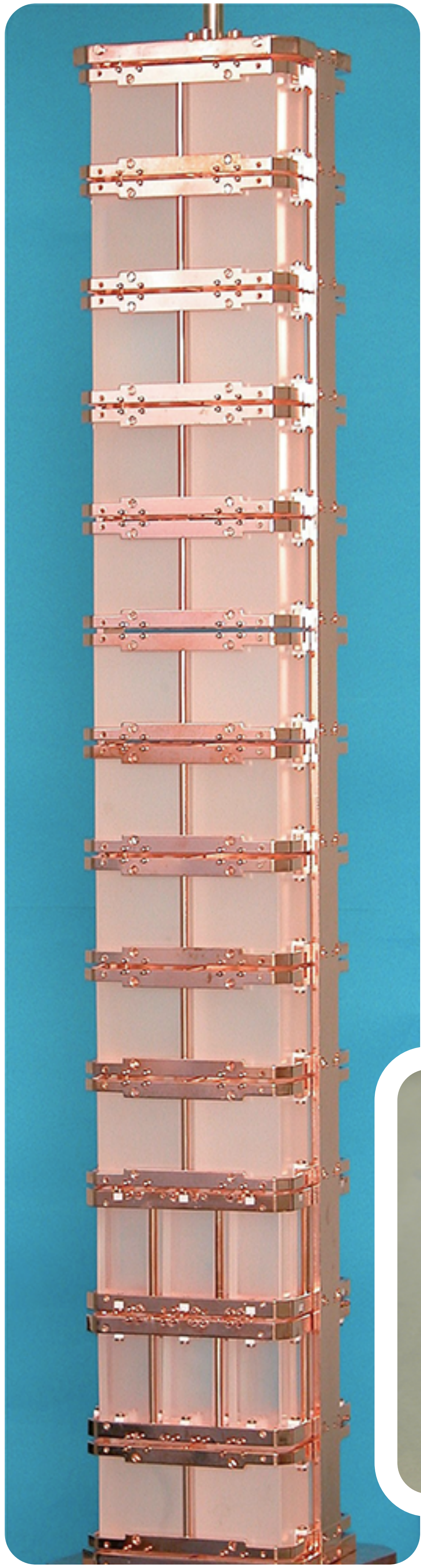

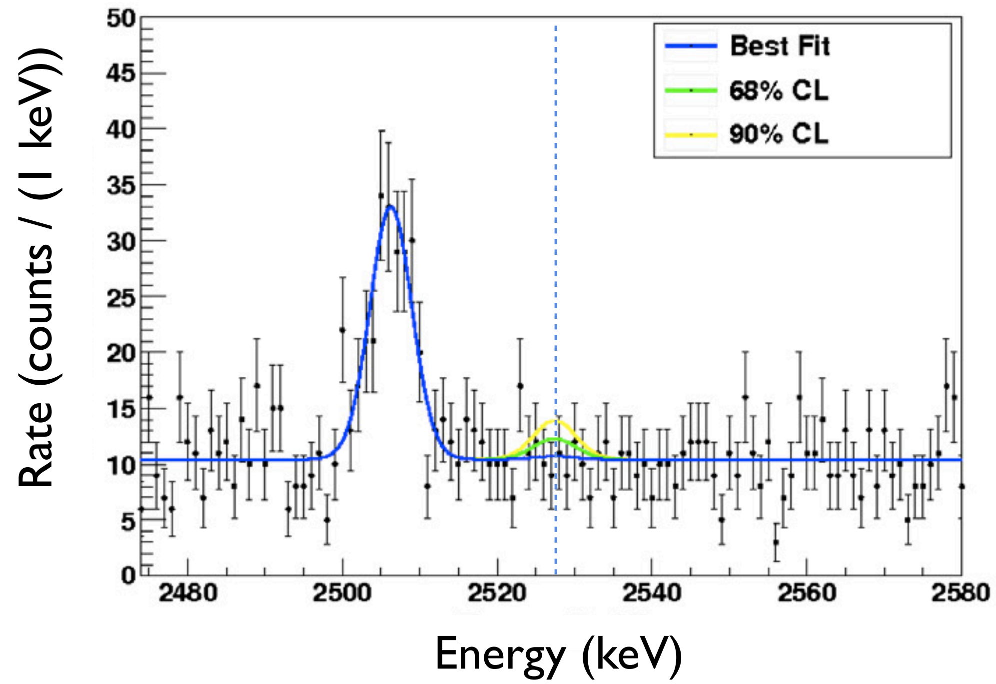

$$T^{0\nu}_{1/2} \geq 2.8 \times 10^{24}\,\mathrm{y}\,(90\%\,\mathrm{c.l.})$$

$$\langle m_{\beta\beta} \rangle < 300 - 710\,\mathrm{meV}$$

Andreotti, E., Astropart. Phys.. **34**, 822 (2011).

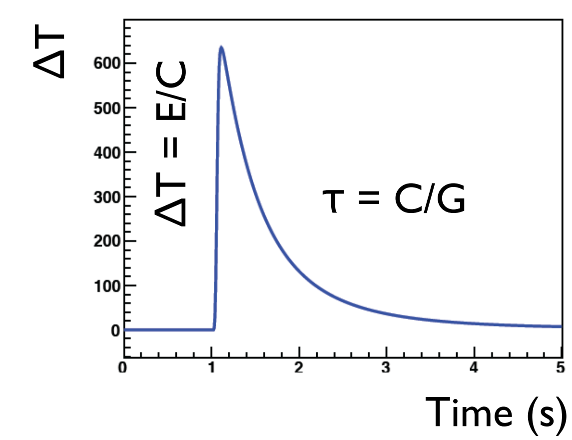

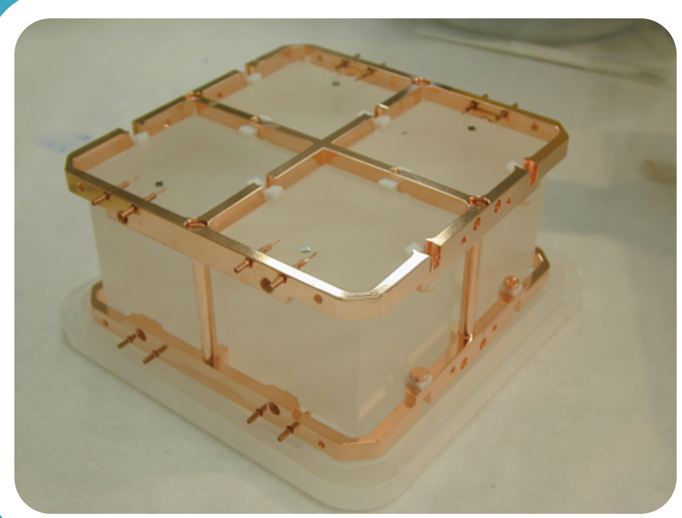

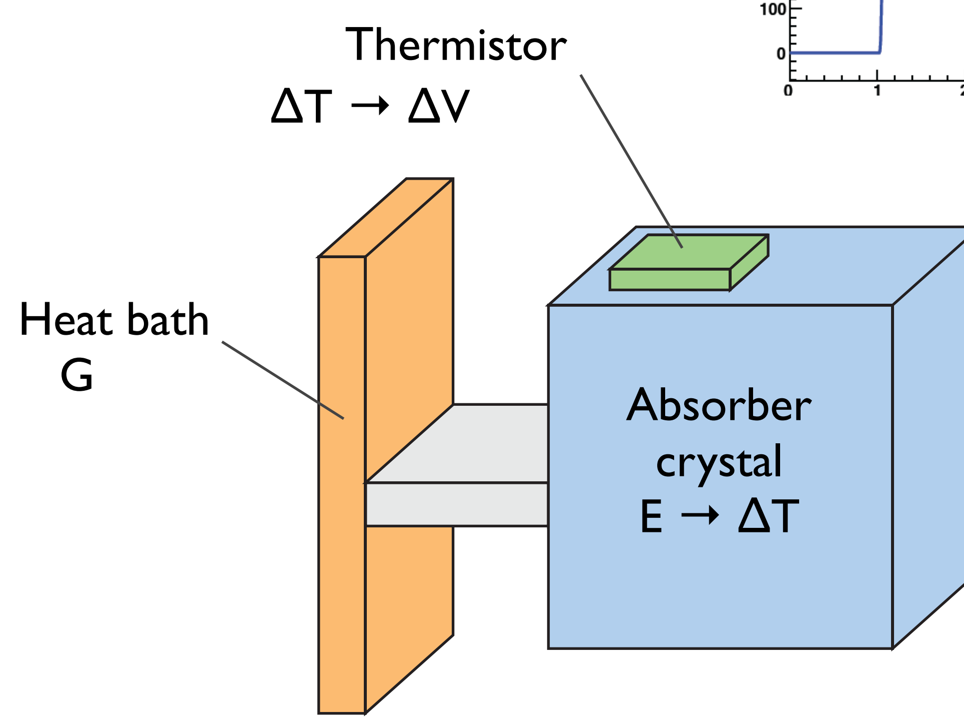

The germanium experiments

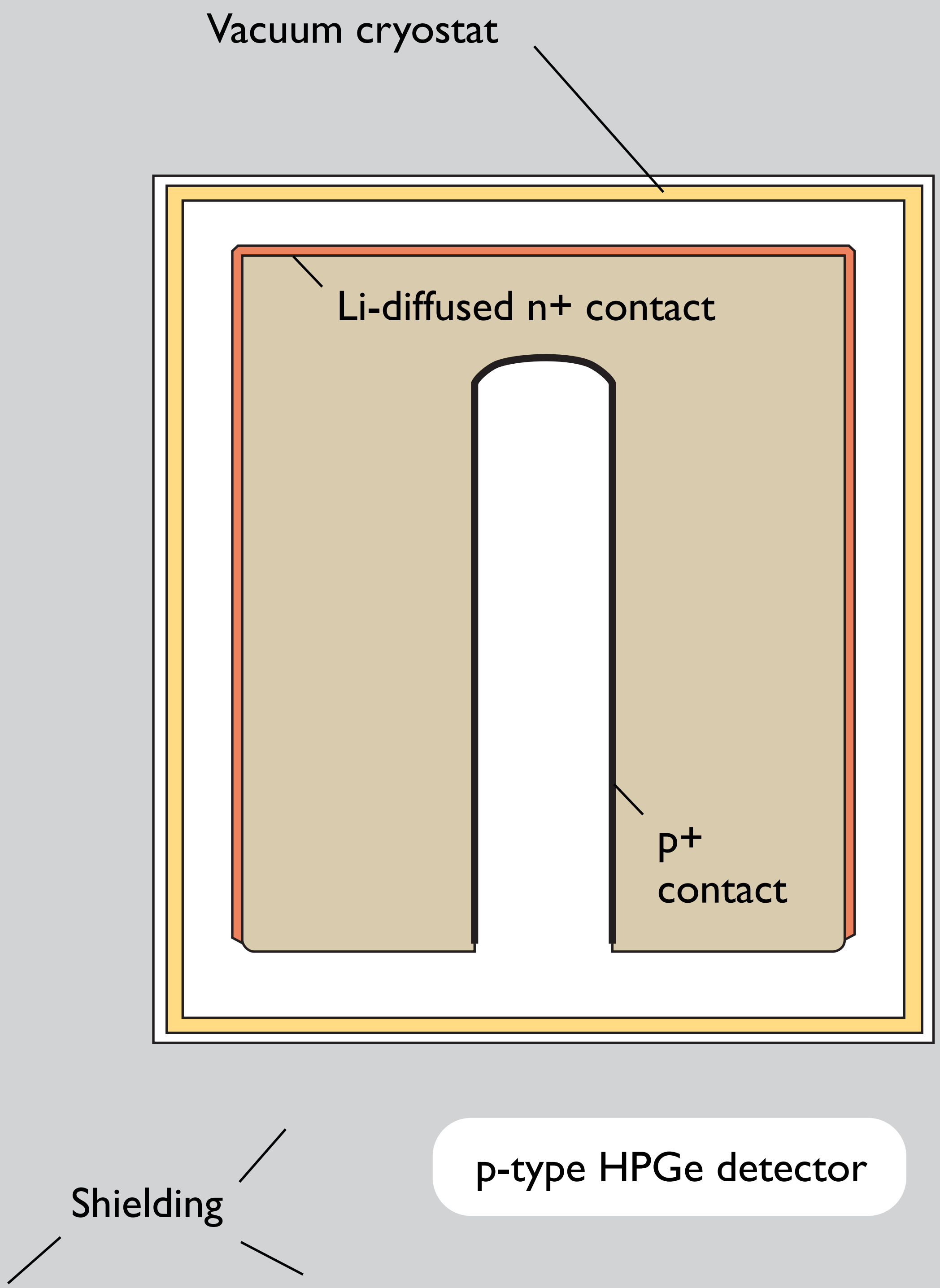

HPGe detectors are an excellent way to search for $0\nu\beta\beta$

- Off-the-shelf technology
- Integrated ^{76}Ge source

  7.8% in natural natural Ge (& enrichable)

- Excellent energy resolution

  $\Delta E_{FWHM} = 0.16\%$ @ $Q_{\beta\beta}$ (2.039 MeV)

The best current limits come from Ge experiments

Two experiments

Heidelberg-Moscow

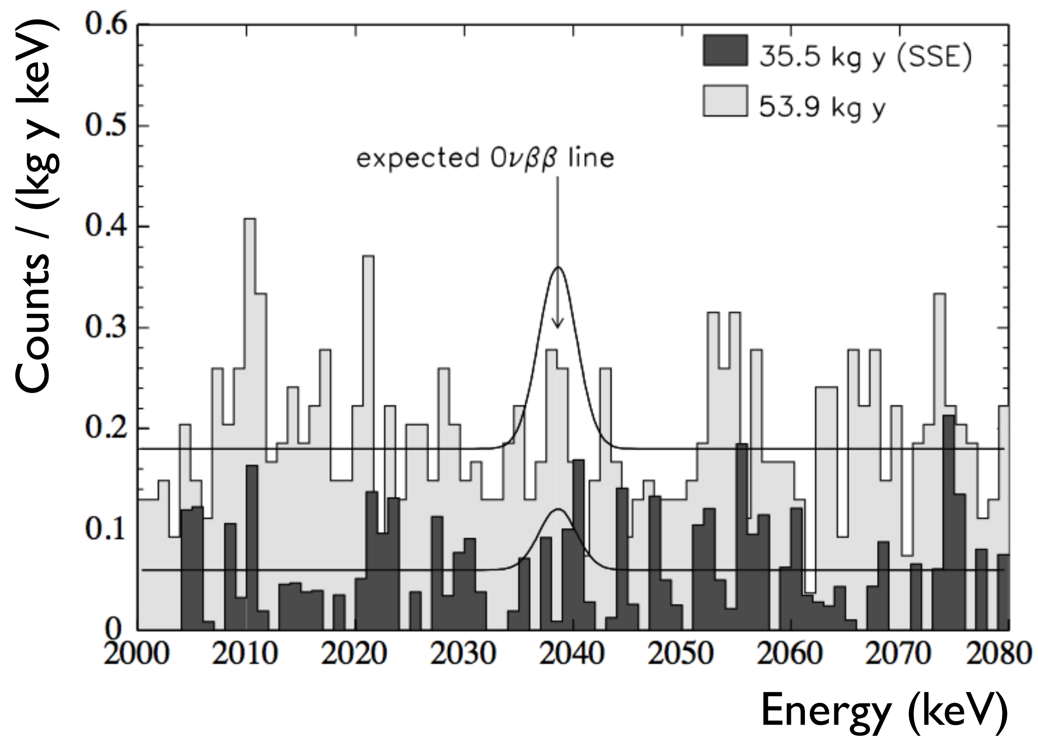

H.V. Klapdor-Kleingrothaus et al., Eur. Phys. J. A **12,** 147-154 (2001).

71.7 kg × y exposure
0.19 ± 0.01 cts / keV·kg·y

$$T_{1/2} > 1.9 \times 10^{25}\,\mathrm{y}\ (90\%\ \mathrm{c.l.})$$

IGEX

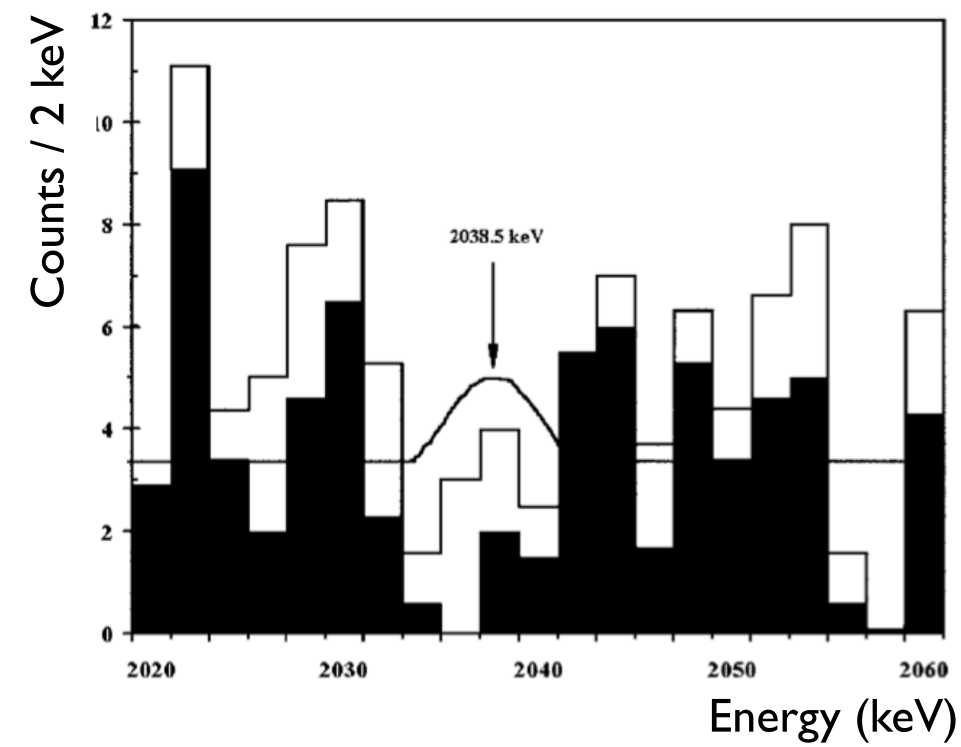

C.E. Aalseth et al., Phys. Rev. D **65,** 092007 (2002).

8.9 kg × y exposure
0.26 ± 0.10 cts / keV·kg·y

$$T_{1/2} > 1.6 \times 10^{25}\,\mathrm{y}\ (90\%\ \mathrm{c.l.})$$

Heidelberg-Moscow

The Claim

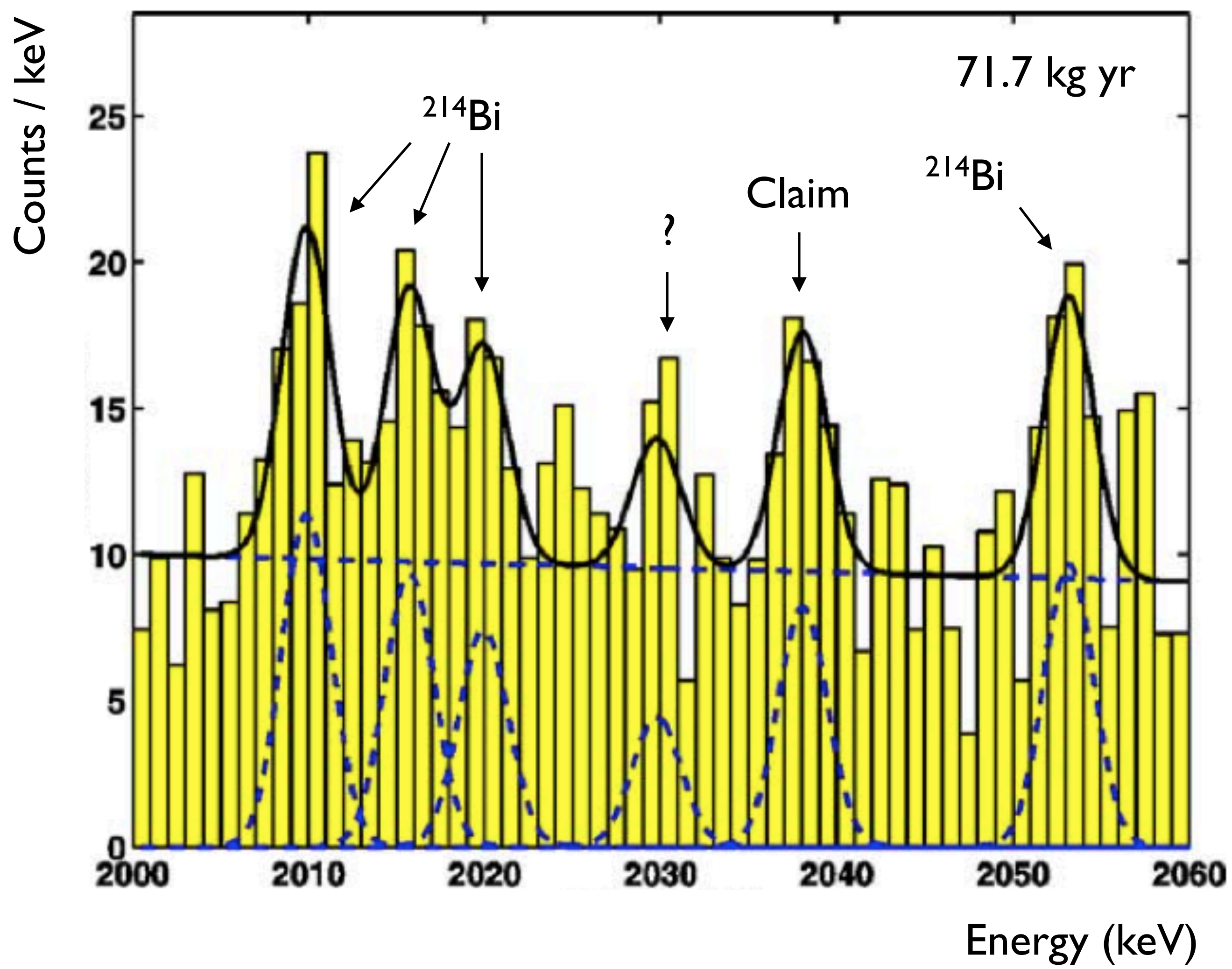

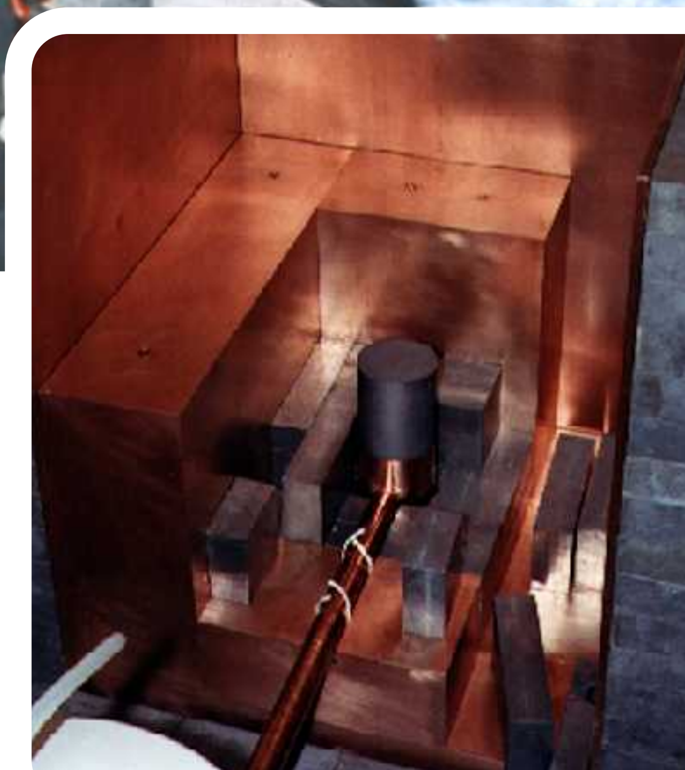

$$T^{0\nu}_{1/2} = (2.23^{+0.44}_{-0.31}) \times 10^{25}\,\mathrm{y}$$

$$\langle m_{\beta\beta} \rangle \sim 300\,\mathrm{meV}$$

5 p-type enriched coaxial HPGe detectors

Stronger claim with more recent PSA: Klapdor-Kleingrothaus, H.V. et al., Mod. Phys. Lett. A **21**, 1547 (2006).

Backgrounds

+ Irreducible $2\nu\beta\beta$
+ Neutrino scattering

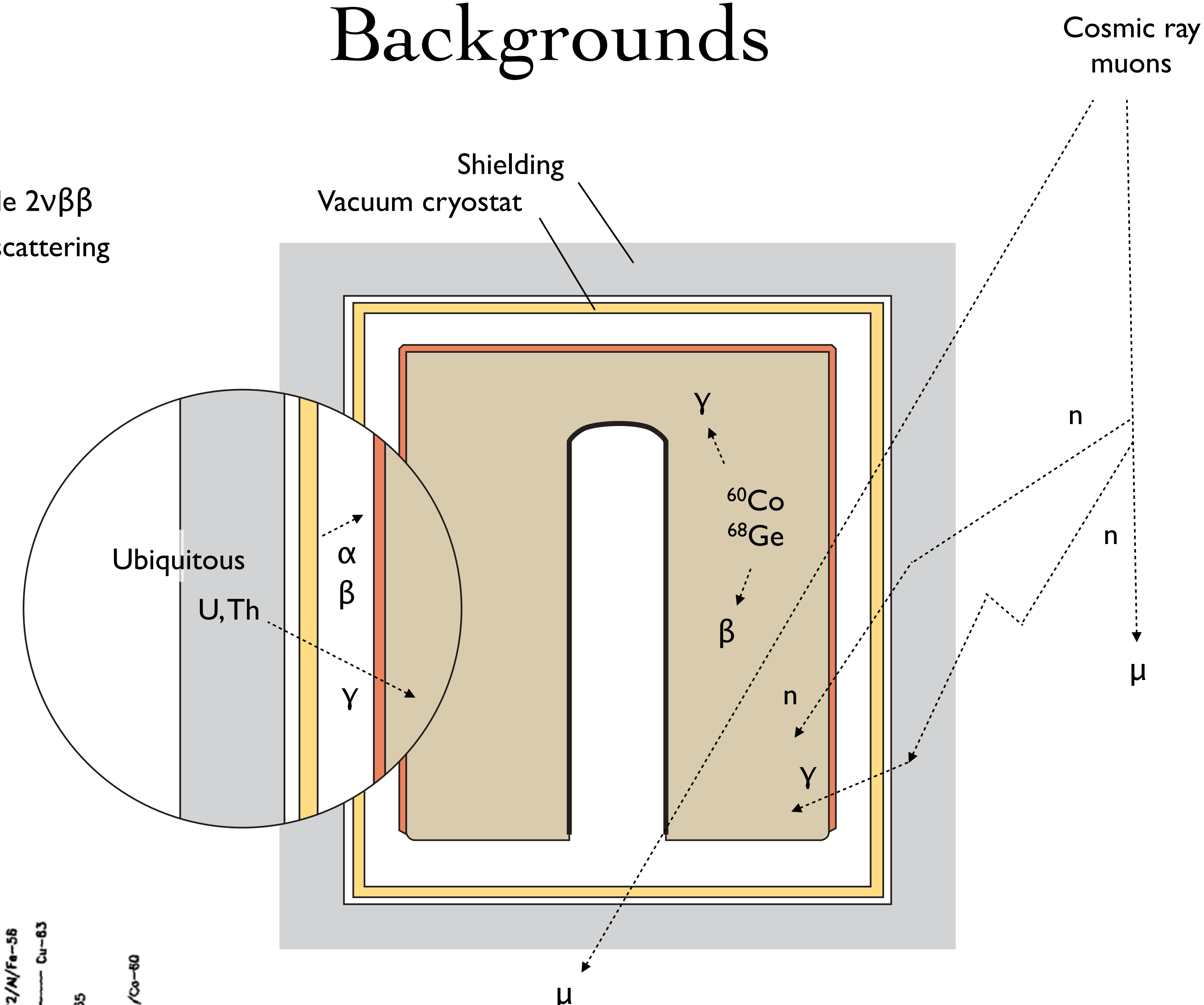

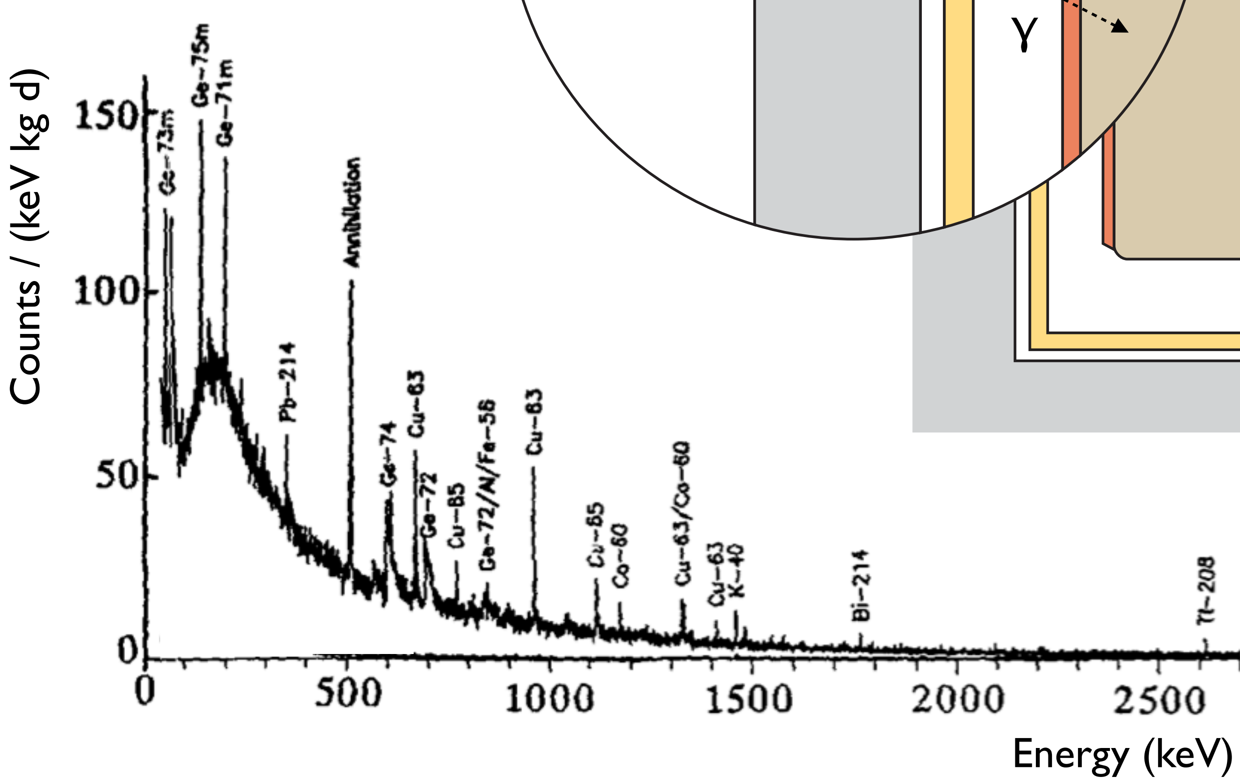

H-M - copper mounts, cryostat

IGEX - radon & cosmogenics

GERDA & MAJORANA

Next generation germanium

GERDA

Naked diodes in liquid argon

MAJORANA

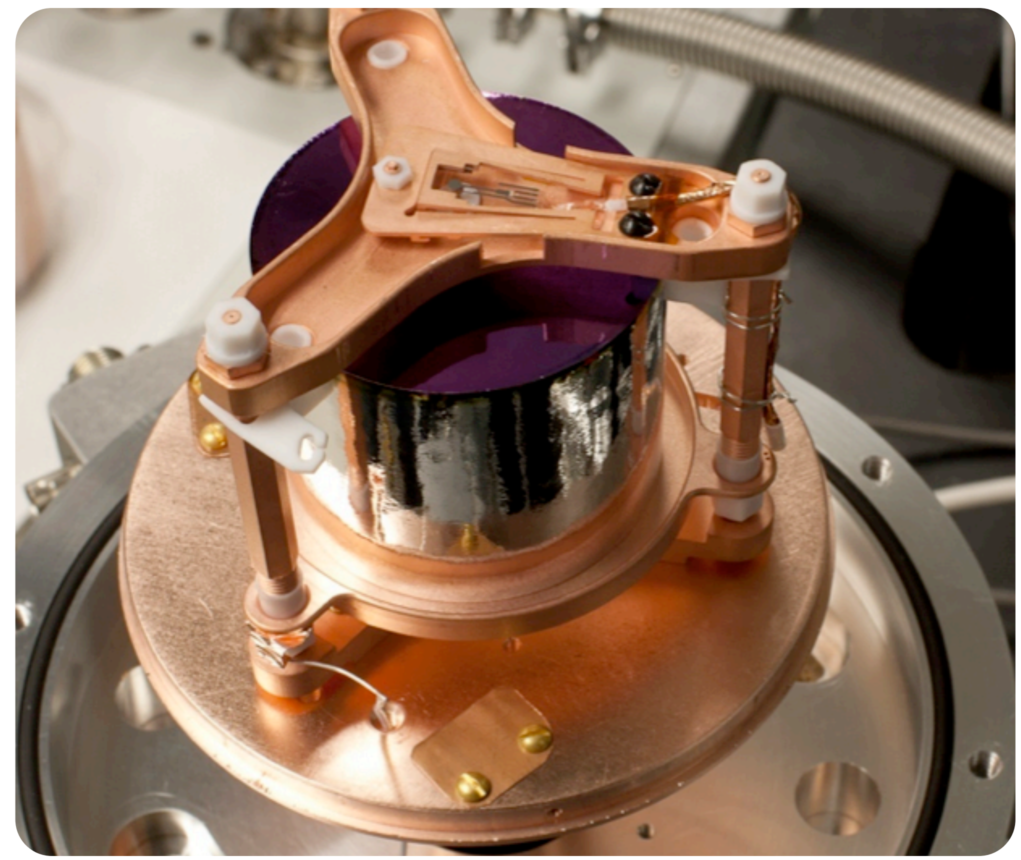

Diodes in vacuum cryostats

Cooperation and an understanding to merge for the tonne-scale

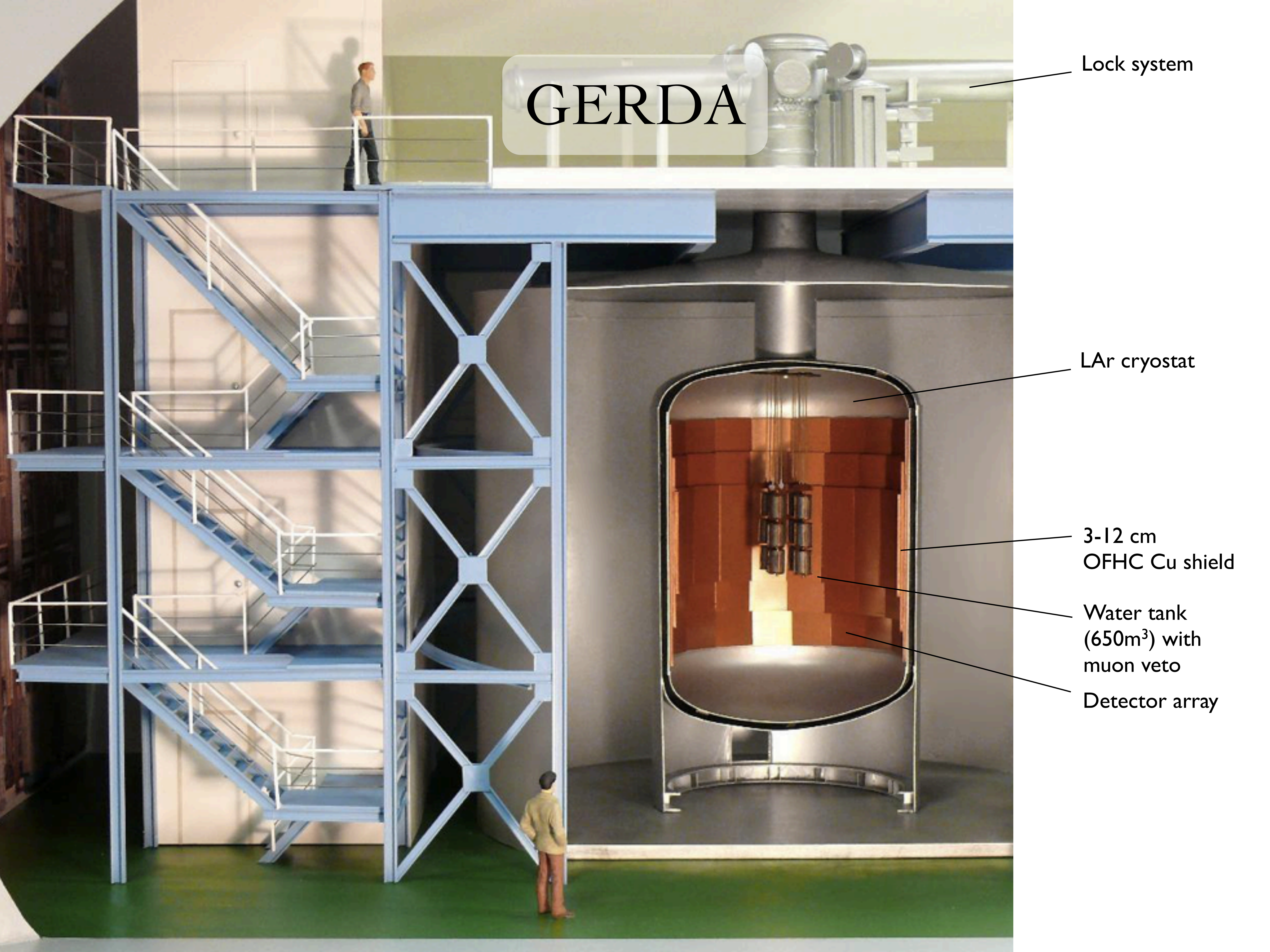
GERDA
Lock system
LAr cryostat
3-12 cm
OFHC Cu shield
Water tank
(650m³) with
muon veto
Detector array

GERDA

Phase I

Enriched detectors from H-M and IGEX

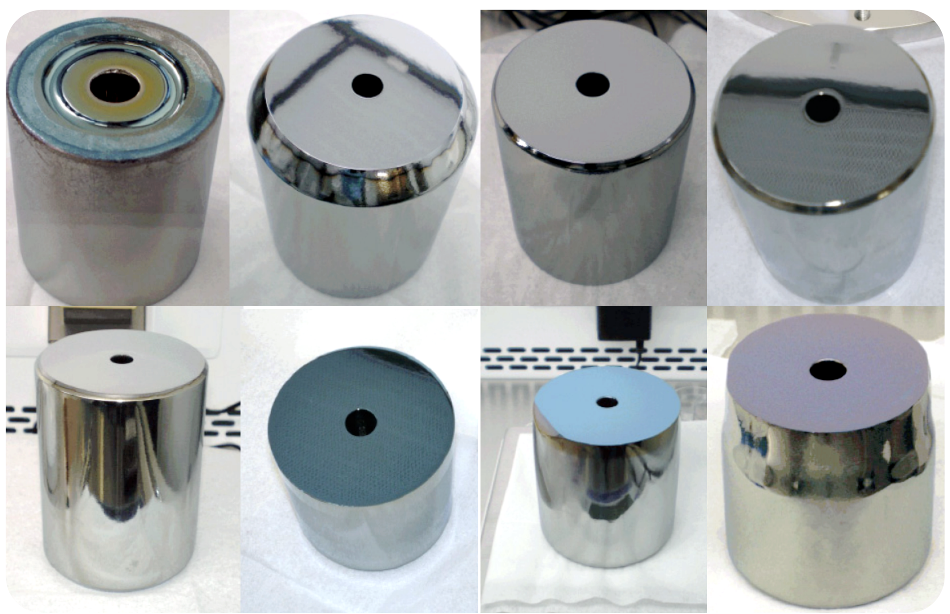

17.66 kg total

+ natural detectors

Deployed Nov 1st 2011 & taking data

Background substantially improved compared to H-M

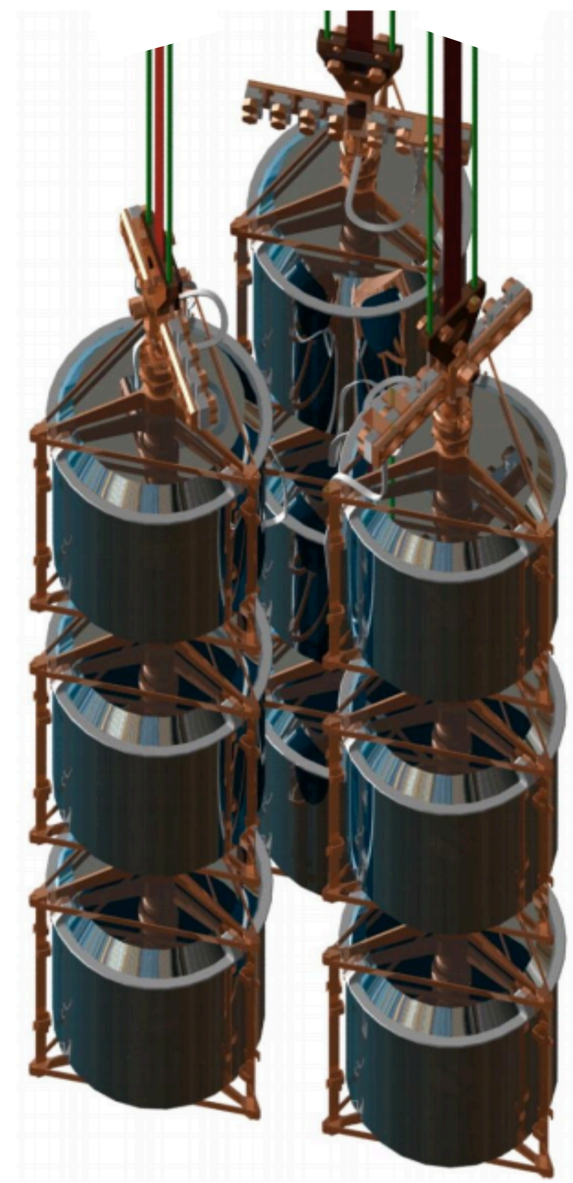

GERDA

Phase I

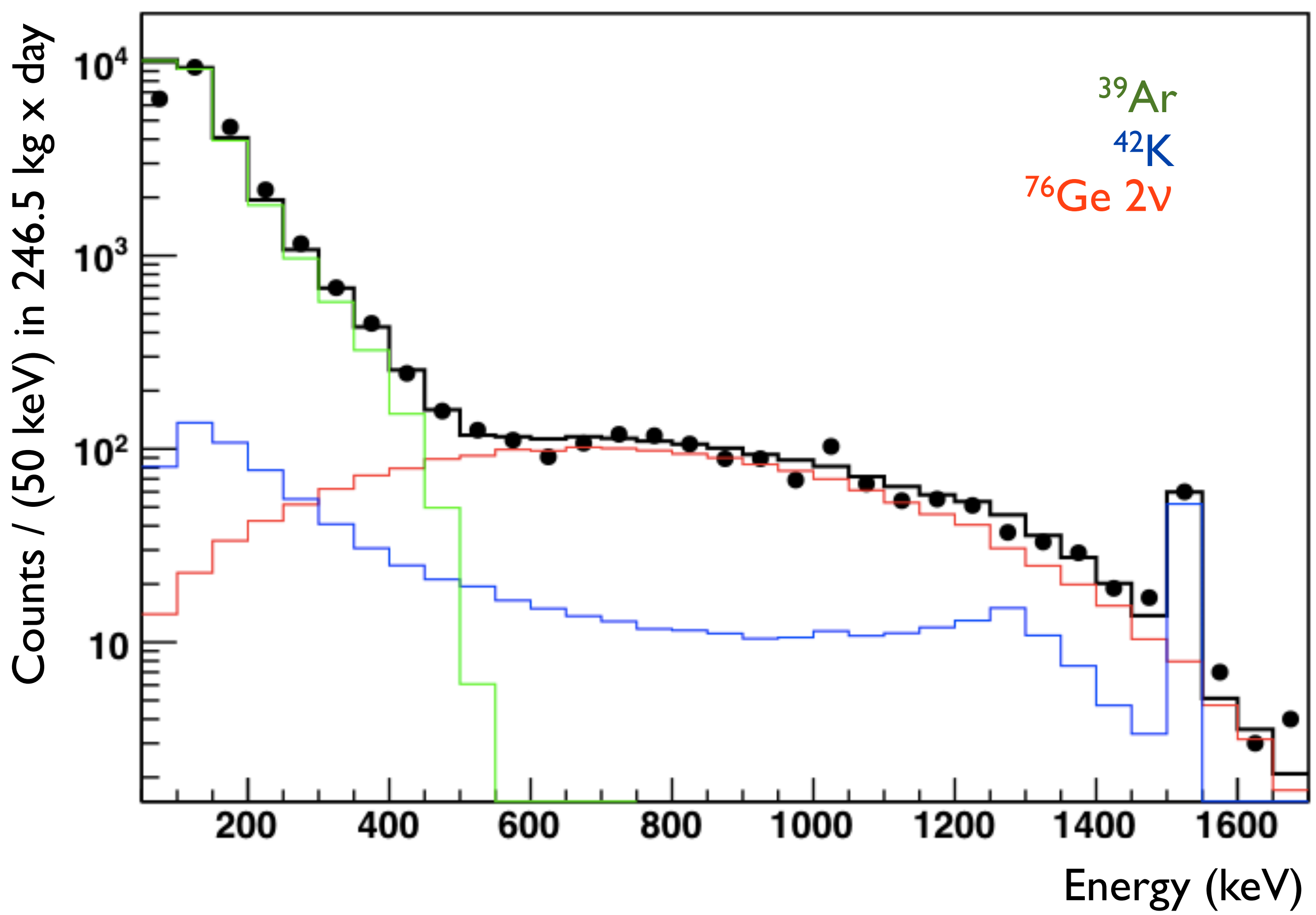

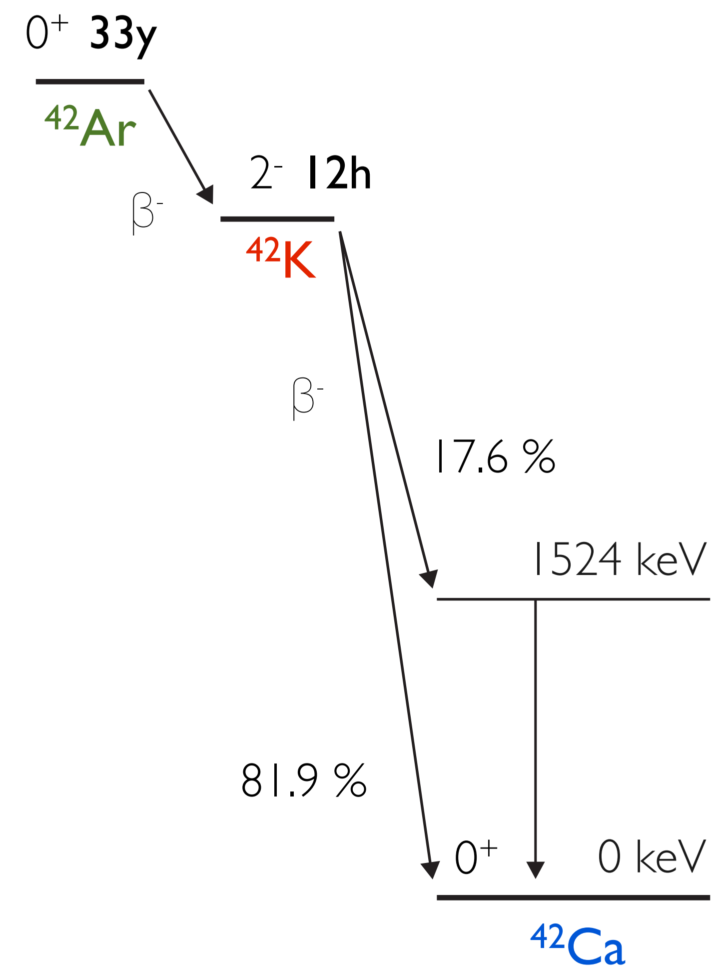

Expect the unexpected in a new type of experiment

GERDA

Phase I

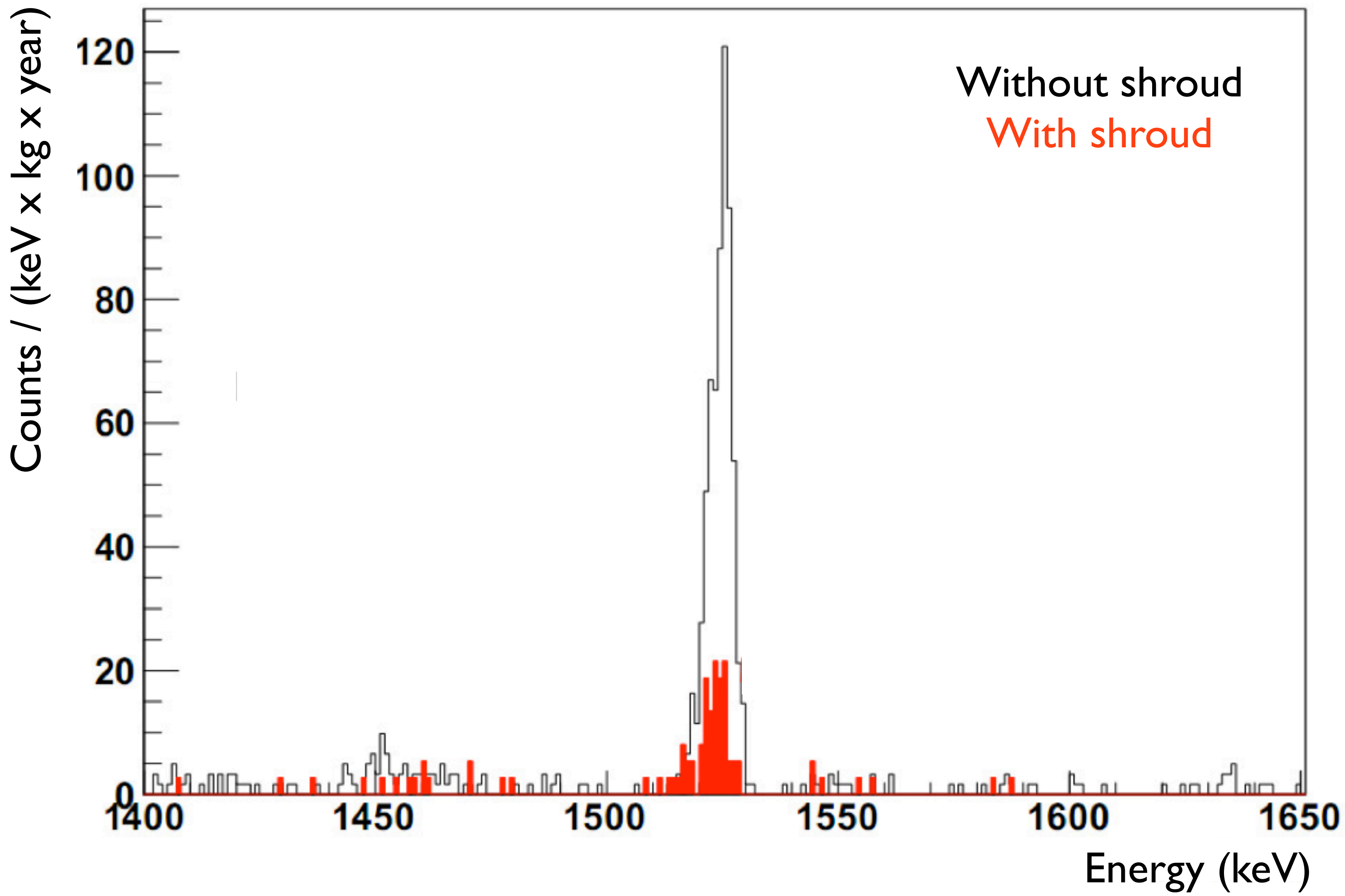

Expect the unexpected in a new type of experiment

MAJORANA

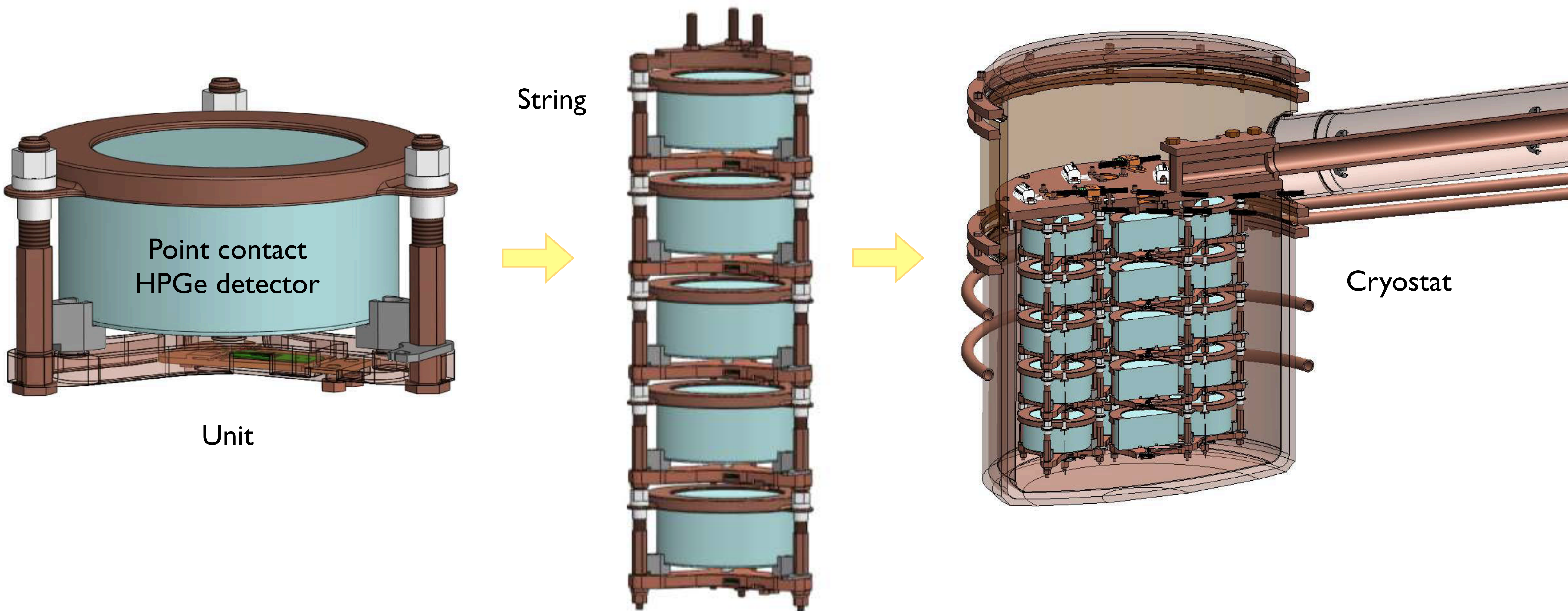

Technical

- Demonstrate backgrounds low enough to justify a tonne-scale Ge experiment
- Establish feasibility of constructing and fielding modular arrays of Ge detectors

Science goals

- Test the claim for observation of $0\nu\beta\beta$ in ^{76}Ge
- Exploit low-energy sensitivity to search for dark matter & axions

Majorana

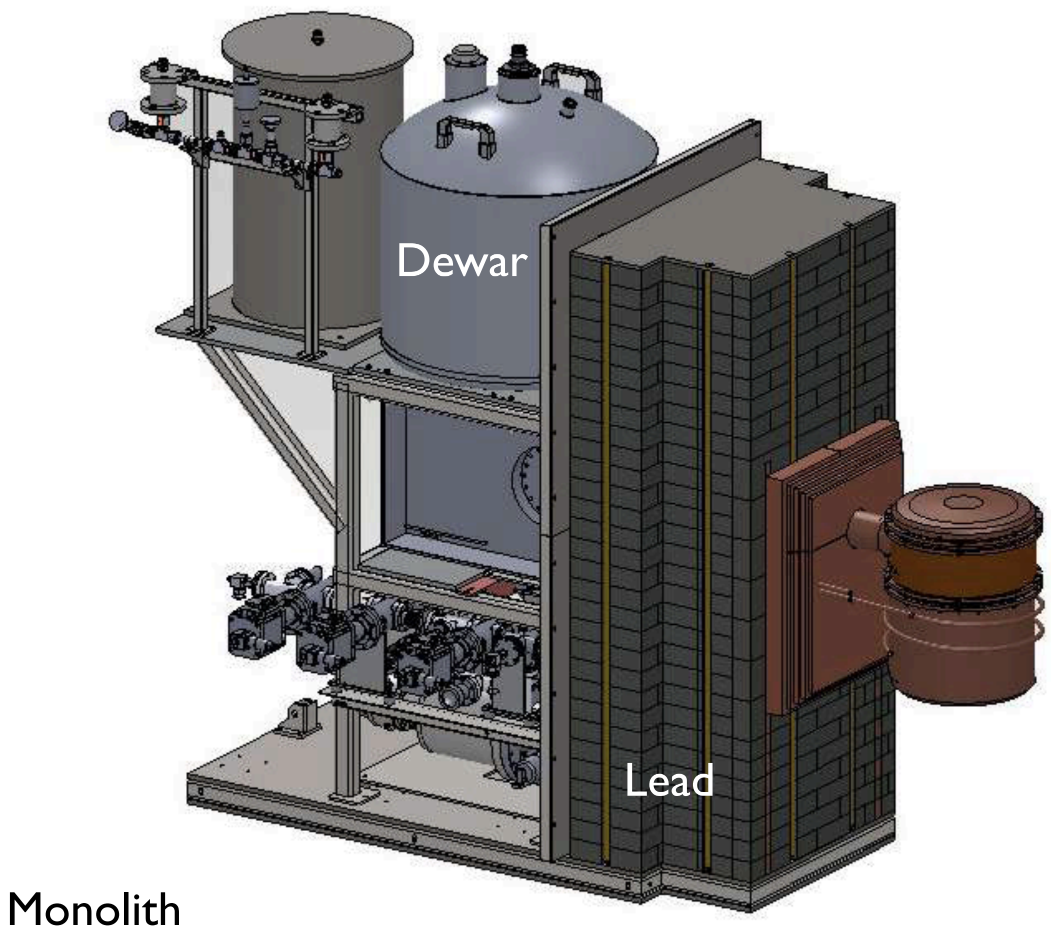

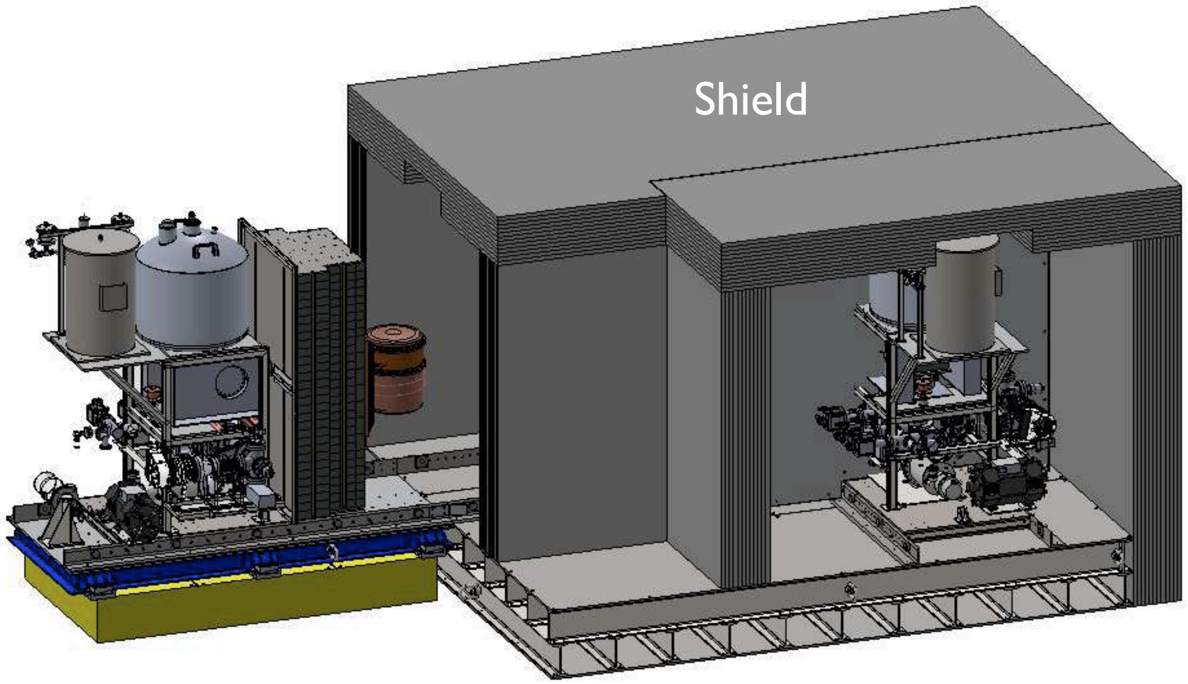

Technical

- Demonstrate backgrounds low enough to justify a tonne-scale Ge experiment
- Establish feasibility of constructing and fielding modular arrays of Ge detectors

Science goals

- Test the claim for observation of $0\nu\beta\beta$ in ^{76}Ge
- Exploit low-energy sensitivity to search for dark matter & axions

MAJORANA

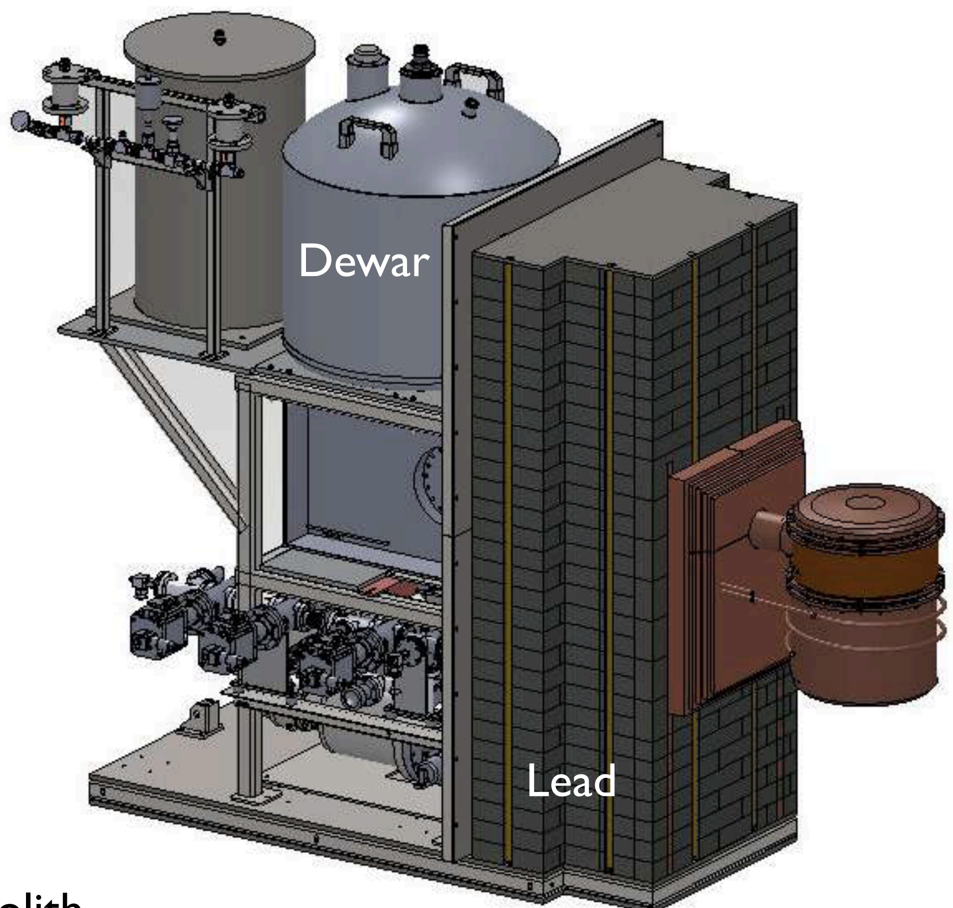

Monolith

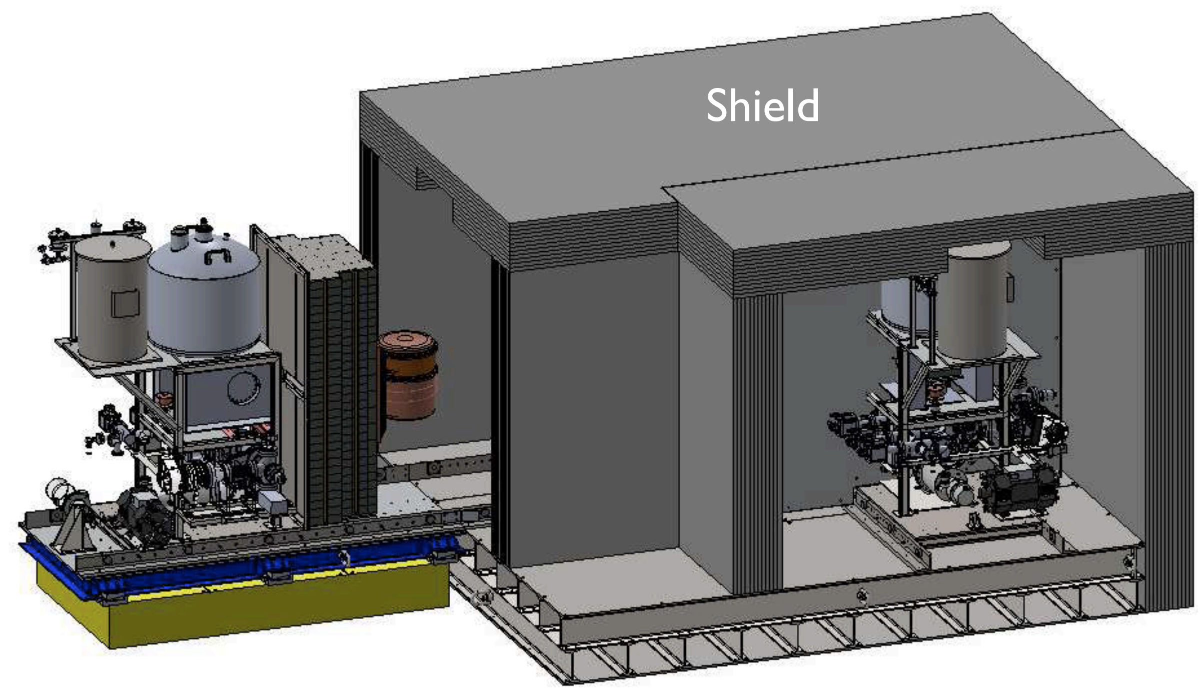

Three phase implementation

Prototype cryostat (2 strings ^{nat}Ge)	**Fall 2012**
Cryostat I (3 strings ^{enr}Ge, 4 string ^{nat}Ge)	**Fall 2013**
Cryostat II (up to 7 strings ^{enr}Ge)	**Fall 2014**

Backgrounds

Goal is ~ 3 counts/ROI/t/y

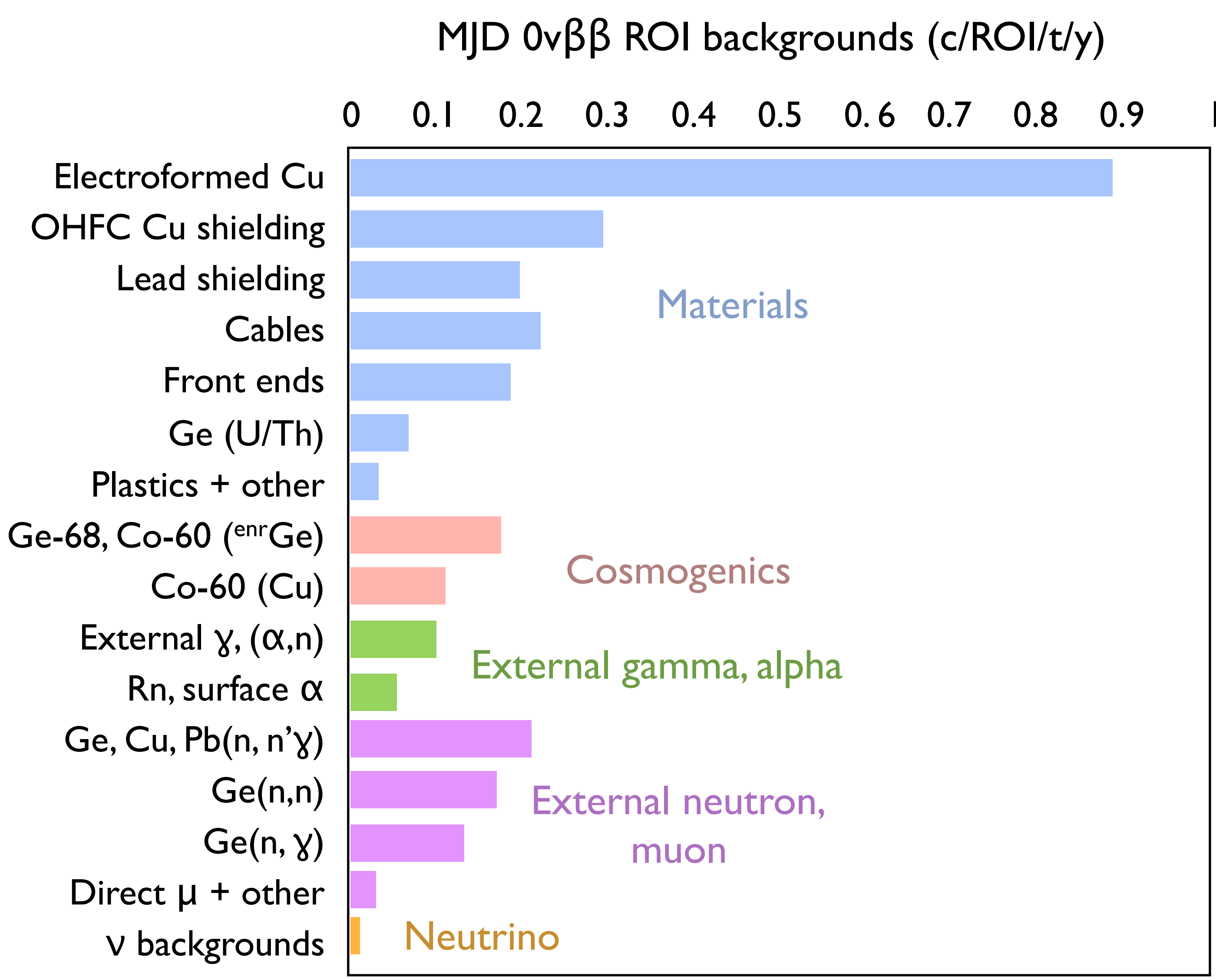

ROI = 4 keV region at 2039 keV

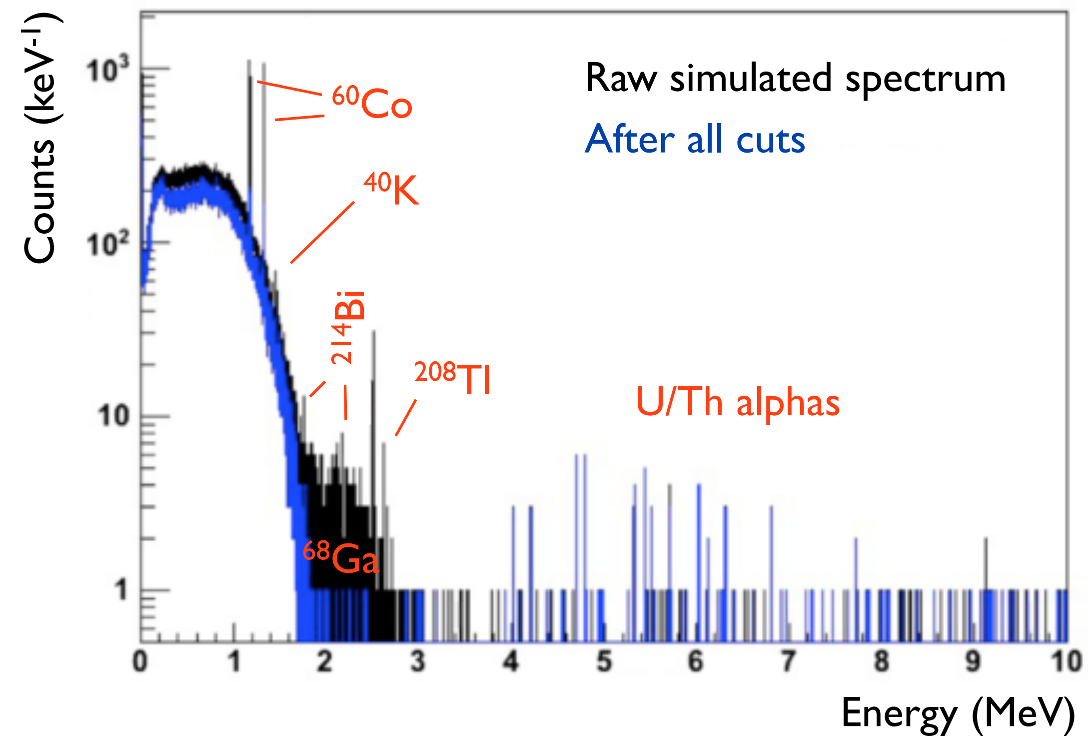

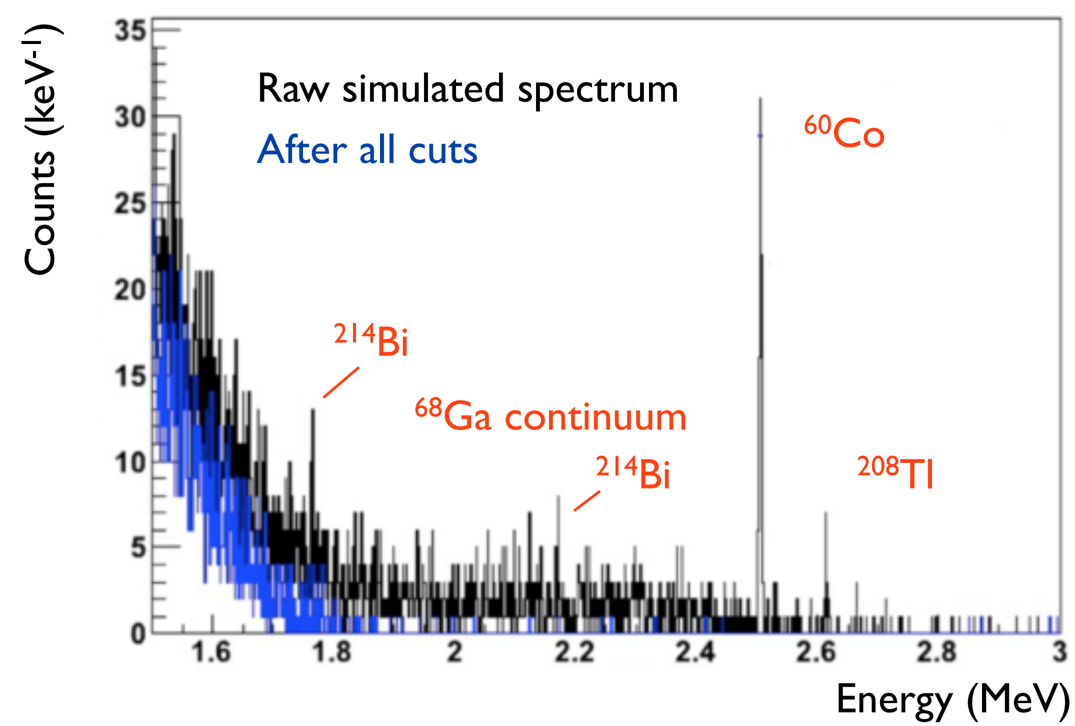

Davis Campus

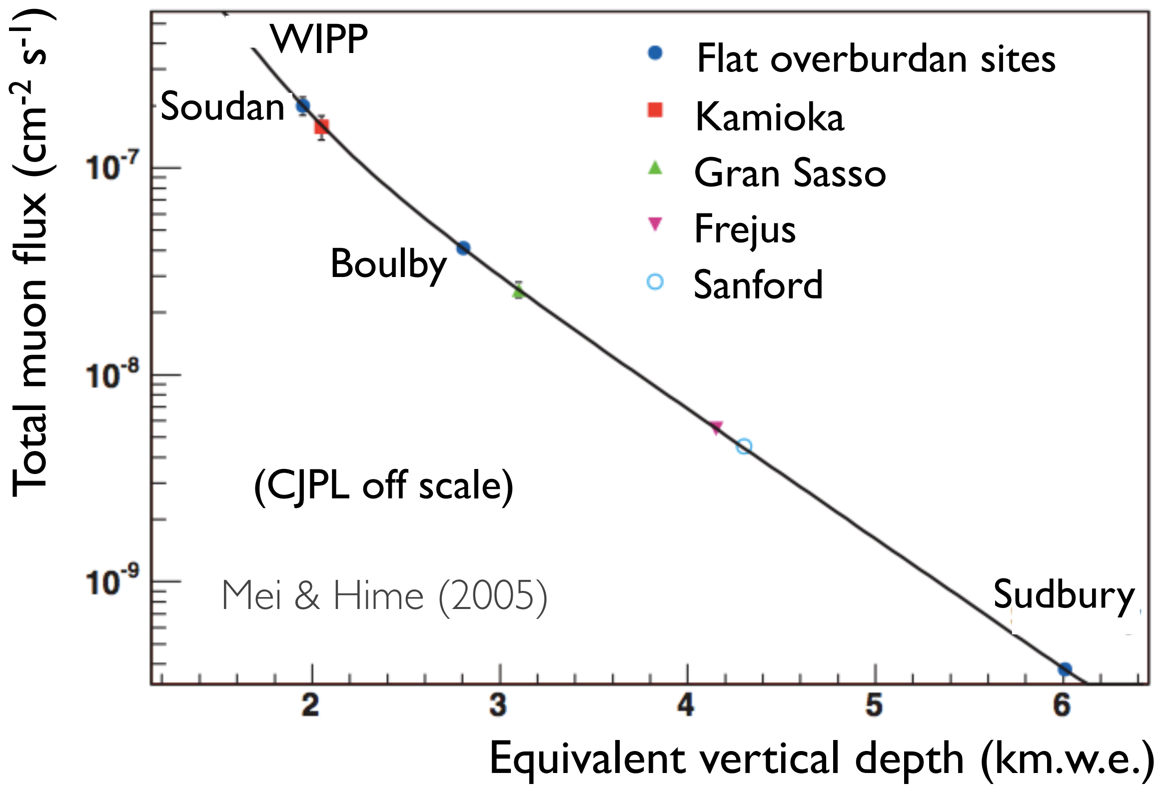

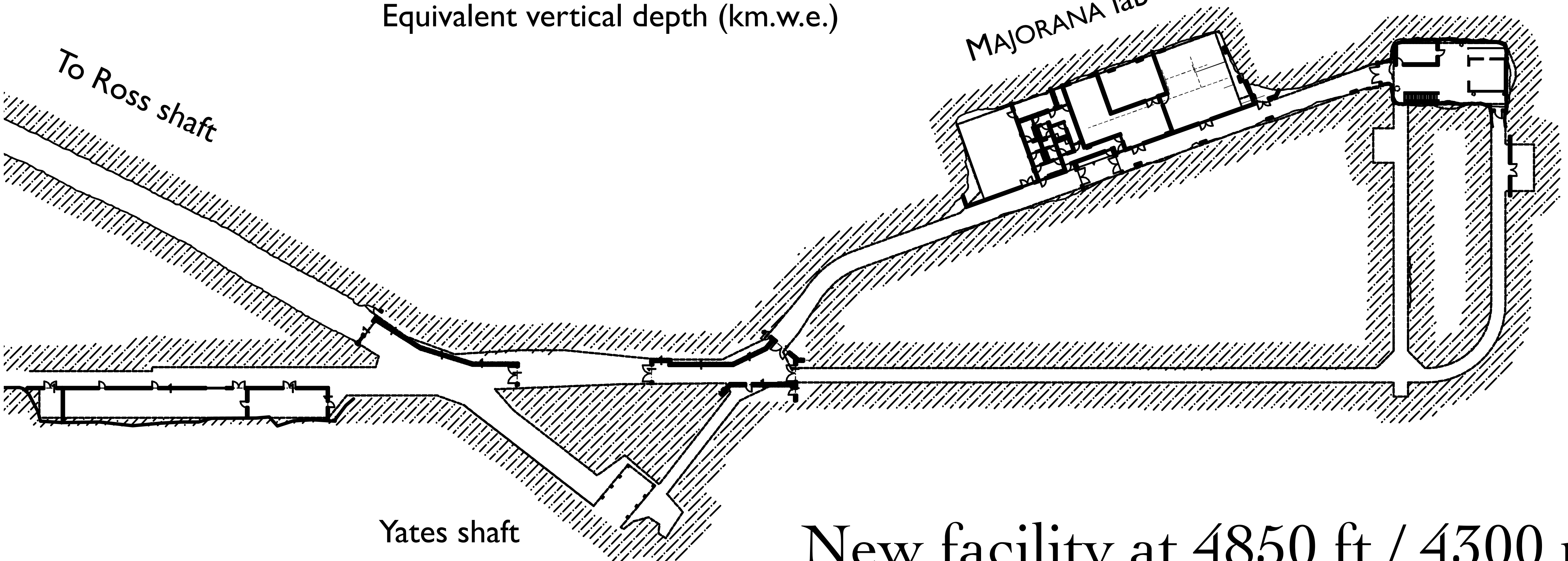

New facility at 4850 ft / 4300 m.w.e.

MAJORANA lab

Assembly room

Electroforming laboratory

Glovebox

Electroforming lab operational since mid-2011

Equipment currently being installed in assembly room

Copper

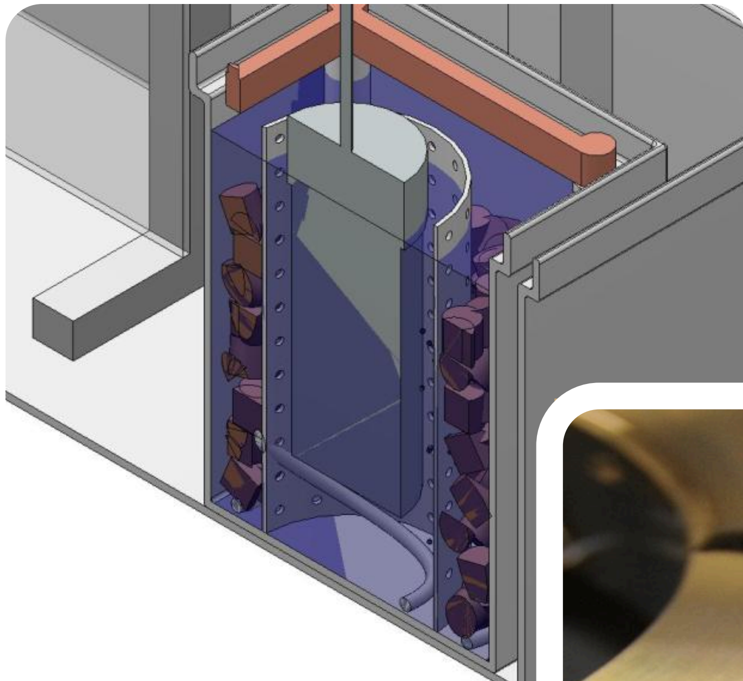

Growth at
70 um / day

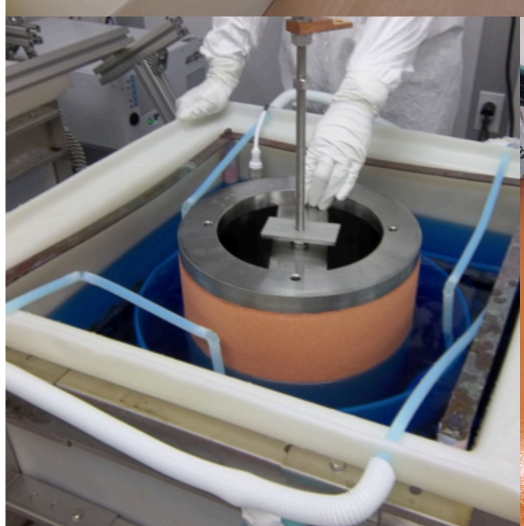

Demonstrated purity **< 1uBq / kg**

Goal **0.1-0.3 uBq / kg**

Ultra-clean copper parts made from electro-formed copper

Copper

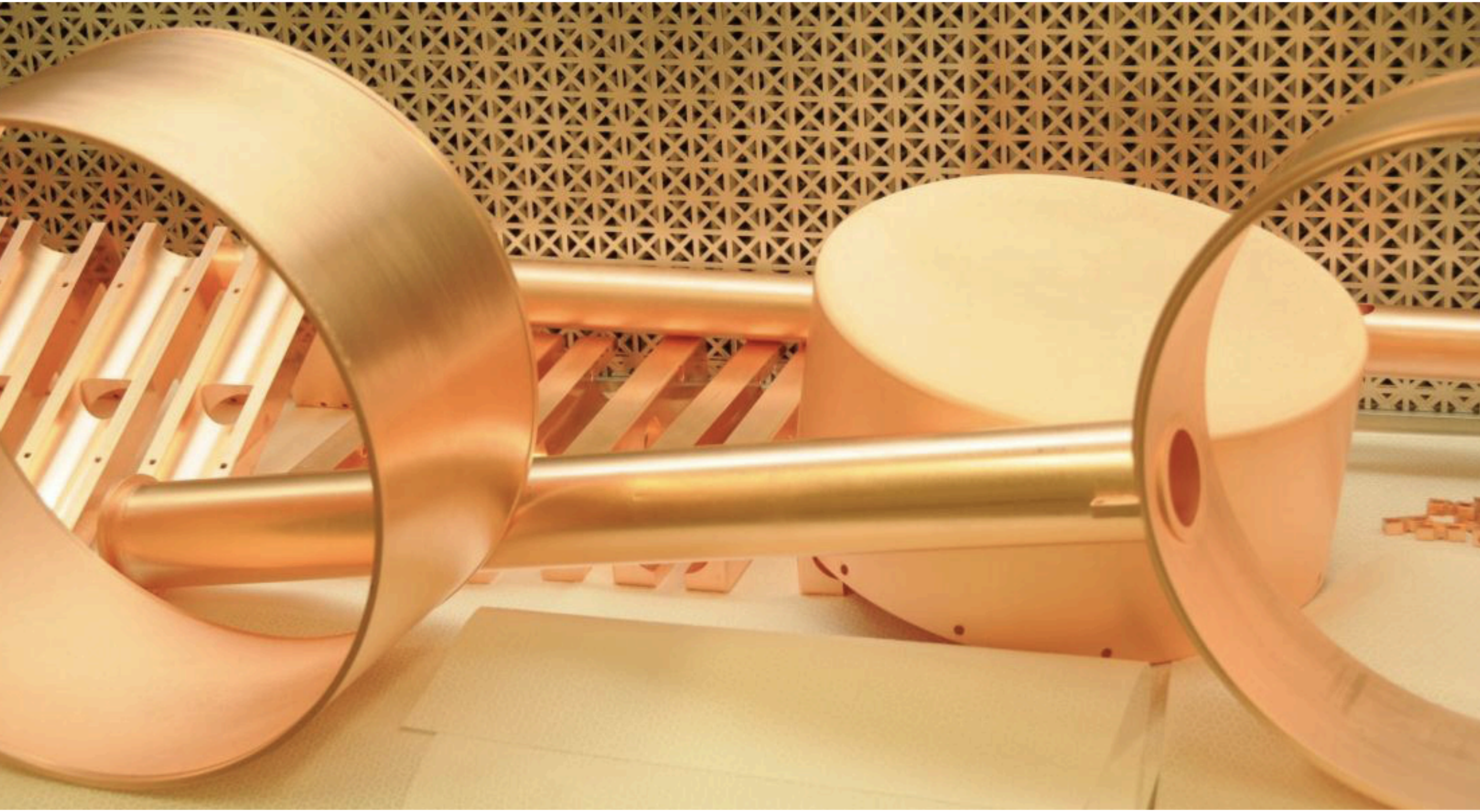

Detectors

Enriched material

Iron transportation container

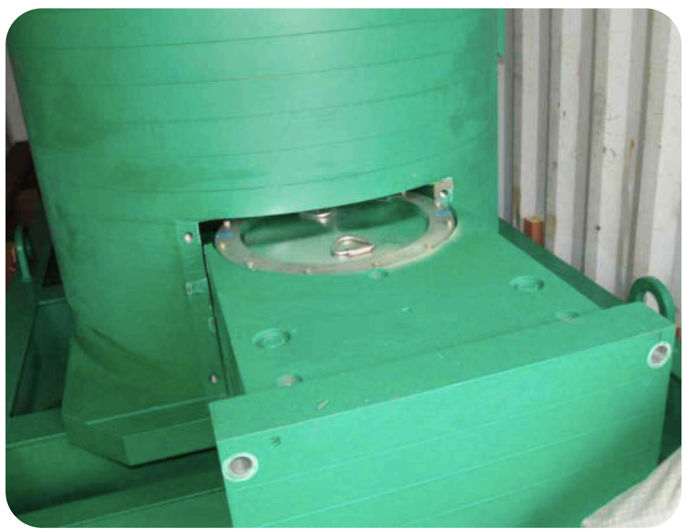

28.5 kg $^{enr}GeO_2$ delivered

Enrichment: 88%
Chemical purity: 99.98%

Enrichment removes cosmogenic isotopes

Including Ge-68

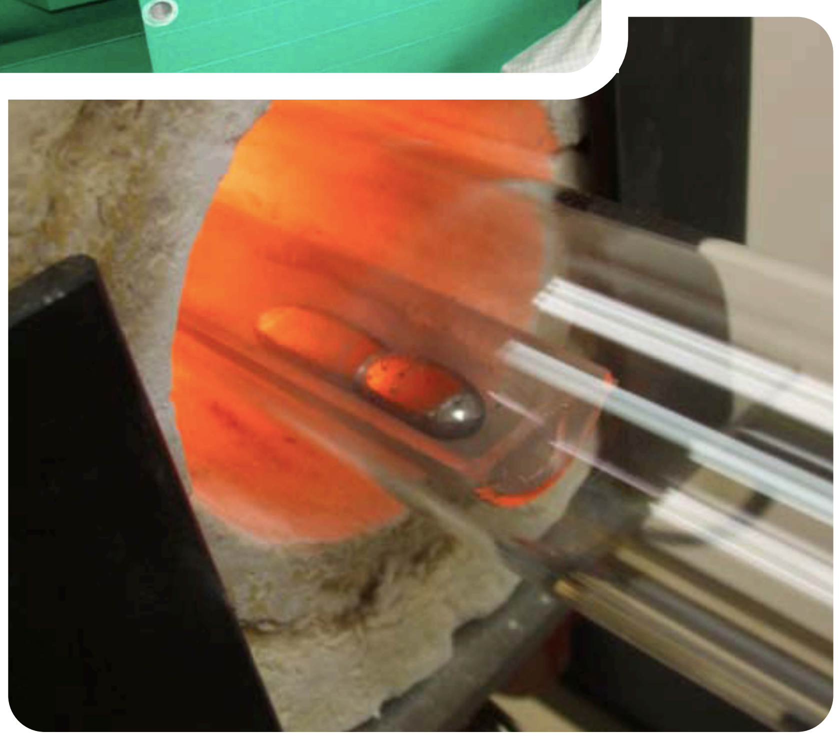

Reduction

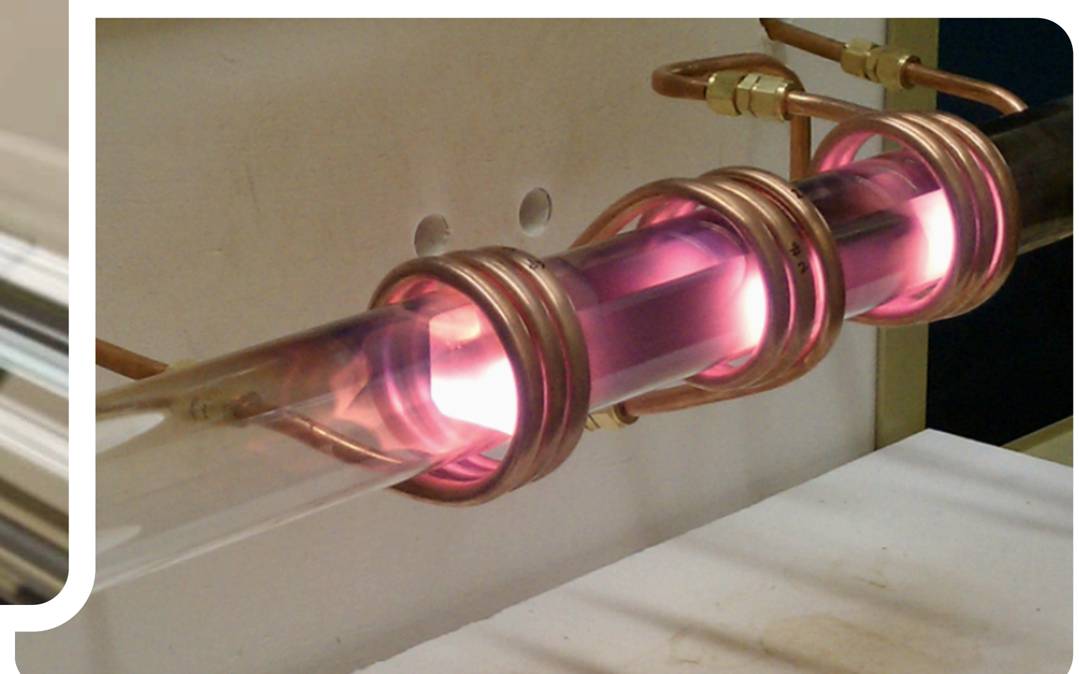

Zone refinement

Electronic-grade Ge

Detectors

Coaxial

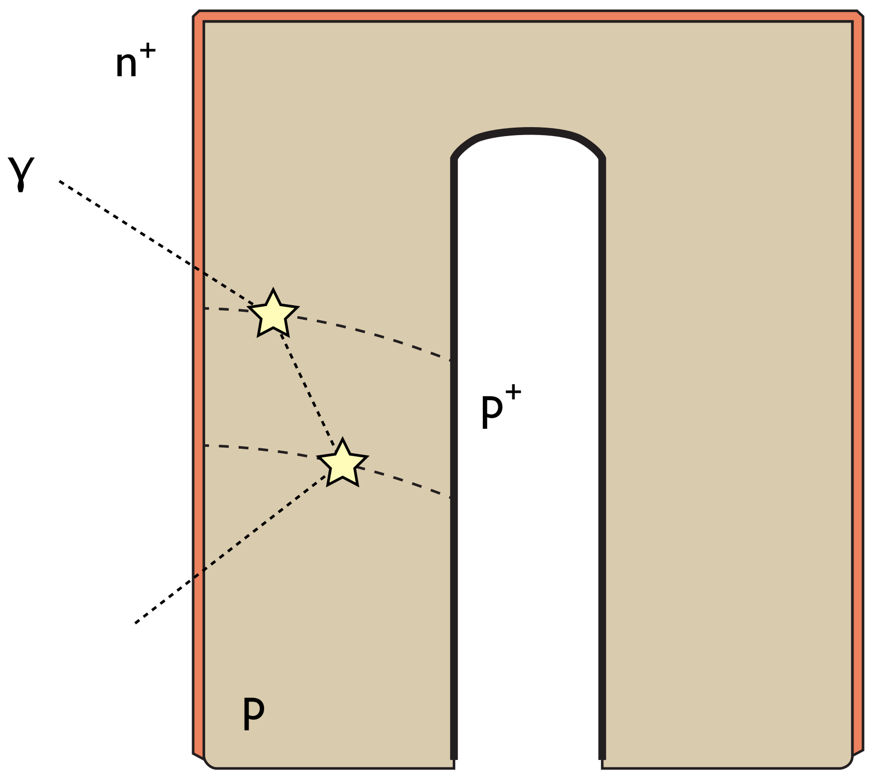

p-type coaxial

Point contact

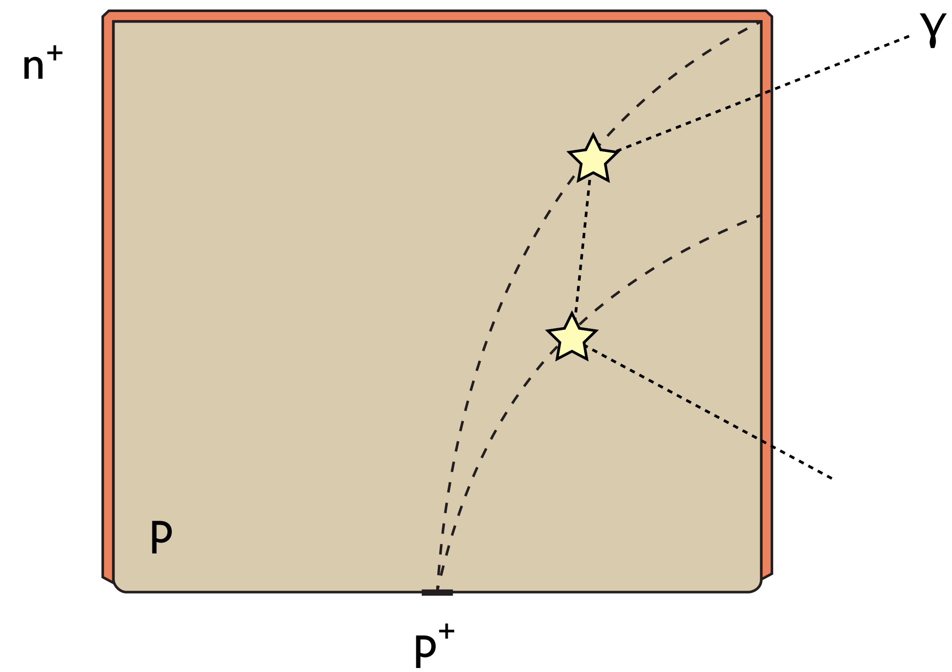

p-type point contact (PPC)

Low-capacitance

Peaked weighting fields

P. N. Luke et al., IEEE T. Nucl. Sci. **36** (1989) 926.

S. Barbeau et al., J. Cosmol. Astropart. Phys. **0709** (2007) 009.

Detectors

Single site

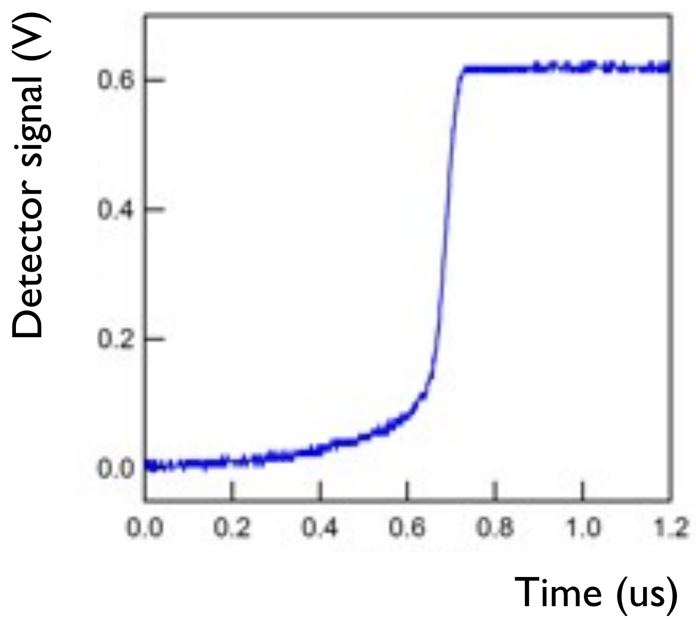

Such as 0νββ

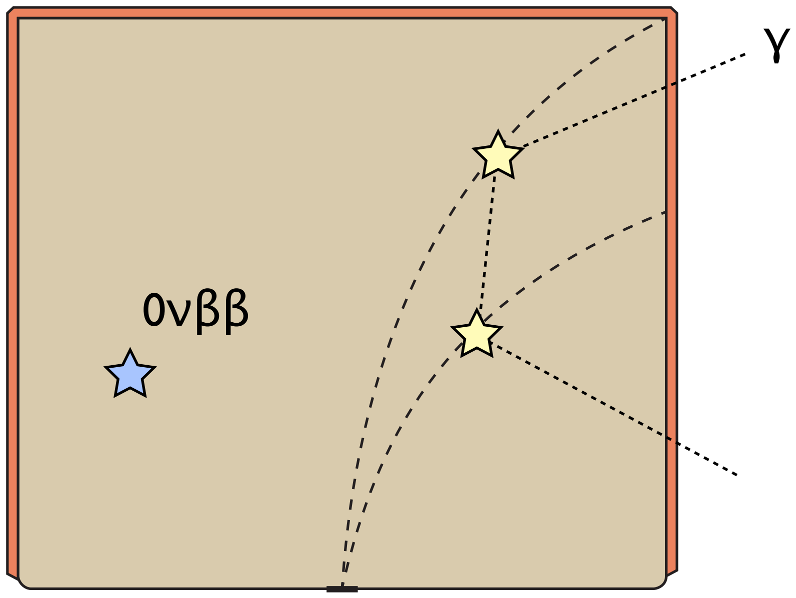

Multiple site

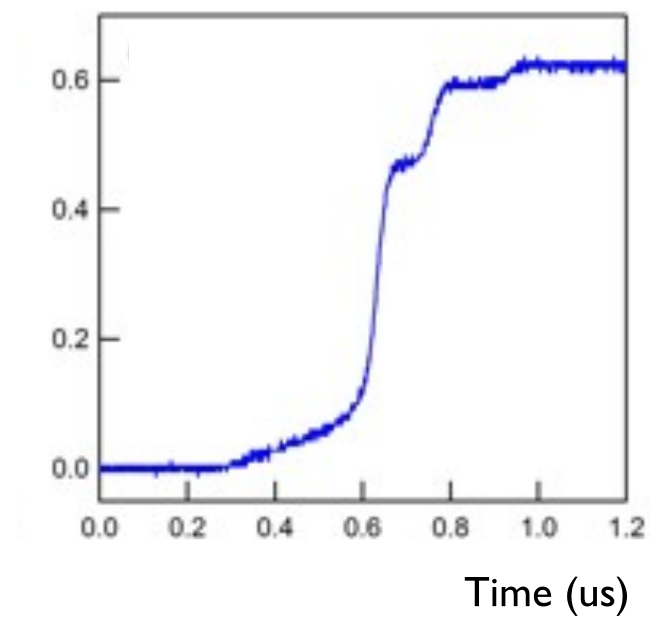

Such as γ scatters

Easy discrimination between single and multiple site events

Powerful background rejection

Detectors

Single site

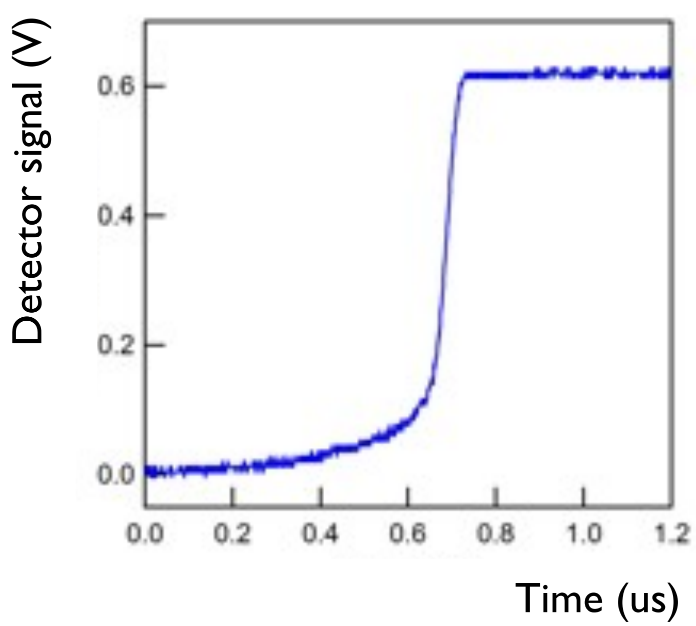

Such as 0νββ

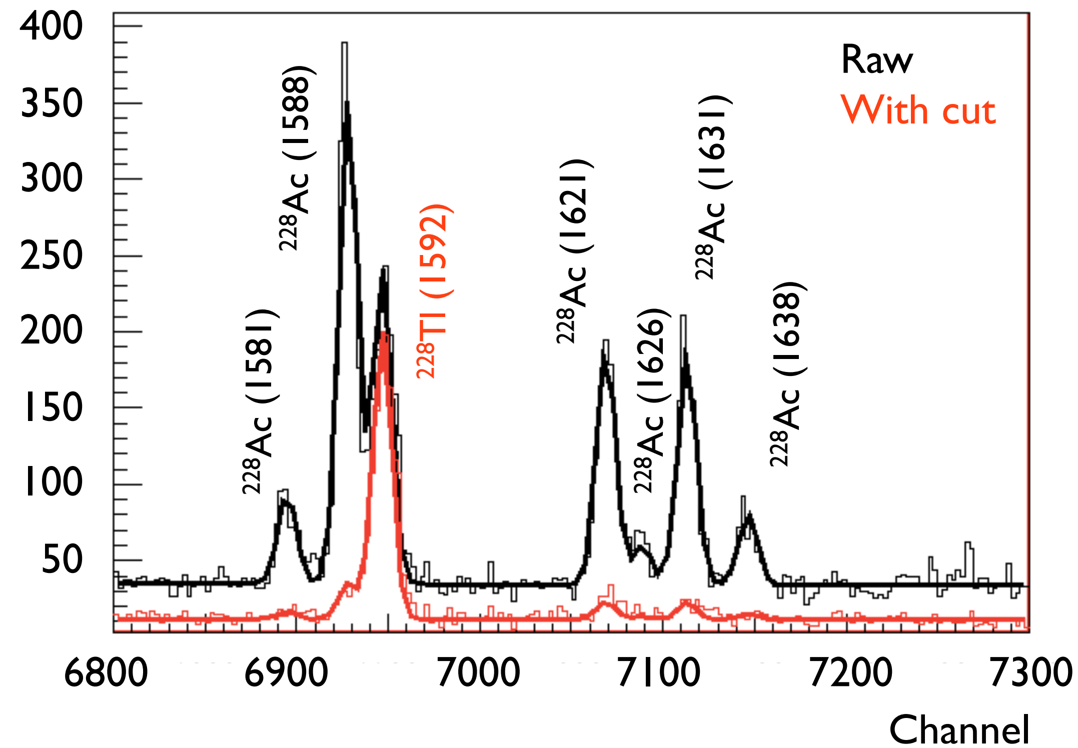

Multiple site

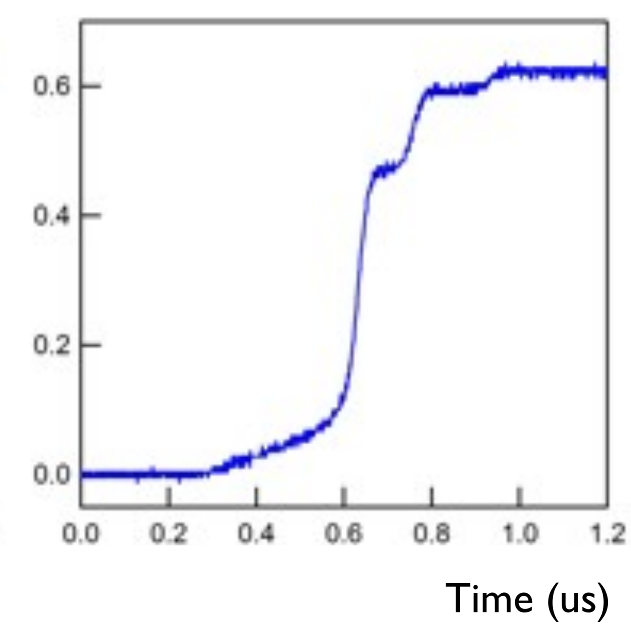

Such as γ scatters

Easy discrimination between single and multiple site events

Powerful background rejection

Detectors

C.E. Aalseth et al., PRL 101 251301 (2008).

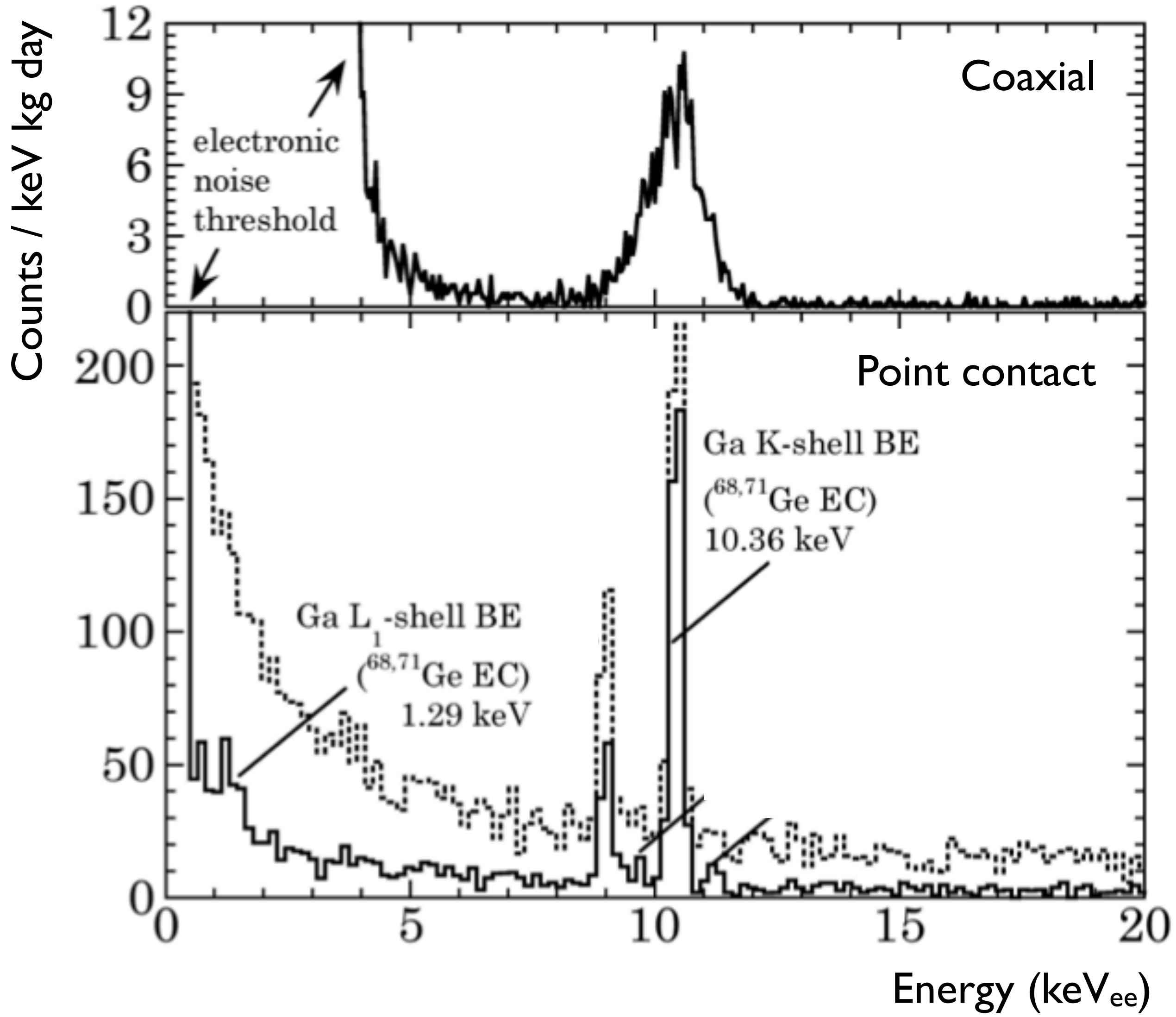

- Dark matter & axions
- Background-tagging

LBNL-fabricated PPC

Low noise therefore low energy thresholds

Detectors

C.E. Aalseth et al., PRL 101 251301 (2008).

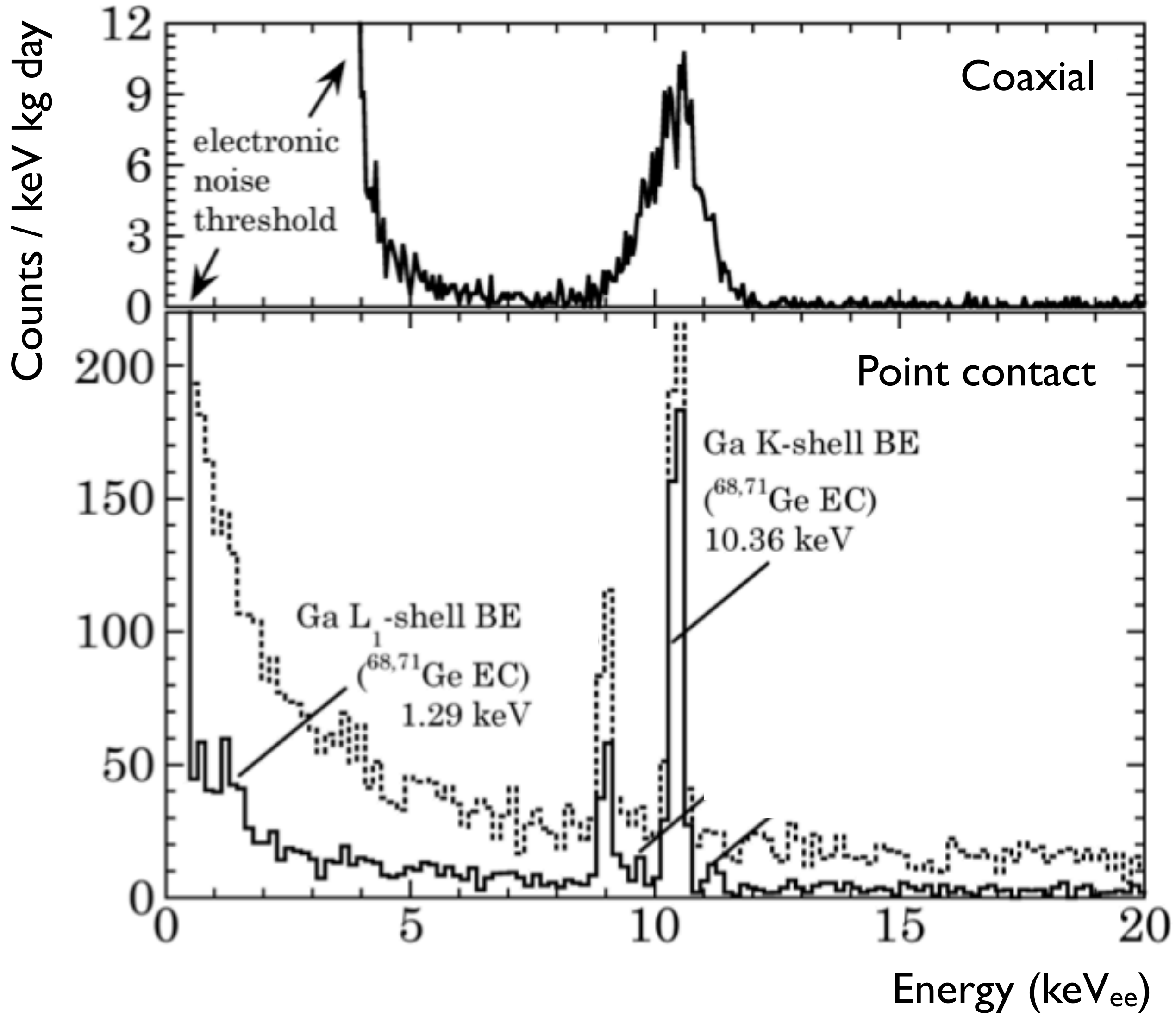

- Dark matter & axions
- Background-tagging

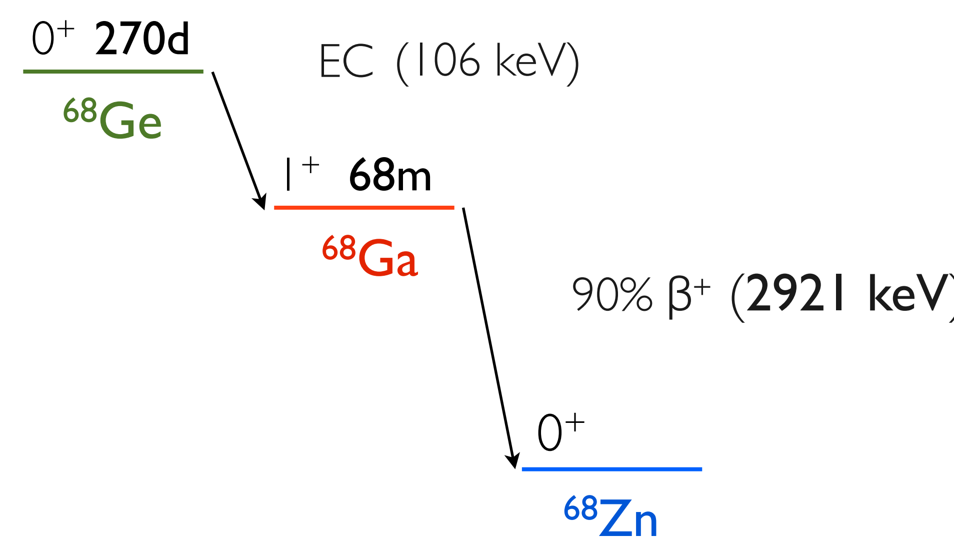

Low noise therefore low energy thresholds

Electronics

Resistive feedback

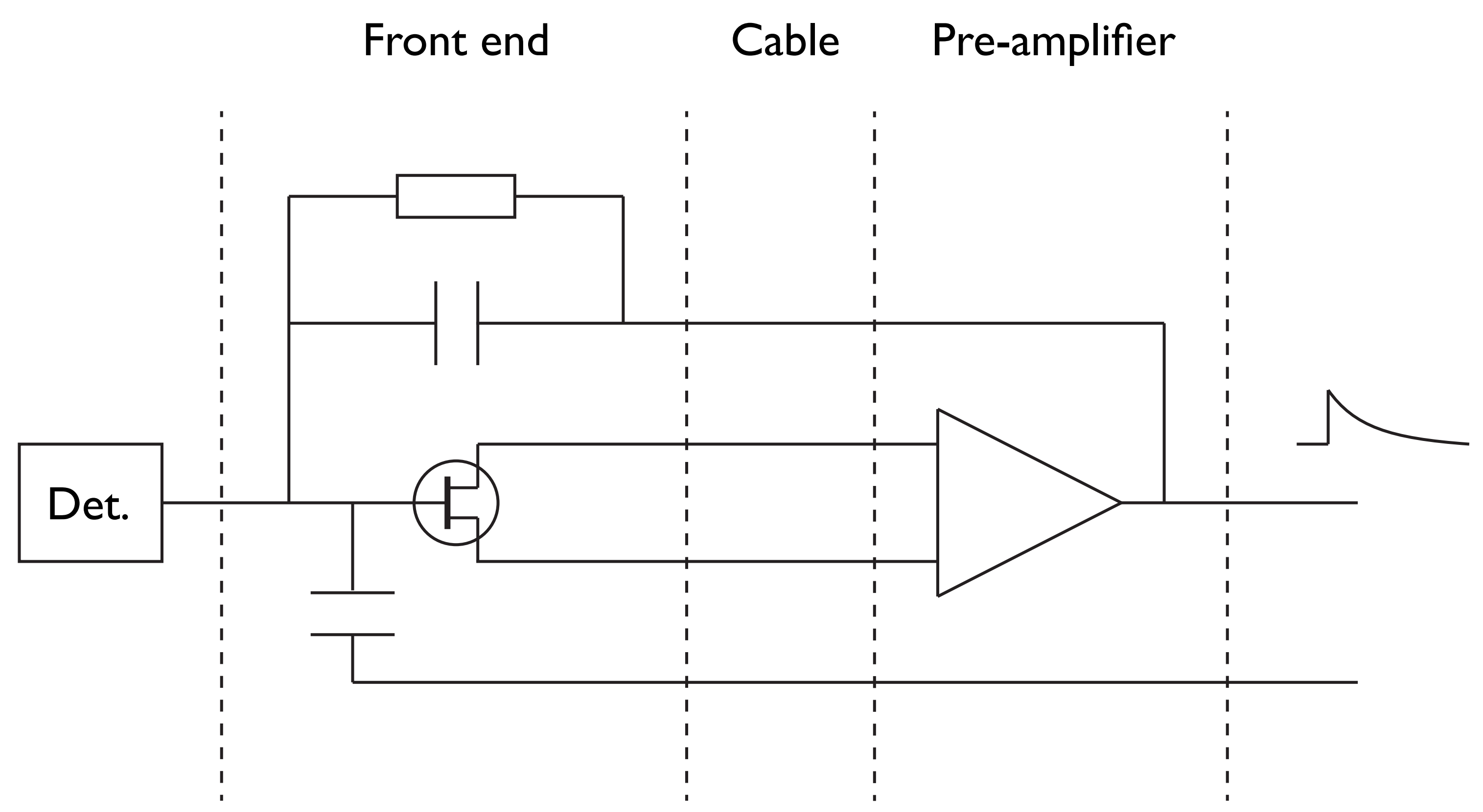

Aiming for :

- Low radioactivity
- Low noise

Radioactivity within the cryostat is minimized

Electronics

Front end

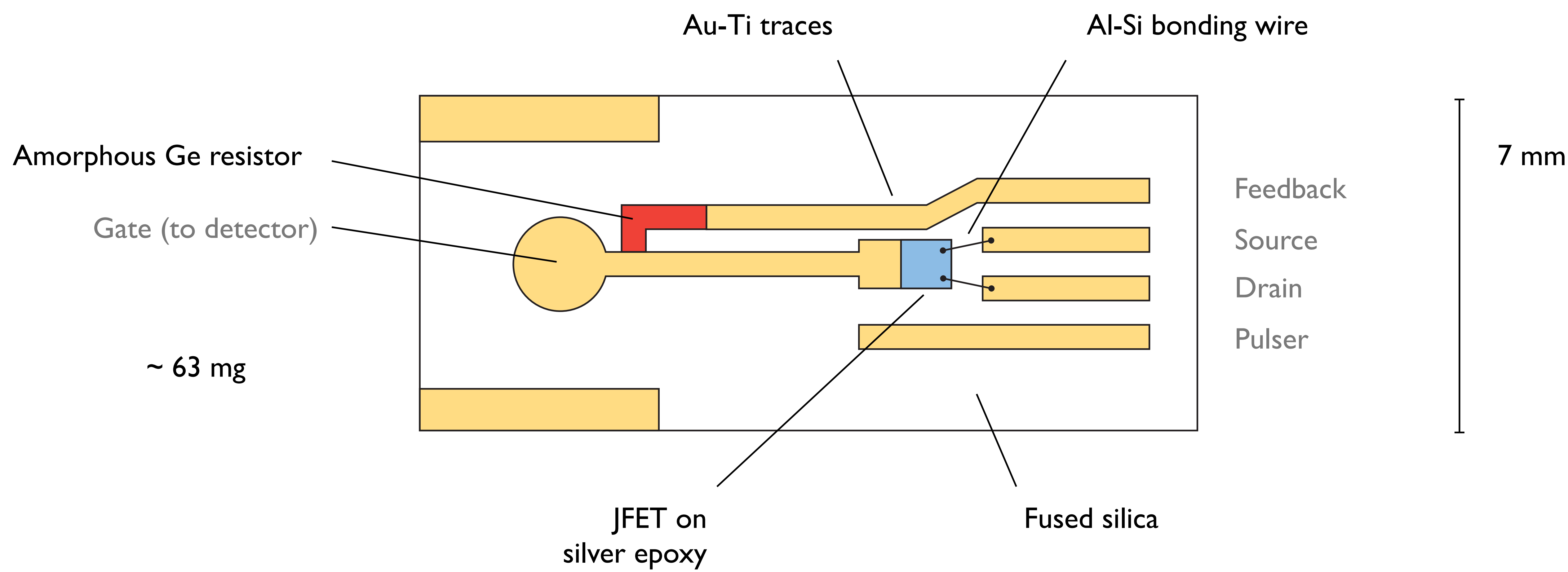

Fused silica (high purity, low dielectric losses, low thermal conductivity)
Amorphous Ge film for R_f (high purity, low noise)
Stray capacitance for C_f

$R_f \sim 10 - 100\ G\Omega$ (77K)
$C_f \sim 0.2$ pF

Electronics

Front end

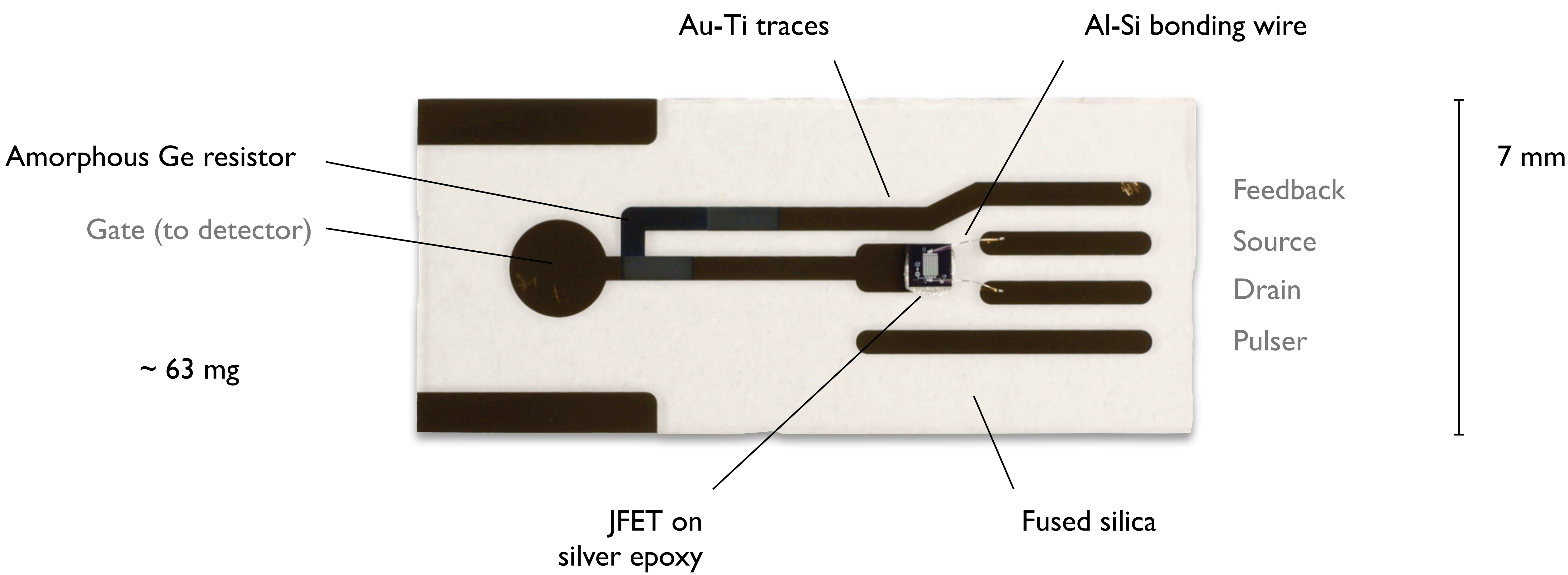

Fused silica (high purity, low dielectric losses, low thermal conductivity)

Amorphous Ge film for R_f (high purity, low noise)

Stray capacitance for C_f

$R_f \sim 10$ - $100\ G\Omega$ (77K)

$C_f \sim 0.2$ pF

Electronics

Ultra-pure

Component	Material	Purity (g / g)	
		^{232}Th	^{238}U
Substrate	Fused silica	101×10^{-12}	284×10^{-12}
Resistor	a-Ge	5×10^{-9}	5×10^{-9}
Traces	Au	$47(1)\times10^{-9}$	$2.0(0.3)\times10^{-9}$
Traces	Ti	$< 400\times10^{-12}$	$< 100\times10^{-12}$
FET	FET die	$< 2\times10^{-9}$	$< 141\times10^{-12}$
Bonding wire	Al	$91(2)\times10^{-9}$	$9.0(0.4)\times10^{-12}$
Epoxy	Silver epoxy	$< 70\times10^{-9}$	$< 10\times10^{-9}$

Ultra-low-noise

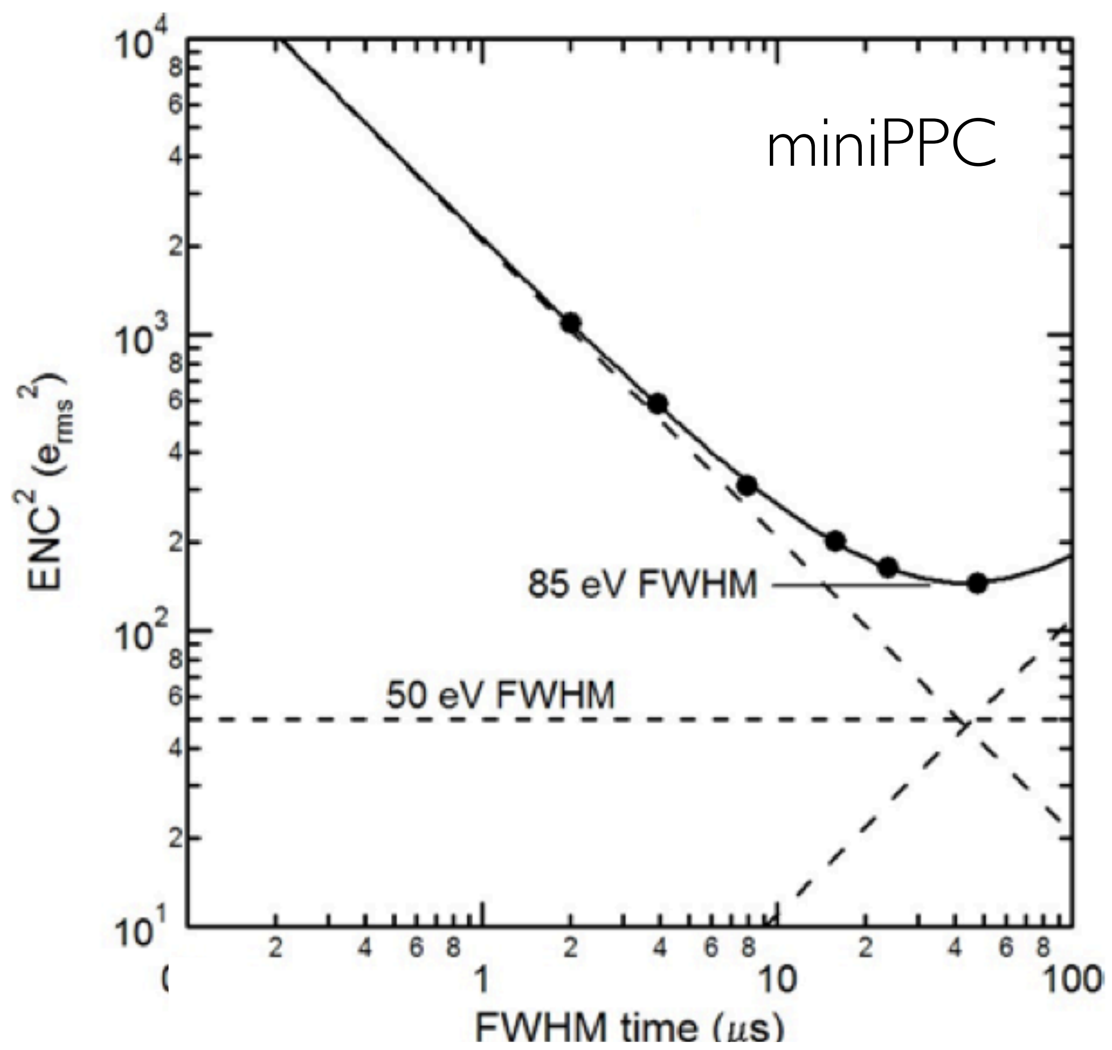

Electronics

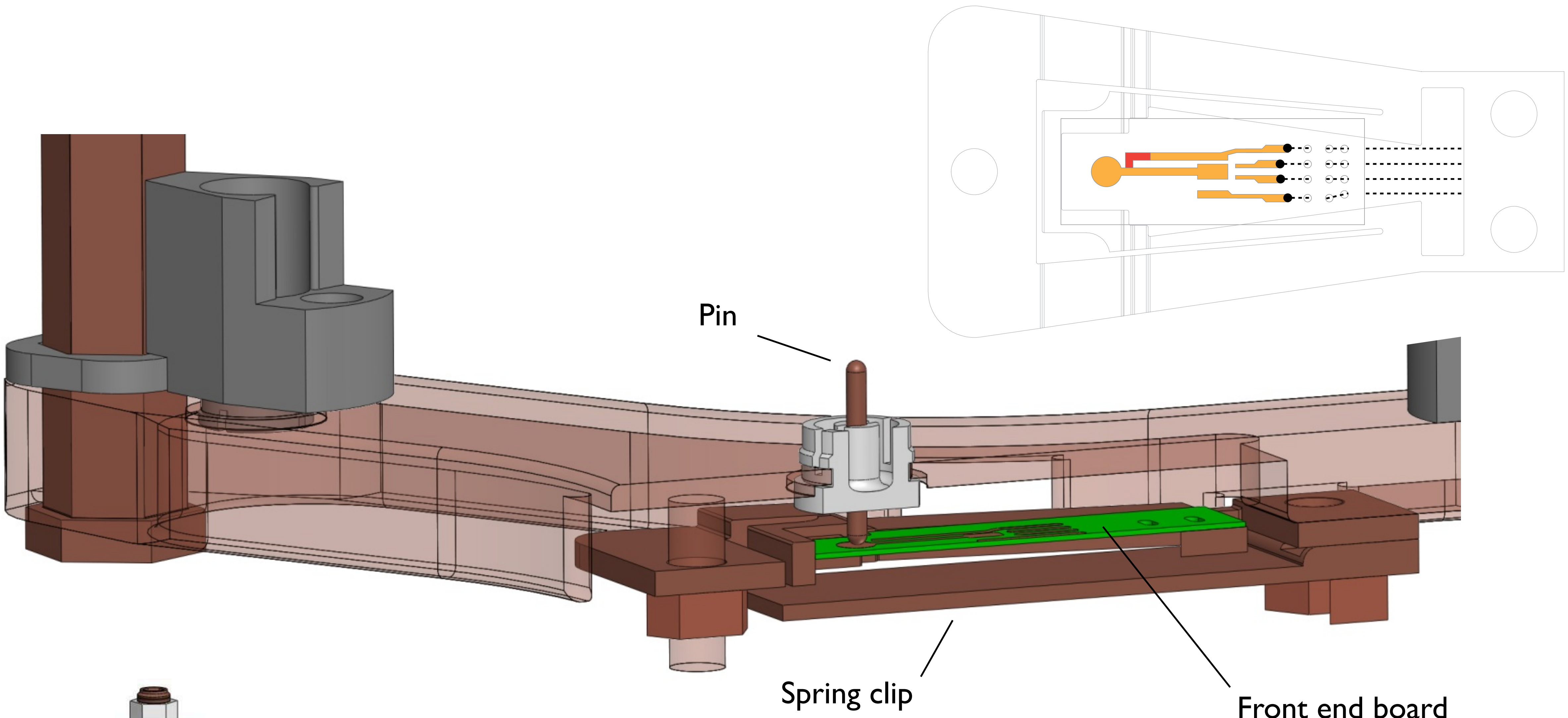

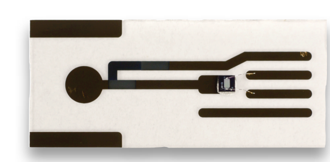

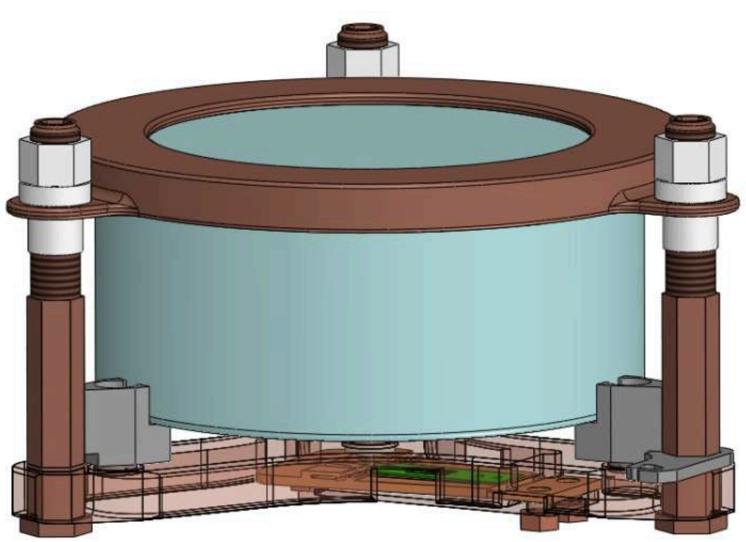

The board in held in a spring-clip,
the glass withstanding the force

Mounts

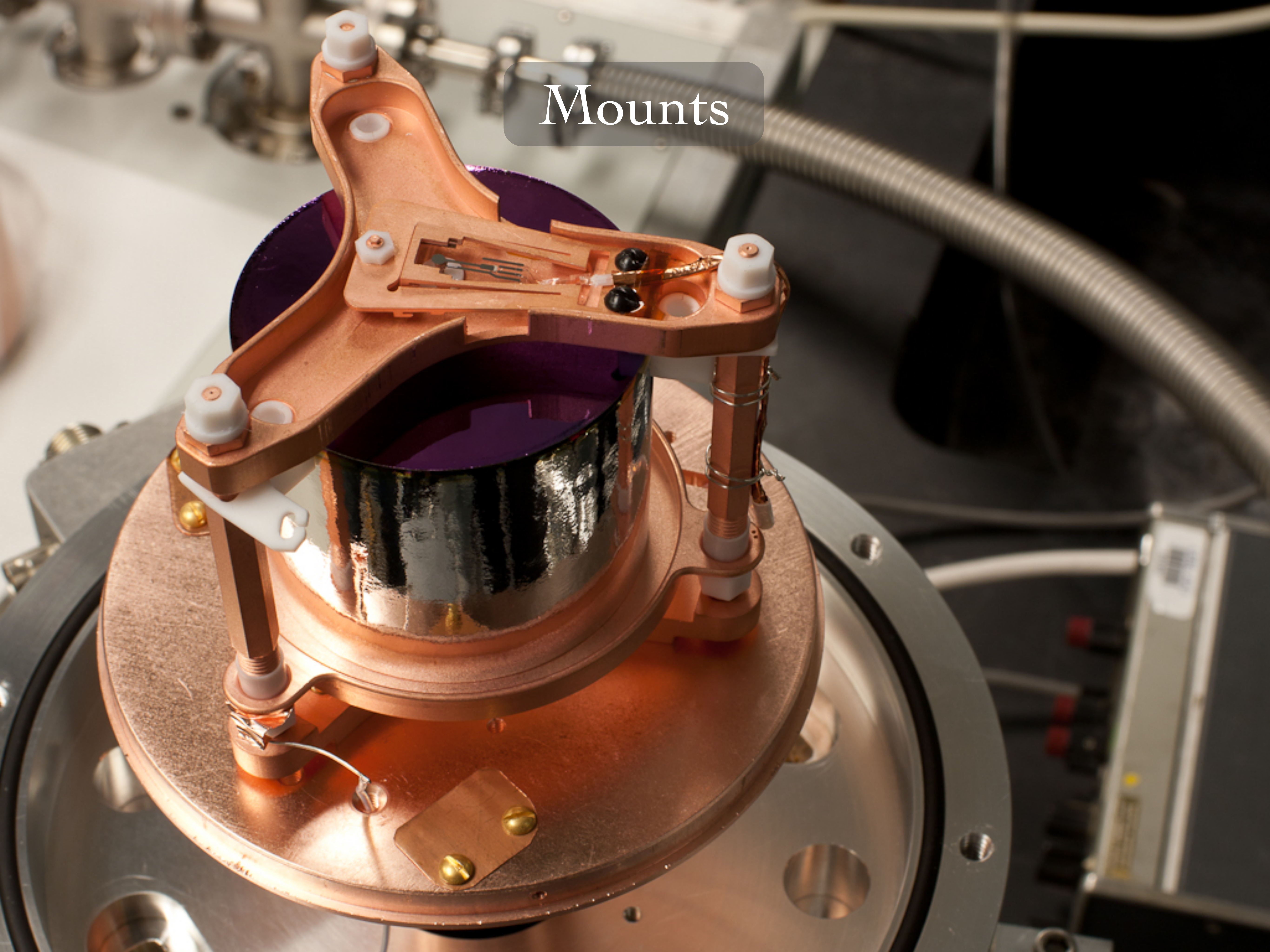

Sensitivity

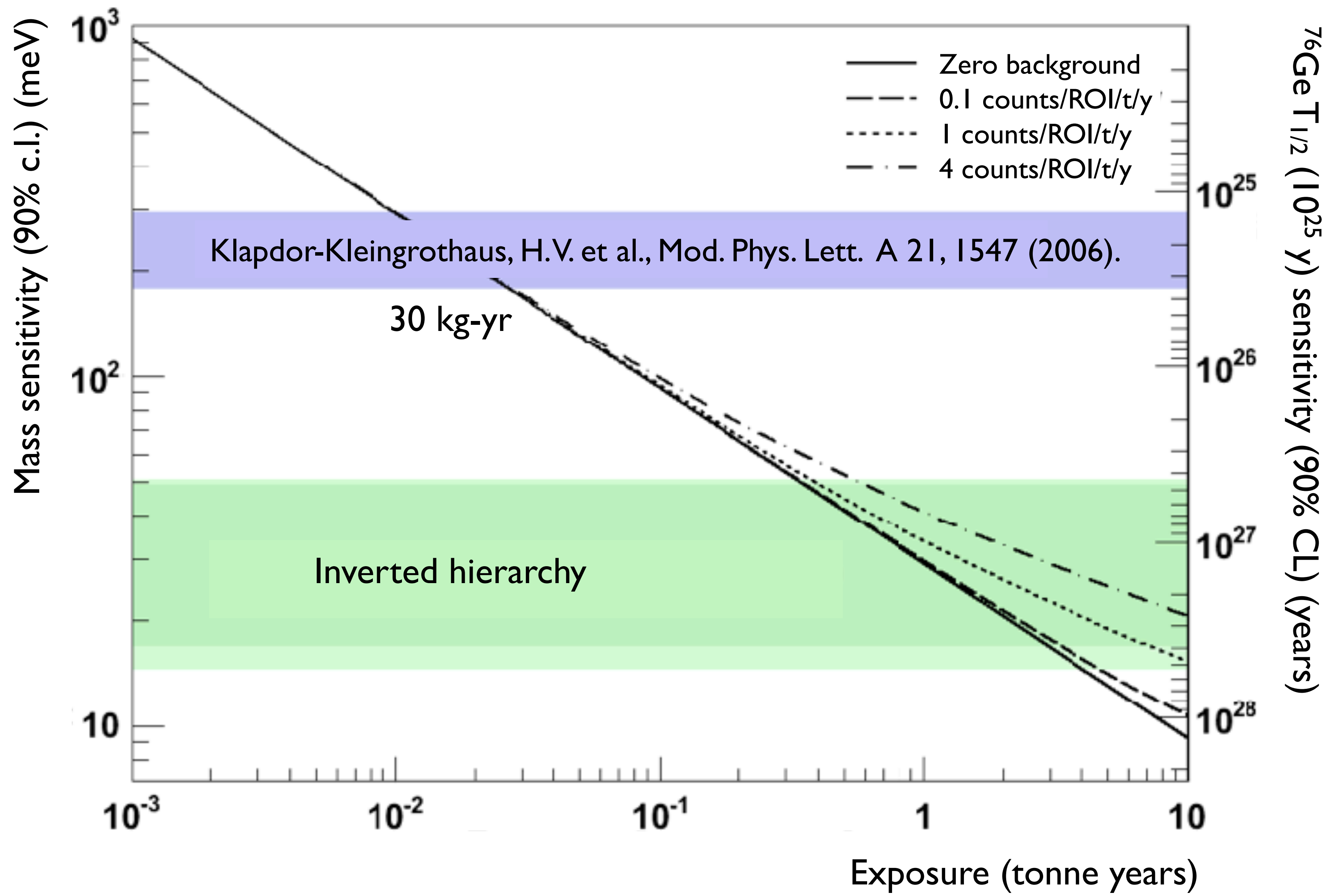

The claim can be tested with a year's data

1TGe

Future large-scale Ge

GERDA

Naked diodes in liquid argon

MAJORANA

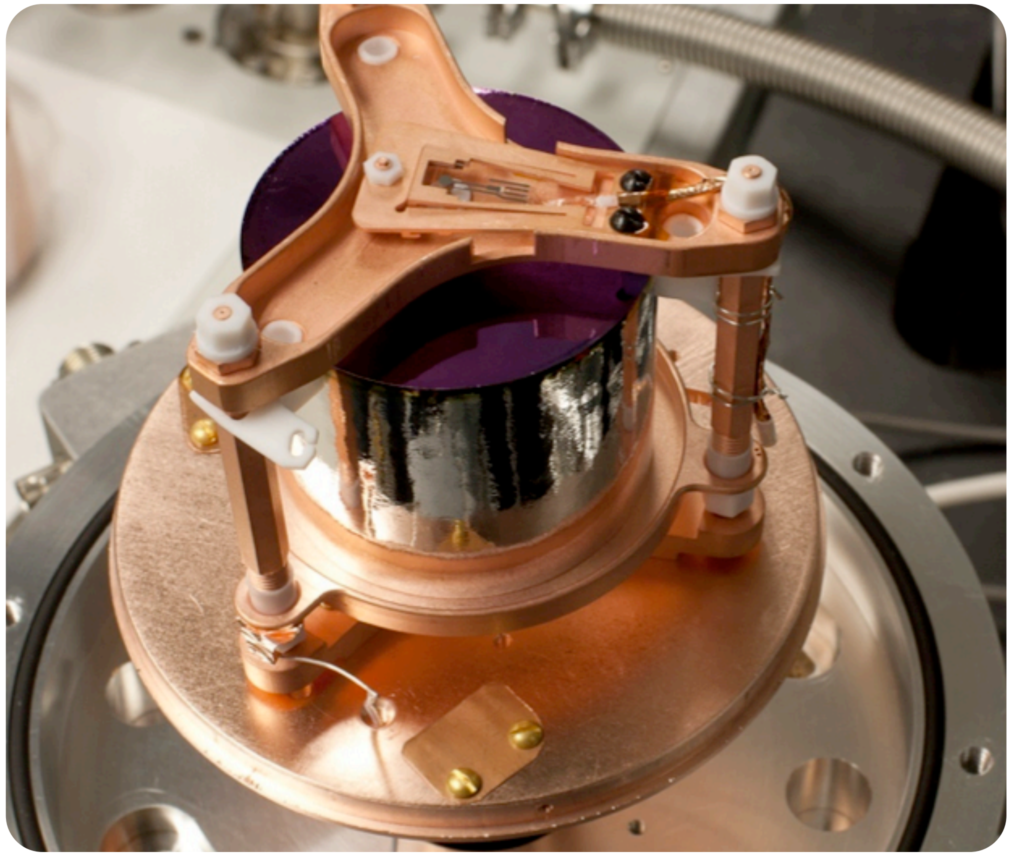

Diodes in vacuum cryostats

Cooperation and an understanding to merge for the tonne-scale

Alternative shield concepts

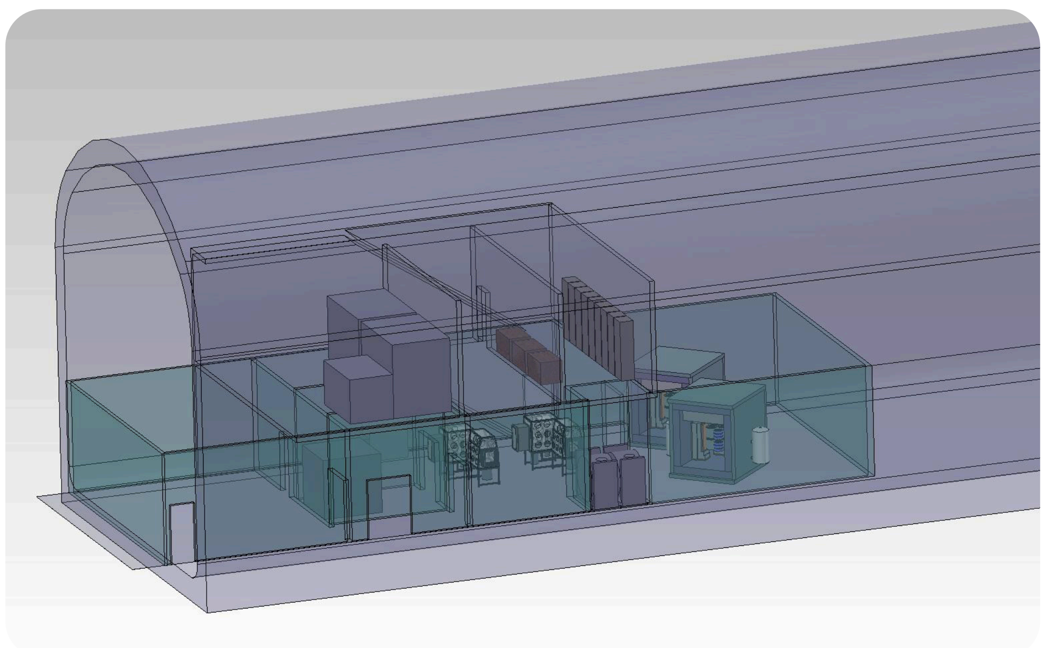

Compact shield

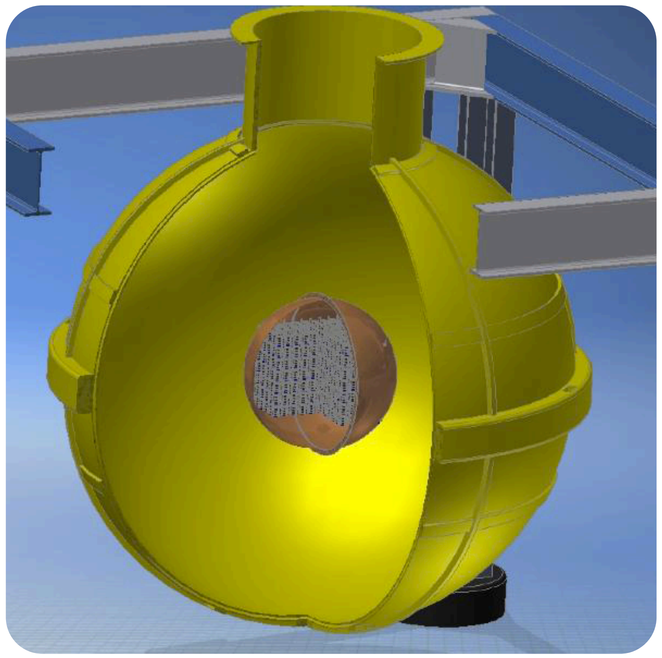

Vacuum cryostat immersed in liquid Ar, H_2O, scintillator

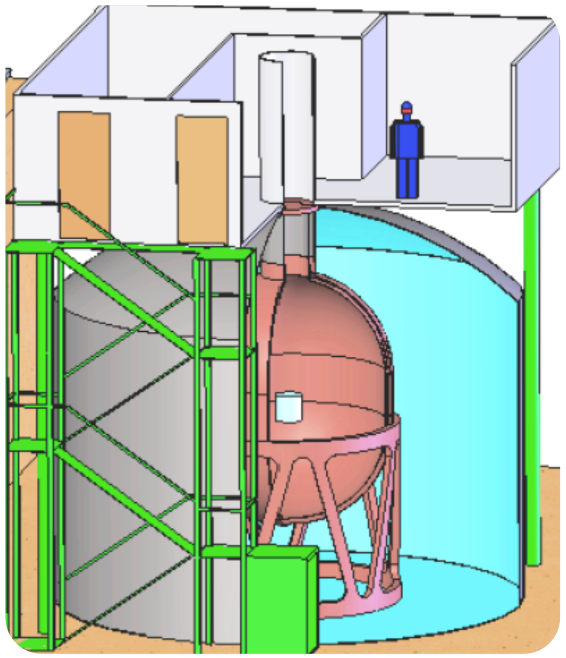

Vacuum cryostat immersed in liquid Ar, H_2O

Studied through grants from NSF (S-4) and other channels

Materials & assay R&D, detector studies, small parts, shielding schemes, operational schemes, fabrication techniques

The choice of technology awaits results from Majorana & GERDA

The long view

< 10 kg
- Sensitivity ~ 1 eV
- ~ 10 2ν measurements

30-200 kg
- Sensitivity ~ 100 meV
- Quasi-degenerate
- ~ 8-10 experiments

If 0ν observed

few 100 kg
- Several experiments
- Program to measure rate in several isotopes
- Kinematic meas.

~ 1 T
- Sensitivity ~ 50 meV
- Atmospheric scale
- ~ 3 experiments

If 0ν observed

few T
- > 3 experiments
- Program to measure rate in several isotopes
- Kinematic meas.

> 10 T
- Sensitivity ~ 5 meV
- Solar scale
- ~ 3 experiments

1985 - present | 2007-2015 | 2015-2025 | Future

Summary

GERDA	~15-35 kg	Running
MAJORANA	 ~30 kg	Construction
EXO-200	~100 kg	Running
KamLAND-Zen	~100 kg	Running
CUORE	~200 kg	Construction
SNO+	~120 kg	Construction
NEXT	~100 kg	
SuperNEMO	~7 kg	

Neutrinoless double beta decay is an exciting field with interesting parameter space ahead

The MAJORANA experiment is progressing well

The field has a clear, though challenging, road ahead

Moore's Law

From Elliott & Vogel, unpublished

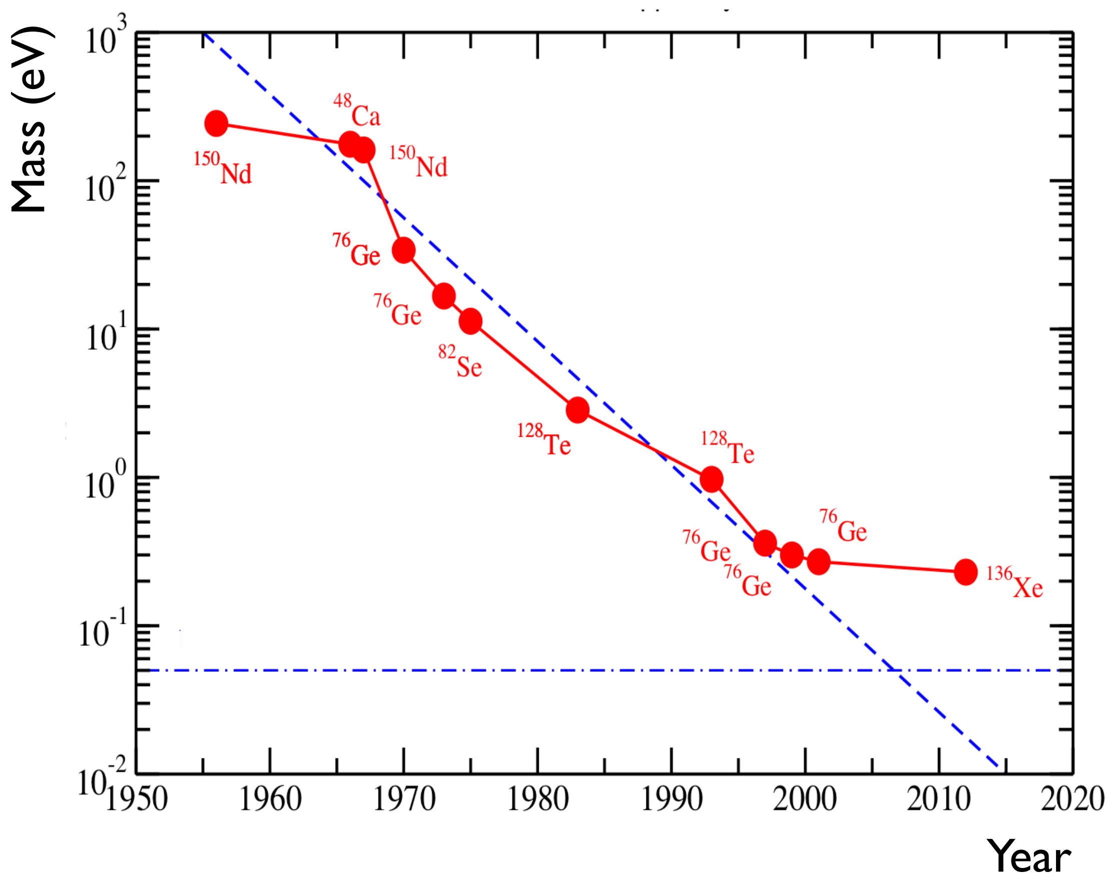

Detectors

Institution	Origin	Size (mm)	Type	Year
LBNL	Paul Luke	50 x 50	NPC	1987
		62 x 50	Segmented-PPC	2008
		20 x 10	Mini-PPCs (x3)	2009
		62 x 50	PPC	2009
	Canberra USA	70 x 30	Mod. BEGe	2011
Univ. Chicago	Canberra France	50 x 44	PPC	2005
	Canberra USA	60 x 30	Mod. BEGe	2008
PNNL	Canberra France	50 x 50	PPC	2008
LANL	PHDs	72 x 37	PPC	2008
	Canberra USA	70 x 30	Mod. BEGe (x39)	2009-11
	ORTEC	62 x 51	PPC	2009
		67 x 54	PPC	2010
	PGT	70 x 30	PPC	2010
UNC	Canberra USA	61 x 30	Mod. BEGe (low bgd)	2009
		61 x 32	Mod. BEGe	2010
		70 x 30	Mod. BEGe (x3)	2011

Size is (diameter x height)

Detectors

BEGe

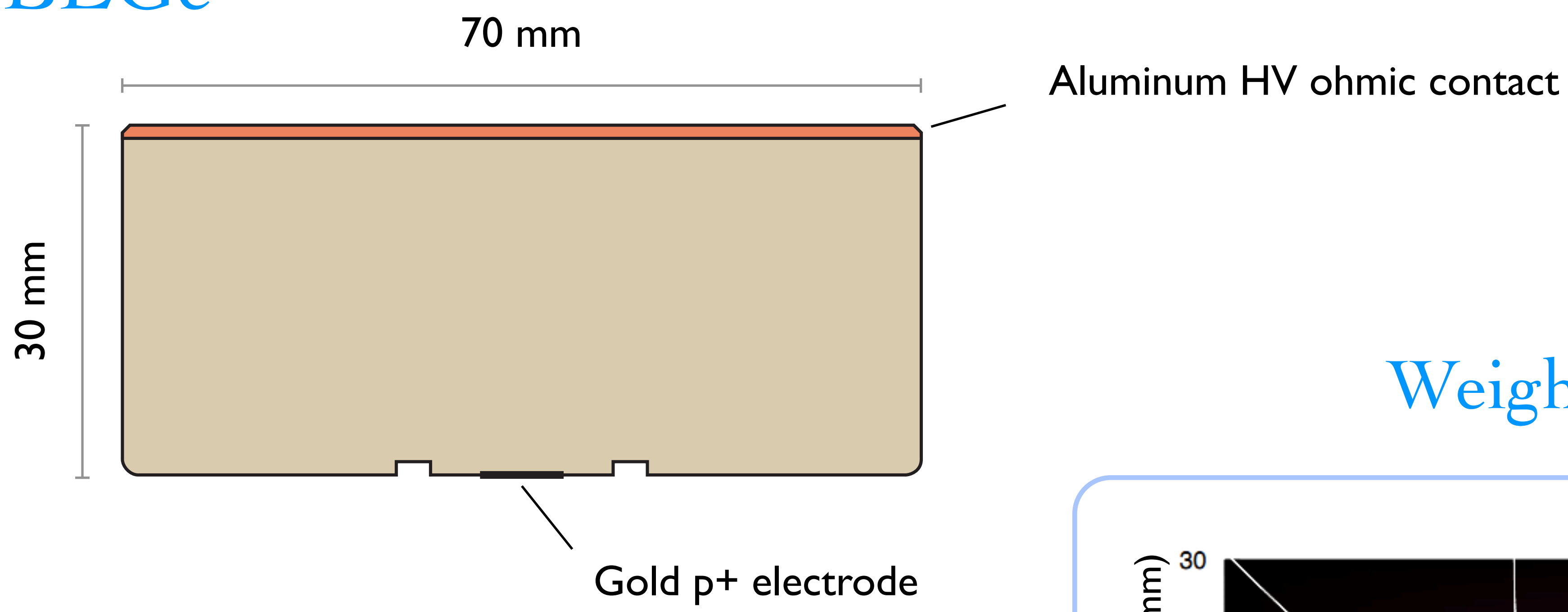

Modified Canberra BEGe detectors

- smaller contact
- non-thinned front faced
- re-positioned HV contact

39 ^{nat}Ge detectors purchased

- most stored underground, others for R&D

Weighting potential

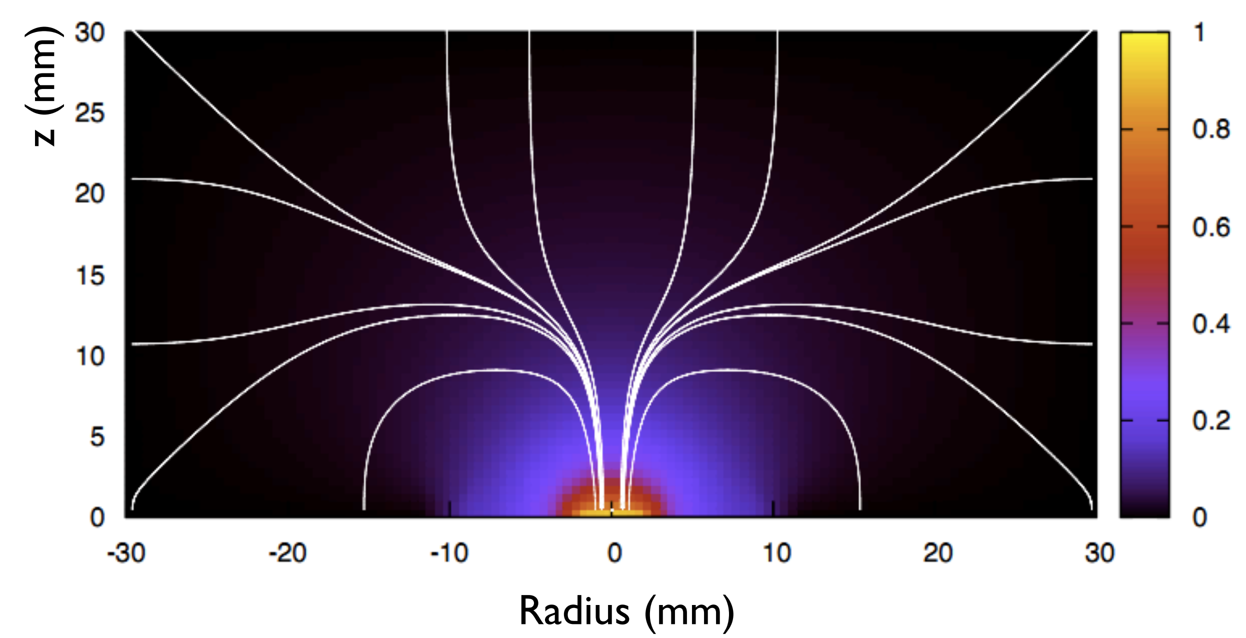

Cables

Picocoax

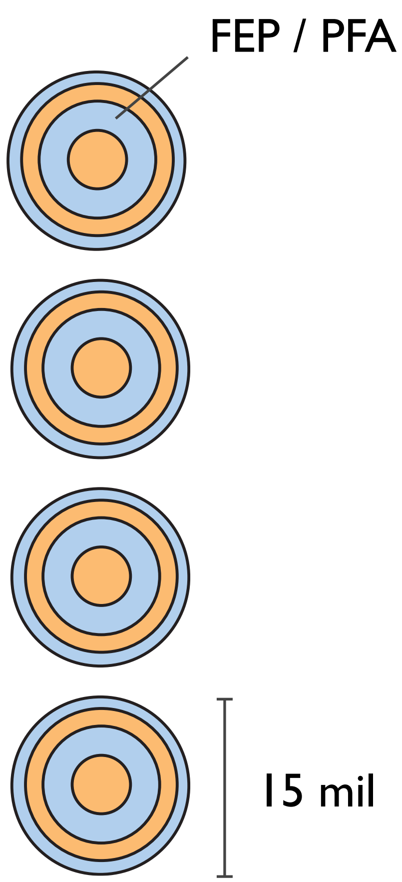

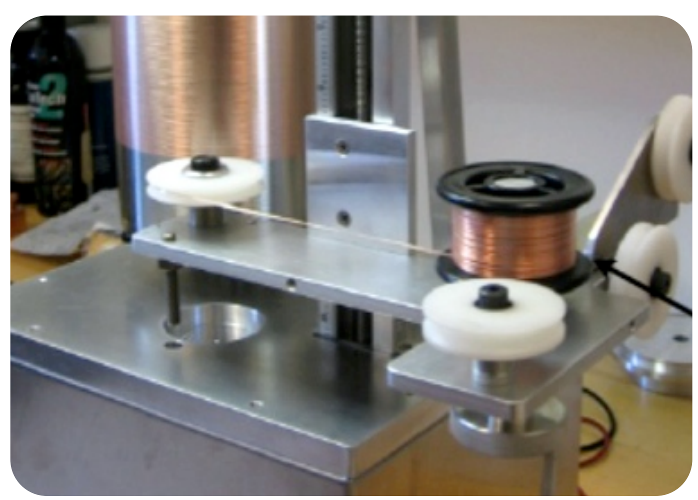

Parylene

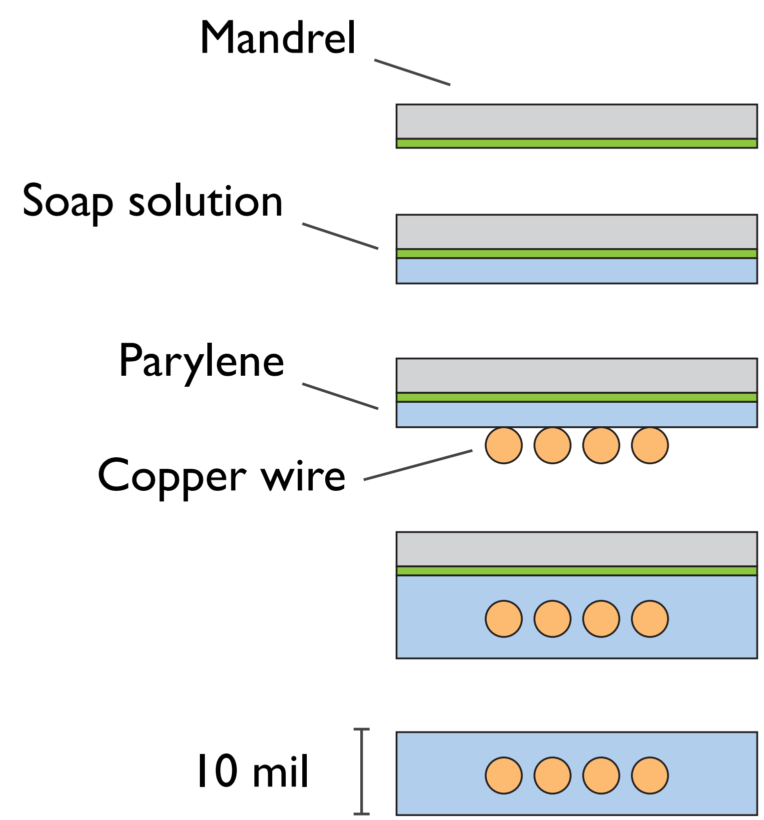

Critical small parts

Heidelberg-Moscow

Experimental configuration

- 5 p-type enriched (~88%) coaxial HPGe detectors
  - 10.96 kg total active volume
  - Enriched to 86-88% in ^{76}Ge
- Two shielding configurations

Heidelberg-Moscow

The claim

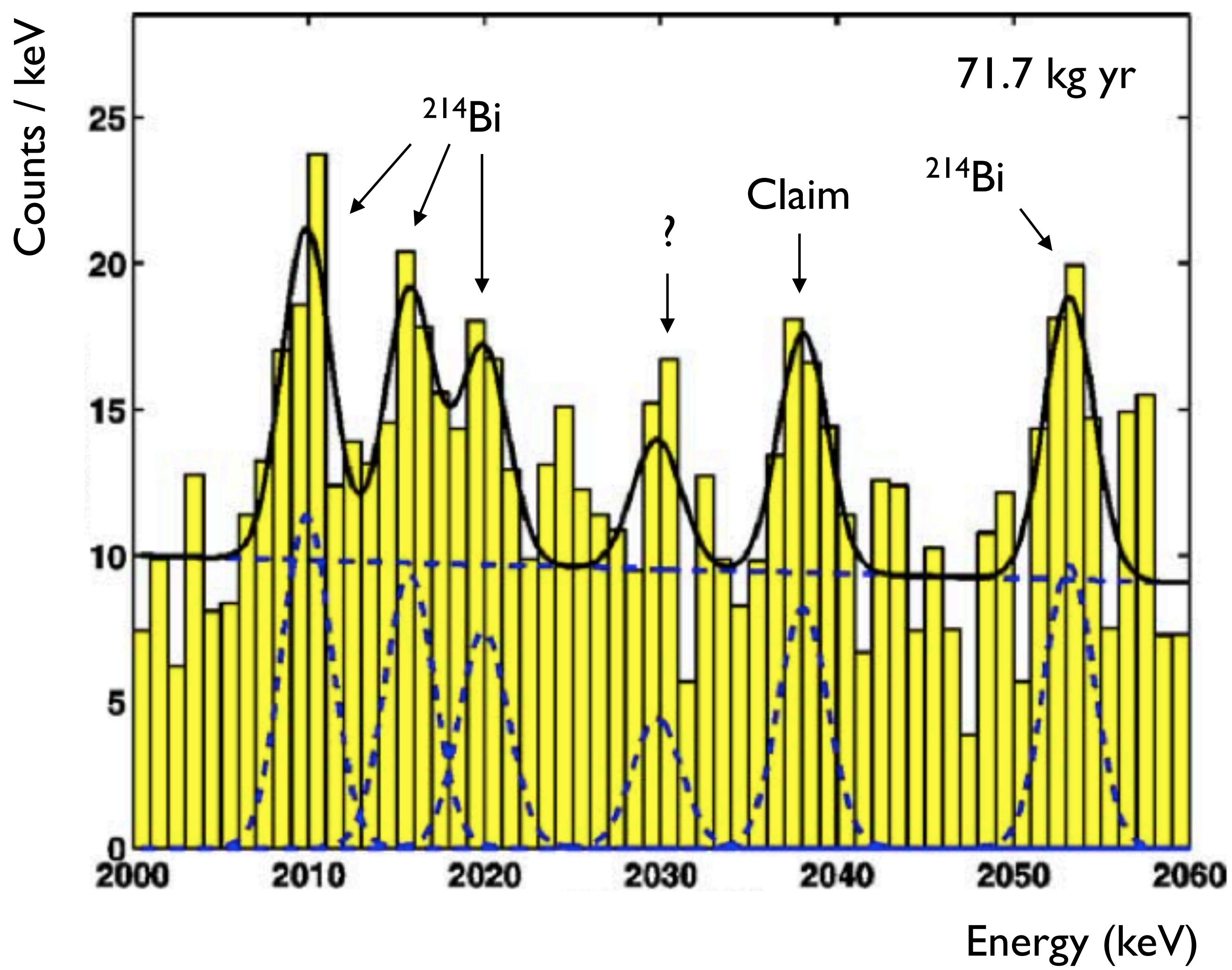

Linear background + peaks

Excess of 28.75 ± 6.86 events at $Q_{\beta\beta}$

4.2 σ significance

Claimed observation

$$T^{0\nu}_{1/2} = (2.23^{+0.44}_{-0.31}) \times 10^{25}\,\mathrm{y}$$

$$\langle m_{\beta\beta} \rangle \sim 300\,\mathrm{meV}$$

Even stronger (6 sigma) claim with more recent PSA:
Klapdor-Kleingrothaus, H.V. et al., Mod. Phys. Lett. A **21**, 1547 (2006).

Klapdor-Kleingrothaus, H.V., et al., Phys. Lett. B **586**, 198 (2004).
(Plot annotated by me.)

Heidelberg-Moscow

The claim

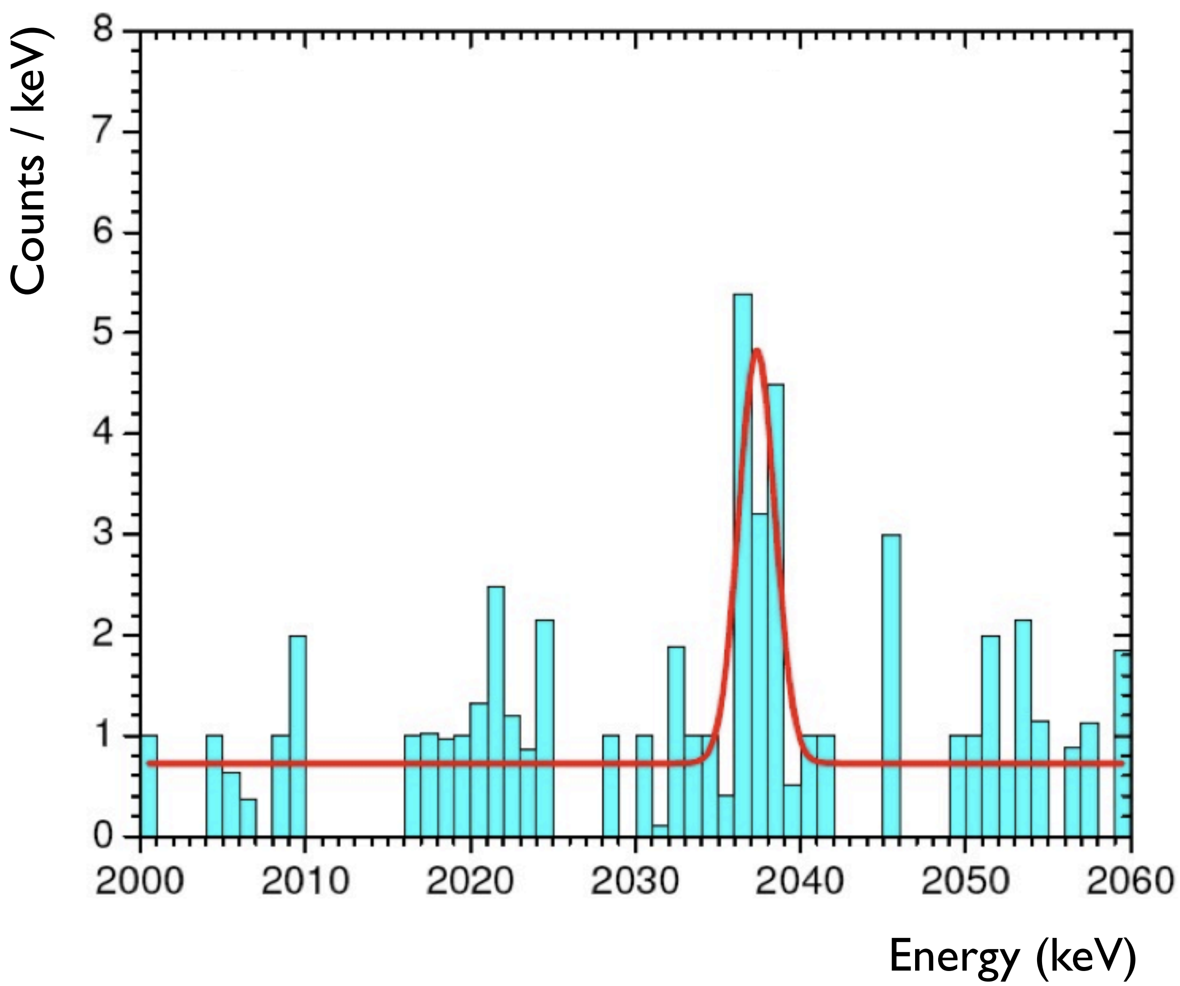

Klapdor-Kleingrothaus, H.V. et al., Mod. Phys. Lett. A **21**, 1547 (2006).

Linear background + peaks

Excess of 28.75 ± 6.86 events at $Q_{\beta\beta}$

4.2 σ significance

Claimed observation

$$T^{0\nu}_{1/2} = (2.23^{+0.44}_{-0.31}) \times 10^{25}\,\mathrm{y}$$

$$\langle m_{\beta\beta} \rangle \sim 300\,\mathrm{meV}$$

Klapdor-Kleingrothaus, H.V., et al., Phys. Lett. B **586**, 198 (2004).
(Plot annotated by me.)

Techniques

Source ≠ Detector

Source in foils, surrounded by instrumentation

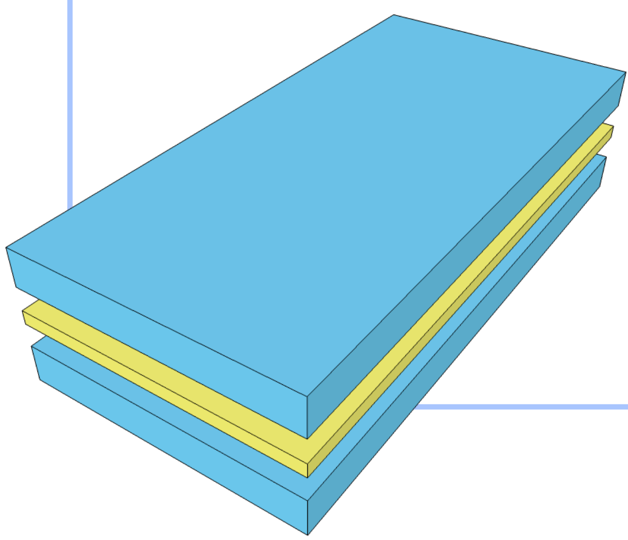

- ▲ Topological background rejection
- ▲ Sensitivity to the mechanism
- ▼ Poor exposure, efficiency, resol^n

Final state ID

Search for anomalous (A, Z+2) in a material containing (A,Z)

Natural source or one specially prepared

Source = Detector

Scintillators, bolometers, diodes, TPCs ...

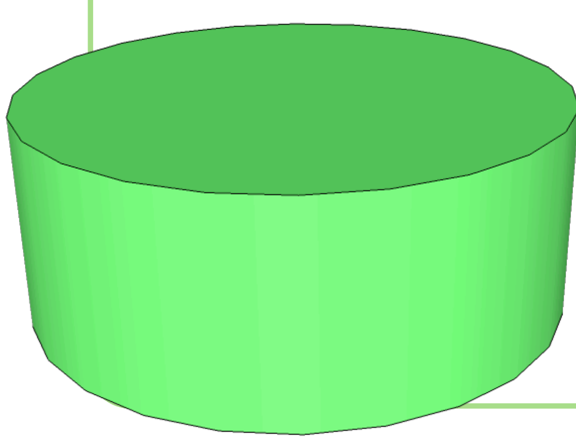

- ▲ Large mass
- ▲ High efficiency
- ● High resolution , moderate tracking possible

Sensitivity

Phase space factor

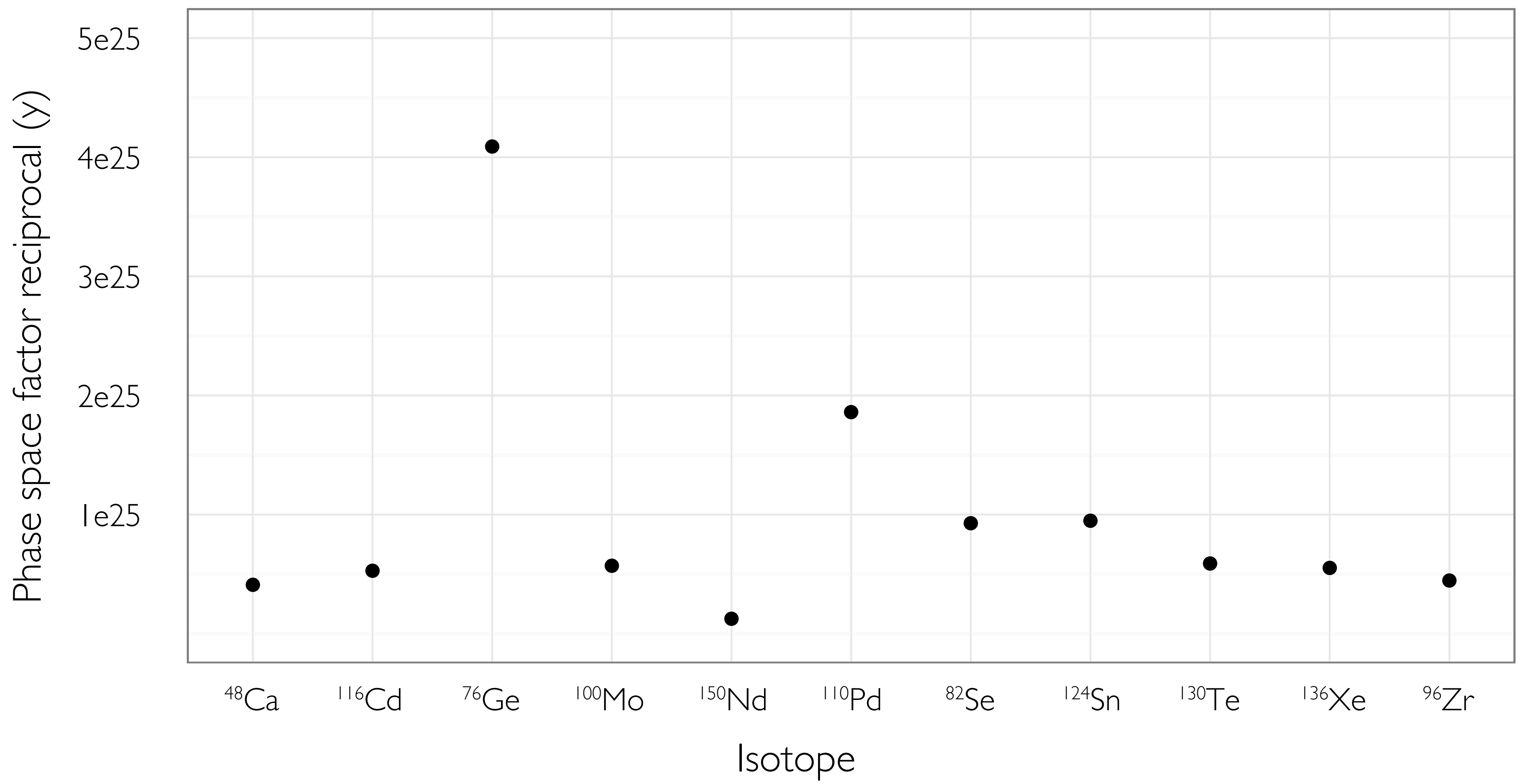

Data from: K. Zuber et al., arXiv:0511009v1 (2005).

$$(T^{0\nu}_{1/2})^{-1} = G_{0\nu}(Q_{\beta\beta}, Z)|M_{0\nu}|^2\langle m_{\beta\beta}\rangle^2$$

Phase space factors affect the predicted rate